Preprints.org

Article

Not peer-reviewed version

# Early Priabonian Larger Benthic Foraminifera from the Vicinity of Verona (N Italy)

Levent Sina Erkızan , György Less * , Cesare Andrea Papazzoni

Posted Date: 24 June 2025

doi: 10.20944/preprints202506.1471.v2

Keywords: north Italy; eocene; priabonian; larger benthic foraminifera; morphometry; taxonomy; biostratigraphy

Preprints.org is a free multidisciplinary platform providing preprint service that is dedicated to making early versions of research outputs permanently available and citable. Preprints posted at Preprints.org appear in Web of Science, Crossref, Google Scholar, Scilit, Europe PMC.

Copyright: This open access article is published under a Creative Commons CC BY 4.0 license, which permit the free download, distribution, and reuse, provided that the author and preprint are cited in any reuse.

Preprints.org (www.preprints.org) | NOT PEER-REVIEWED | Posted: 24 June 2025 doi:10.20944/preprints202506.1471.v2

Peer-reviewed version available at Geosciences 2025, 15, 334; doi:https://doi.org/10.3390/geosciences15090334

from any ideas, methods, instructions, or products referred to in the content.

*Article*

# Early Priabonian Larger Benthic Foraminifera from the Vicinity of Verona (N Italy)

**Levent Sina Erkızan [1], György Less [1,*] and Cesare Andrea Papazzoni [2]**

[1] University of Miskolc, Institute of Exploration Geosciences, H-3515, Miskolc-Egyetemváros, Hungary

[2] Università di Modena e Reggio Emilia, Dipartimento di Scienze Chimiche e Geologiche, I-41125 Modena, Italy

* Correspondence: gyorgy.less@uni-miskolc.hu; Tel.: +36-20-5005907

**Abstract:** The rich Eocene larger benthic foraminiferal (LBF) assemblages from the vicinity of Verona are well-known long since. However, they are described in detail only from the Ypresian to Bartonian interval. Here, we present the results of our morphometrically based study of Priabonian LBF. The lowermost part of the succession, just above the uppermost occurrence of giant *Nummulites* (*N. biedai*) is outcropping on Monte Cavro and contains *Heterostegina reticulata multifida* and *Nummulites hormoensis* as major constituents. These taxa clearly determine the earliest Priabonian SBZ 18C shallow benthic zone. Slightly younger strata could be studied in the three studied exposures on the northern side of Castel San Felice. These beds already represent the early Priabonian SBZ 19A Zone based on the first appearing *Spiroclypeus sirottii* and on the presence of *Heterostegina reticulata mossanensis* and *Nummulites fabianii* (replacing *H. r. multifida* and *N. hormoensis*, respectively). The most abundant LBF in these beds are the very diverse and well-preserved orthophragmines represented both by family Discocyclinidae (genus *Discocyclina* and *Nemkovella*) and Orbitoclypeidae (genus *Orbitoclypeus* and *Asterocyclina*). They determine the OZ 14 orthophragmine zone. The distinction of six species of the genus *Discocyclina* (especially that of *D. euaensis* from *D. dispansa*) is discussed in detail. The exposures around Castel San Felice are considered as key localities for the SBZ 19A and OZ 14 Zones containing their key LBF assemblages. Late Lutetian–Priabonian range charts for LBF and separately also for orthophragmine taxa are updated.

**Keywords:** north Italy; eocene; priabonian; larger benthic foraminifera; morphometry; taxonomy; biostratigraphy

## 1. Introduction

Larger benthic foraminifera (LBF) are probably the most widespread fossils in the tropical/subtropical shallow marine rocks of the Tethyan Paleogene (and especially Eocene) deposits, which is reflected also in the name "Nummulitique", widely used earlier in the French literature for the Eocene. LBF have been widely used for biostratigraphical purposes since the middle of the 19th century [1,2]. Due to the intensive work in IGCP projects 286 ("Early Paleogene Benthos") and 393 ("Neritic Events at the Middle–Upper Eocene boundary"), the Tethyan Paleocene and Eocene has been subdivided into twenty shallow benthic (SBZ) zones (SBZ 1–20 [3]), followed with six zones in the Oligo-Miocene (SBZ 21–26 [4]).

Simultaneously, [5,6] worked out the stratigraphic subdivision of Tethyan late Paleocene and Eocene orthophragmines (the families Discocyclinidae and Orbitoclypeidae with similar morphostructure), which was incorporated into the shallow benthic zonation. A separate orthophragmine zonation with eighteen OZ prefixed zones was also developed [6]. Later, this zonation was significantly improved [7] and also geographically widened to the east and south. SBZ and OZ zones were first correlated [6], with the most updated versions being found in [8] and [7]. In addition, the first includes the calibration of the SBZ and OZ zones to the magnetostratigraphic and plankton-based subdivisions.

© 2025 by the author(s). Distributed under a Creative Commons CC BY license.

Preprints.org (www.preprints.org) | NOT PEER-REVIEWED | Posted: 24 June 2025 doi:10.20944/preprints202506.1471.v2

Peer-reviewed version available at Geosciences 2025, 15, 334; doi:https://doi.org/10.3390/geosciences15090334

Because of the discontinuous record (characteristic for shallow marine organisms) these SBZ and OZ units are considered as Oppelzones (for detailed explanation see [9]), which are defined rather by their key assemblages recorded in particular key-localities than by the (very often undetectable) zone boundaries. The vertical succession of zones can be established sometimes by their superposition in the field. More often, however, it is based on the comparison of the evolutionary degree of particular lineages occurring in the neighboring zones. Fortunately, especially in the Eocene, numerous evolutionary lineages run parallel and co-occur in the key localities.

Based on the above reasoning, the detailed knowledge of key LBF assemblages from key localities is essential since they serve as references for the determination of LBF from other localities, which leads to the correct stratigraphic evaluation of the latter. Consequently, the key LBF assemblages (i) should be very rich and diverse, (ii) should contain well preserved and isolated specimens, and (iii) the key localities should be easily accessible. In this paper we present and describe in detail the early Priabonian key LBF assemblage from the vicinity of Verona (N Italy), which fulfill all these three conditions.

## 2. Geological Setting

Verona is located in northeastern Italy, on the southwestern margin of the Lessini Mountains, (Figure 1), which are part of the Southern Alps, originated by the collision of the Adria Plate with the southern European margin during Cenozoic [10–12]. During the Paleogene, the Lessini area formed the so-called "Lessini Shelf" [13], a shallow-marine platform limited on the western side by the Lombardy Basin, on the eastern side by the Belluno Basin, connected north to the emerged land and extending south to the modern Berici Mts. The Lessini Shelf was in turn superimposed to the Early Jurassic Trento Platform [13,14], which drowned starting from Middle Jurassic to become the Trento Plateau [15], a structural high with basinal sedimentation continuing until the early Eocene [13,16,17]. During this time interval, on the Trento Plateau were deposited deep-water sediments belonging to the Rosso Ammonitico Veronese Fm. (upper Bajocian–upper Tithonian; [18]), Maiolica Fm. (upper Tithonian–lower Aptian; [19]), Scaglia Variegata Alpina Fm. (lower Aptian–Cenomanian; [19]), and Scaglia Rossa Fm. (Turonian–Ypresian; [13,16,19]). Then, the Cenozoic shallow-water carbonates started their deposition in the early Eocene on the higher parts of uplifted blocks (e.g., Torbole Limestone, [16]) while in the surrounding deeper areas slope and basinal sediments were deposited (e.g., Malcesine Limestone and Chiusole Formation, [16]).

The Eocene cropping out in the vicinity of Verona is subdivided into three different formations, namely the "Calcari argillosi e marne di colore biancastro" (whitish clayey limestone and marl), attributed to the lower Eocene (also "Calcari di Spilecco" [20] or "Calcari argillosi e marne" [21]), the "Calcari nummulitici" (nummulitic limestone), first deposits of shallow-water paleoenvironment, spanning the lower to middle Eocene, and the "Marne di Priabona" (Priabona marl), belonging to the upper Eocene [22].

Among these formations, the older "Calcari argillosi e marne di colore biancastro" contain abundant planktonic foraminifera, sometimes together with larger benthic foraminifera, mainly *Nummulites*, resedimented from shallower areas into the deeper basins [21].

Similarly, also the lowermost part of the "Calcari nummulitici" may contain resedimented larger benthic foraminifera in the lower Eocene, that could be correlated with the Chiusole Formation [16], also recently reported from the locality of Monte Solane near Fumane (a few km northwest of Verona; [24]). The remaining part of the "Calcari nummulitici", extensively cropping out just north of the city of Verona, is attributed to the Lutetian and Bartonian, with different (partly giant) *Nummulites* in its uppermost part (see the Monte Cavro section in [25]).

The "Marne di Priabona" is commonly cropping out on top of the "Calcari nummulitici" in the hills north of Verona (see geological map [22]). They contain mainly orthophragmines and subordinately nummulites, all indicating a Priabonian age [20–22]. Near Verona the Priabona marl is locally covered by middle Miocene calcarenites ("Arenarie e calcari di S. Urbano" [20]), the top of the Eocene and the Oligocene are most probably eroded and/or non-deposited [13,21,22,26].

© 2025 by the author(s). Distributed under a Creative Commons CC BY license.

Preprints.org (www.preprints.org) | NOT PEER-REVIEWED | Posted: 24 June 2025 doi:10.20944/preprints202506.1471.v2

Peer-reviewed version available at Geosciences 2025, 15, 334; doi:https://doi.org/10.3390/geosciences15090334

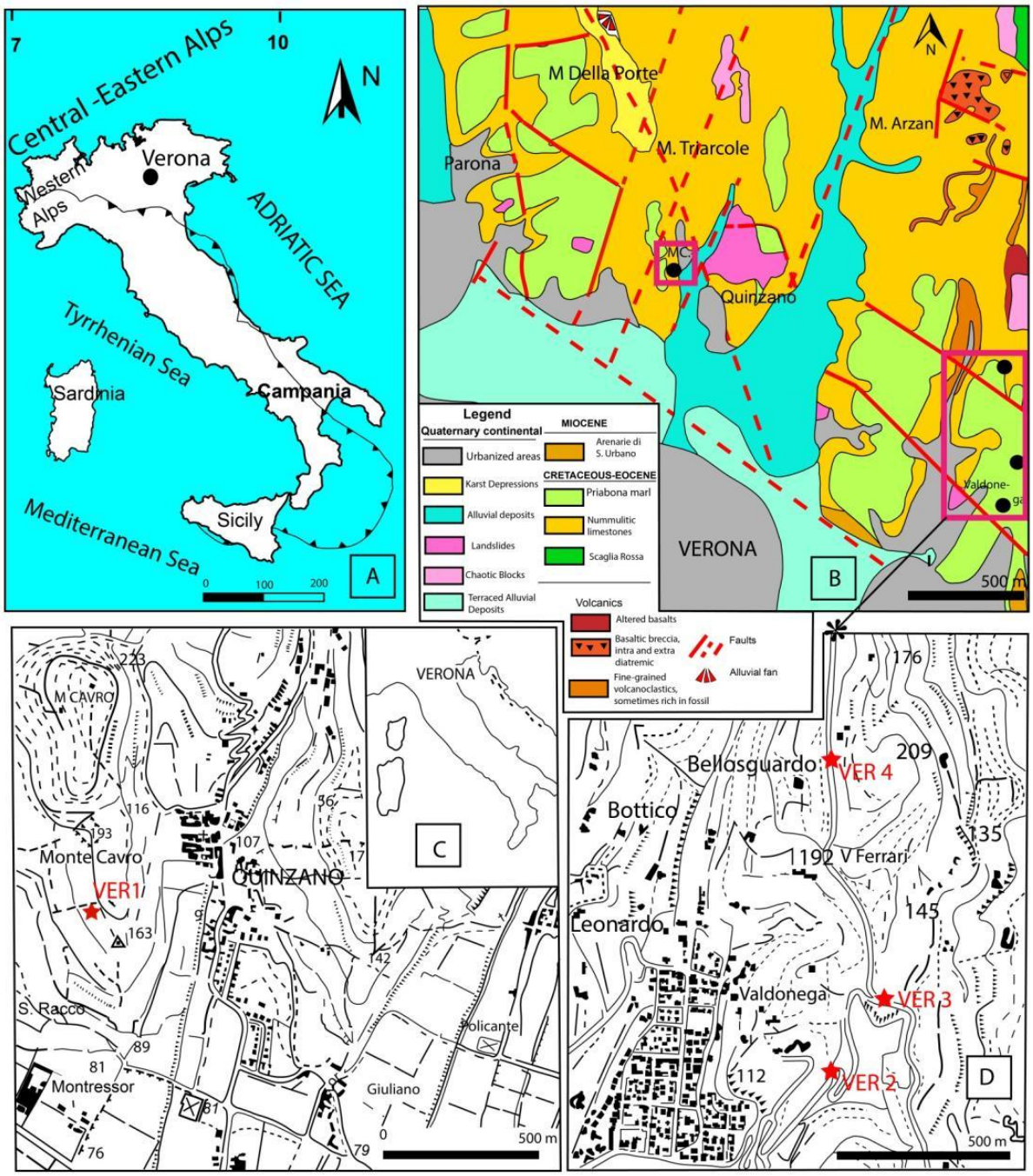


**Figure 1.** Location maps with sample locations, A: Map of Italy showing the location of Verona, B: geology map of the vicinity of Verona (N Italy) and locations of the studied samples: VER 1 (Monte Cavro 4), and VER 2–4 (Castel S. Felice) [23], slightly modified, C: topographic map of the vicinity of Monte Cavro with the location of the sample VER 1, D: topographic map of the vicinity of Verona, Castel San Felice with the location of the samples VER 2–4.

## 3. Previous LBF Studies from the Vicinity of Verona

The Eocene larger foraminifera from the Verona area were subject of several studies, starting at least from the 19th century [27–29]. These papers, however, contain only faunal lists, and lack descriptions and illustrations of LBF. Later, in the early 20th century [30] widely treated the Veronese Eocene in the frame of the whole Veneto area and gave also only faunal lists. [26] already focused strictly on the vicinity of Verona and reported, for the Eocene, the presence of "*Nummulites perforata*" (= *N.* ex gr. *perforatus*) and "*N. complanata*" (= *N.* ex gr. *millecaput*) from the "strati di S. Giovanni

© 2025 by the author(s). Distributed under a Creative Commons CC BY license.

Preprints.org (www.preprints.org) | NOT PEER-REVIEWED | Posted: 24 June 2025 doi:10.20944/preprints202506.1471.v2

Peer-reviewed version available at Geosciences 2025, 15, 334; doi:https://doi.org/10.3390/geosciences15090334

Ilarione" (Lutetian), the "*Nummulites* cfr. *Brongniarti*" (= *N. brongniarti*) and "*N. contorta*" (= *N. striatus*) from the "strati di Roncà" (Bartonian), and "*Orthophragmina ephippium*" (= *Discocyclina* spp.) from the "strati di Priabona" (Priabonian)

In concentrating on the systematics of orthophragmines Paul Brönnimann used also material from the Priabona marl of Verona, Castel San Felice. He presented excellent photos and drawings on *Aktinocyclina radians* ([31], re-evaluated as *Discocyclina radians labatlanensis* by [5]) and on *D.* aff. *varians* ([32], re-evaluated as *D. dispansa umbilicata* by [5]). According to our recent studies, however, these re-evaluations are questionable, since there is a contradiction between the enlargements of drawings and photographs of the same individuals in Brönnimann's publications above. If we consider the magnifications given for the drawings, then the correct re-evaluation is *D. radians radians* and *D. dispansa dispansa*, respectively. This is confirmed by the fact that the dimensions in the text [31] confirm the magnifications given in the drawings.

Lukas Hottinger and Hans Schaub used the description and geological map in [26] for investigating the alveolines [33] and nummulitids [34,35] from Calcari nummulitici, which they subdivided into three parts. The lower part (Calcaire de la Vallé Gallina) is attributed to the middle-late Cuisian (late Ypresian) based on *Alveolina indicatrix*, *Nummulites* aff. *nitidus*, *N.* aff. *irregularis*, *N.* cf. *distans* and *Assilina* aff. *laxispira*. The middle part (Calcaire d'Avesa) is attributed to the middle-upper Lutetian based on *Alveolina munieri*, *A.* aff. *munieri*, *A.* aff. *prorrecta*, *A.* cf. *elliptica nuttalli*, *Nummulites crassus*, *N.* aff. *crassus*, *N.* aff. *meneghinii*, *N. lorioli*, *N. alponensis*, *N.* cf. *millecaput*, *N. discorbinus*, *N.* aff. *biarritzensis*, *Assilina exponens* and *A. gigantea*. They are marked as key LBF assemblage for the SBZ 15 Zone in [3]. The upper part of Calcari nummulitici (Calcaire à Algues) is attributed to the Biarritzian (=Bartonian) based on *Alveolina fragilis*, *Nummulites* cf. *perforatus*, *N.* cf. *dufrenoyi*, *N. lyelli* and *N. brongniarti* (this latter is only in [34]).

Ref. [36] studied the sedimentological aspects of Calcari nummulitici in detail and interpreted it as a nummulitic bank in general. They mostly repeated the list of nummulitids by [34] with the addition of some other forms. This fauna has, however, never been taxonomically described and illustrated.

An unpublished MSc thesis [23], conducted under the supervision of the late Prof. Achille Sirotti, identified from the Priabona Marl of this area *Nummulites chavannesi*, *N. cunialensis*, *N. fabianii*, *N. incrassatus*, *N. pulchellus*, *N. stellatus*, *Operculina alpina*, *O. canalifera gomezi*, *Spiroclypeus granulosus*, *Grzybowskia reticulata*, *Pellatispira madaraszi*, *Discocyclina aspera*, *D. augustae*, *D. sella*, *Aktinocyclina radians*, *Orbitoclypeus nummuliticus*, *Asterocyclina stella*, *A stellaris*, *A stellata*, and *A taramellii*. [23] concluded that here the transition between the middle and upper Eocene (= Bartonian–Priabonian) is continuous, differently that in the Priabona stratotype; however, he also noticed that the transition is often not visible because of the detritus or vegetation cover.

In the frame of the study of nummulite biostratigraphy at the Middle/Upper Eocene boundary [25] investigated also the Monte Cavro sequence representing the uppermost part of Calcari nummulitici. According to them the lower part (samples MC 1–3) containing still giant *Nummulites* (*N. biedai*) belongs to their *N. biedai* Zone. The other LBF in these samples are *N. chavannesi*, *N. hormoensis*, *N.* cf. *hormoensis*, *N. stellatus*, *N. striatus*, *N. variolarius/incrassatus*, *Operculina* aff. *alpina*, *Heterostegina reticulata*, *Discocyclina discus*, *D. pratti*, *Orbitoclypeus varians*, *O.* sp., *Asterocyclina stella*, *A.* sp., *Asterigerina* sp., *Calcarina* sp., *Fabiania* sp., *Gypsina linearis*, *G.* sp., *Haddonia heissigi*, *Silvestriella tetraedra* and *Sphaerogypsina globula*. Giant *Nummulites* are already absent in the upper part (samples MC 4 and 5), and the LBF fauna (belonging already to the *Nummulites variolarius/incrassatus* Zone) is much poorer. Beside the nominate taxon it consists also of *N.* cf. *hormoensis*, *N. striatus*, *Orbitoclypeus* sp., *Asterigerina* sp., *Gypsina linearis*, G. sp., *Silvestriella tetraedra* and *Sphaerogypsina globula*. [25] stated that the *N. biedai* Zone still represents the Middle Eocene (Bartonian), the *N. variolarius/incrassatus* Zone, however, can be arranged both into the Middle and Upper Eocene.

It is clear from the above that the LBF from Calcari nummulitici have been studied more intensively than those from the Priabona marl. Therefore, in this article we focus on the latter. This work has already begun with [37,38]. Nummulitids (*Heterostegina* and *Spiroclypeus*, respectively) with

© 2025 by the author(s). Distributed under a Creative Commons CC BY license.

Preprints.org (www.preprints.org) | NOT PEER-REVIEWED | Posted: 24 June 2025 doi:10.20944/preprints202506.1471.v2

Peer-reviewed version available at Geosciences 2025, 15, 334; doi:https://doi.org/10.3390/geosciences15090334

secondary chamberlets have been studied from Monte Cavro (sample MC 4, see above) and from the Priabona Marl near Castello San Felice on the northern edge of Verona. The results are summarized and briefly presented in this article as well, since the sites are identical.

## 4. Materials and Methods

### *4.1. Localities*

We examined four sites (Figure 2) representing two levels of the Eocene sequence near Verona. The samples were collected in 1990 by the first and last author of this article under the guidance of the late Dr. Achille Sirotti, former professor at the University of Modena.

Sample Verona (VER) 1 (45° 28′ 10.284″ N, 10° 58′ 14.604″ E) comes from the stratigraphically lower level outcropping in Monte Cavro (just about 4–5 km NNW of Verona), and it is identical with sample Monte Cavro (MC) 4 in [25]. It represents the uppermost part of Calcari nummulitici lacking already giant *Nummulites* and belonging to the *N. variolarius/incrassatus* Zone in the above paper. Isolated LBF specimens can be collected from the weathered surface of the limestone. Small nummulitids dominate over orthophragmines in the LBF assemblage, and almost all specimens from both groups are megalospheric (A-forms).

The other three samples [Verona (VER) 2: hairpin bend – 45° 27′ 12.57″ N, 11° 00′ 26.989″ E; VER 3: Villa Devoto – 45° 27′ 19.146″ N, 11° 00′ 32.335″ E and VER 4: Villa Le Are – 45° 27′ 38.856″ N, 11° 00′ 26.64″ E] come from the overlying Priabona marl, near Castello San Felice, on the northern edge of Verona. The direct transition between the Calcari nummulitici and the Priabona marl is not visible near Verona. The relative stratigraphic position of the three samples cannot be determined in the field. Wash residues contain abundant isolated LBF, among which orthophragmines strongly dominate over nummulitids. In these samples, too, microspheric (B) forms are very rare.

### *4.2. Preparation and Depository*

The identification of nummulitids and orthophragmines (the two most widespread LBF in the Tethyan Eocene, along with alveolinids) is based primarily on their internal features, in addition to their external features. The internal characteristics can best be studied in the equatorial section. This was revealed in the Verona material by snapping the specimens with pliers into two, due to their good or even excellent preservation. The specimens were then stained with purple ink to make the morphology of the equatorial section more visible. The procedure is described in detail in [39]. The two main advantages of the method are: (i) it is very productive and (ii) it exposes the equatorial layer perfectly, along the weakest surface containing stolons; thus, they become visible. Meanwhile, since the equatorial layer is never completely flat, this can cause sharpness problems when photographing.

All equatorial sections were photographed and measured in the Geological Department of the University of Miskolc using the microscopes Discovery.V20 and Imager. A2m (Zeiss) and the Axio Vision SE 64 Rel.4.8 software.

Figured specimens prefixed by E. are stored in the Eocene collection of the Supervisory Authority for Regulatory Affairs of Hungary (formerly Geological Institute of Hungary) in Budapest.

### *4.3. Taxon Determination*

Recently, there has been a general agreement among LBF experts working on different groups on the existence of long-lived evolutionary lineages. There are two different approaches to their treatment (see also [9]). Representatives of the Basel School [33,35,40,41] working mainly in the Eocene [where in the case of all three major LBF groups (i.e., nummulitids, orthophragmines and alveolinids) a considerable number of co-occurring evolutionary lineages run parallel] use a typological approach. They use this method not only for the separation of lineages but also for the characterization of the evolution within them. In this approach a lineage is a succession of typical

© 2025 by the author(s). Distributed under a Creative Commons CC BY license.

Preprints.org (www.preprints.org) | NOT PEER-REVIEWED | Posted: 24 June 2025 doi:10.20944/preprints202506.1471.v2

Peer-reviewed version available at Geosciences 2025, 15, 334; doi:https://doi.org/10.3390/geosciences15090334

forms each including the holotype and the population from the type locality as well. Hence, these types (interpreted as distinct species) serve as central, favored moments of the development of the given evolutionary lineage and the related populations from other sites are grouped around them.

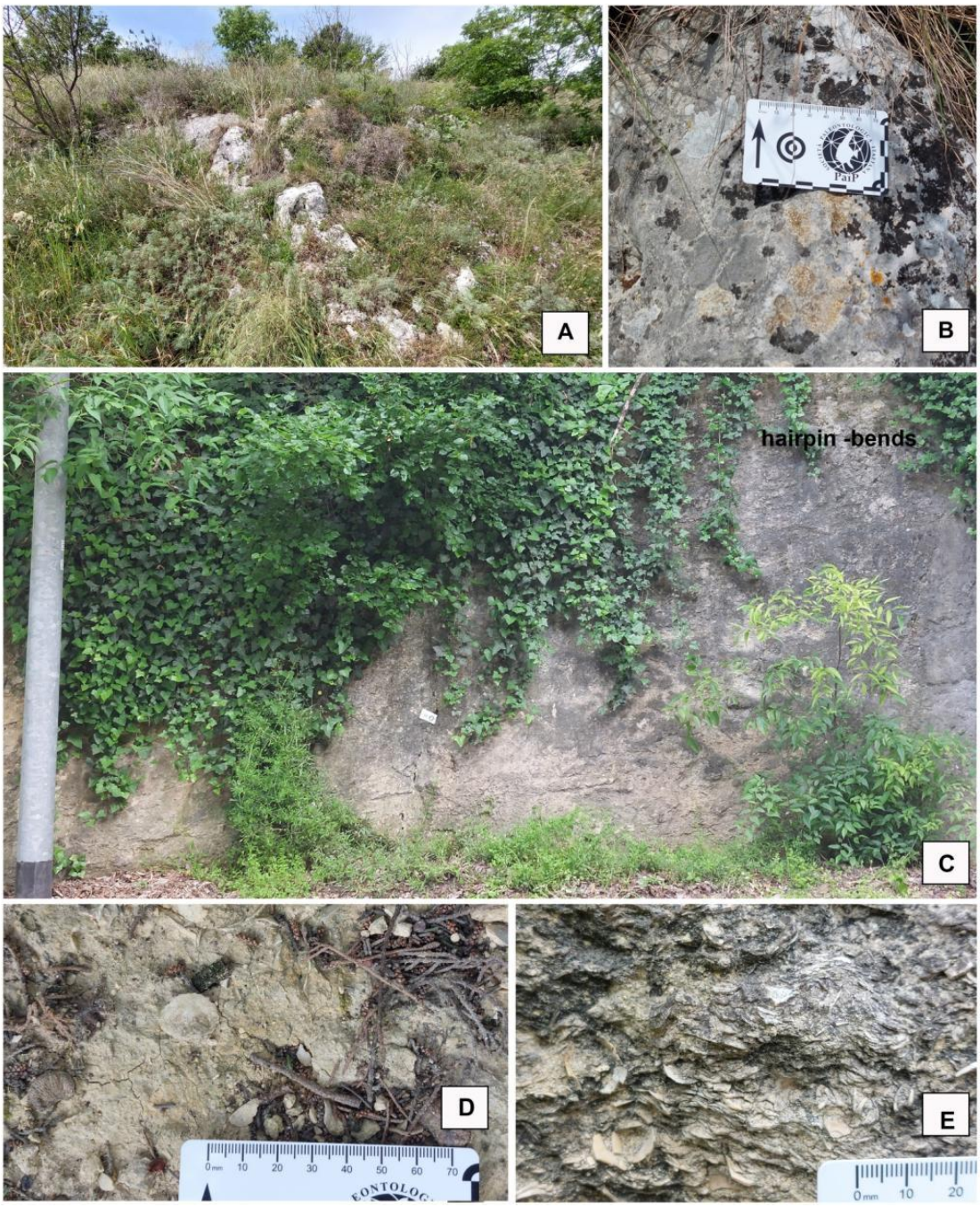


**Figure 2.** Photos of sampling sites. A–B. Monte Cavro, site VER 1: A. general view; B. close-up view. C–E. Castel San Felice: C. general view of site VER 2, hairpin bend; D. close up view of site VER 3, Villa Devoto; E. close-up view of site VER 4, Villa le Are. Photos: C.A. Papazzoni (2025).

In contrast, the morphometric Utrecht School (working mainly in the Upper Cretaceous and Oligo-Miocene where only very few lineages of particular genera run parallel) does not characterize the evolution with the help of "central moments" but subdivides it by artificial limits using a well-measurable, rapidly evolving quantitative parameter of the given lineage (as summarized in [42]). Simultaneously, the existence of numerous simultaneously running evolutionary lineages in the Eocene was questioned [42,43], which was considered as an artifact of the typological method using

© 2025 by the author(s). Distributed under a Creative Commons CC BY license.

Preprints.org (www.preprints.org) | NOT PEER-REVIEWED | Posted: 24 June 2025 doi:10.20944/preprints202506.1471.v2

Peer-reviewed version available at Geosciences 2025, 15, 334; doi:https://doi.org/10.3390/geosciences15090334

many discriminating ("yes/no") qualitative parameters instead of the quantitative ones used in the morphometric method.

In revising Tethyan orthophragmines the above two methods were combined by the typological separation of lineages and their morphometrical subdivision [5,6]. Responding to the criticism by [42], in a case-study from the late Ypresian site of Horsarrieu (SW France) [44] showed the co-occurrence of numerous lineages both typologically and morphometrically. With this, [44] certified the validity of the much quicker typological method in this respect and gave therefore priority to it. At the same time the morphometric method appears to be much more objective in subdividing the lineages, thus it is highly recommended in this respect.

In practice, this means that (according to the protocol by [42]) the LBFs in each sample are determined in three steps (experienced experts usually perform the first two steps at once). In the first step, the specimens are typologically grouped into populations whose members are clearly distinguishable from specimens of other populations in the same sample.

Since in most cases these populations are members of a lineage or phylum, in the second step the populations are typologically identified with these lineages (by units, not by individuals). Experienced experts perform the first two steps usually at once. In the case of orthophragmines and genus *Heterostegina*, the lineages correspond to species, while in the case of nummulitids (other than *Heterostegina*) they constitute a series of chronospecies.

Then, in the third step, the evolutionary degree of the given populations within the corresponding lineage is estimated morphometrically. Many lineages are used for biostratigraphic purposes after being artificially segmented into chronospecies (or chronosubspecies in the case of orthophragmines and *Heterostegina*) separated by arbitrary biometric boundaries of a characteristic numerical evolutionary parameter.

In some populations, the mean of the defining parameter may be very close (closer than 1 s.e. of the mean) to the limit of two neighboring species/subspecies. In this case we need an intermediate notation in the species/subspecies units, and a two-species/subspecies exemplum intercentrale notation (abbreviated as ex. interc.) is used in which the prevalent species/subspecies unit will be ranked first, the closest specific/subspecific unit in the other as the second part of the determination. If the population consists of only a single specimen, no species/subspecies is determined, in the case of only two or three specimens, the species/subspecies is determined as "cf.". Samples close to each other and containing practically the same assemblages with similar parameters are evaluated both separately and jointly. However, the species/subspecies determination is given for the joint sample.

## 5. Results

The LBF composition of the four samples is shown in Table 1. The assemblage VER 1 (Monte Cavro 4) from the uppermost part of the Calcari nummulitici is the least diverse. Nevertheless, the presence of *Nummulites hormoensis* (typical of SBZ 18) and *Heterostegina reticulata multifida* (typical of SBZ 18C only), taking also into account the absence of the genus *Spiroclypeus* (first reported in SBZ 19) are crucial in the definition of SBZ 18C Subzone [3,8,37,45]. In [3,37], the SBZ 18C is still placed in the late Bartonian, but the last paper places it in the earliest Priabonian due to the revision of the Bartonian/Priabonian boundary [46,47]. Since orthophragmines are rare in the VER 1 sample, it cannot be precisely placed within the orthophragmine zonation in [5,6]. Based on the composition of the LBF, in which nummulitids dominate over orthophragmines, this sample represents a relatively protected, low-energy inner platform environment [25].

The LBF assemblages of the overlying Marne di Priabona (samples VER 2–4 from the Castel San Felice area) differ significantly from that of sample VER 1. The LBF fauna of the three samples is very similar (especially in samples VER 3 and 4), in the diverse assemblages orthophragmines strongly dominate over nummulitids, suggesting an outer platform environment. Sample VER 2 differs from the other two in three respects. These are: (i) the presence of reticulate *Nummulites* (*N. fabianii*), (ii) the presence of *Discocyclina euaensis*, which is replaced by *D. dispansa* in samples VER 3 and 4, and (iii) the evolutionary degree of *Orbitoclypeus varians*, which is slightly less advanced in sample VER 2

© 2025 by the author(s). Distributed under a Creative Commons CC BY license.

Preprints.org (www.preprints.org) | NOT PEER-REVIEWED | Posted: 24 June 2025 doi:10.20944/preprints202506.1471.v2

Peer-reviewed version available at Geosciences 2025, 15, 334; doi:https://doi.org/10.3390/geosciences15090334

(with *O. v. scalaris*) than in the other two samples (with *O. v. varians*). However, the latter does not necessarily mean that sample VER 2 is slightly older than the other two, since at the same time *Heterostegina reticulata mossanensis* appears to be slightly less developed in the VER 3 and 4 samples. Thus, their relative stratigraphic position cannot be clearly assessed.

**Table 1.** Distribution of LBF in the studied early Priabonian samples from Verona. +: common, ×: sporadic.

| Locality | Sample | *Discocyclina augustae augustae* | *D. dispansa dispansa* | *D. euaensis* | *D. pratti minor* | *D. radians* cf. *radians* | *D. trabayensis elazigensis* | *Nemkovella strophiolata tenella* | *N. daguini* | *Orbitoclypeus varians scalaris* | *O. varians varians* | *Asterocyclina alticostata* indet. ssp | *A. alticostata danubica* | *A. stellata* cf. *stellaris* | *A. stellata stellaris* | *Nummulites hormoensis* | *N. fabianii* | *N. chavannesi* | *N. incrassatus* | *N. budensis* | *N. pulchellus* | *Assilina alpina* | *Operculina* ex gr. *gomezi* | *Heterostegina reticulata multifida* | *H. reticulata mossanensis* | *Spirocypeus sirottii* |
|---|---|---|---|---|---|---|---|---|---|---|---|---|---|---|---|---|---|---|---|---|---|---|---|---|---|---|
| M. Cavro | VER 1 | | | | | | | | | | | × | | × | | + | | | + | × | | | | + | | |
| Castel San Felice | VER 2 | + | | + | | | × | + | | × | | | × | | + | | + | + | + | × | | × | | | + | + |
| | VER 3 | + | + | | | | × | + | | | × | | × | | + | | | × | × | | | + | × | | + | + |
| | VER 4 | + | + | | + | × | + | + | × | | + | | × | | + | | | × | | | × | + | × | | + | + |

Although they are in minority in samples VER 2–4, nummulitids play a key role in determining the SBZ 19A Subzone (as defined in the papers listed two paragraphs up). These samples already contain *Spiroclypeus sirottii* (first reported from SBZ 19), *Heterostegina reticulata mossanensis* (SBZ 19A only) and *Nummulites fabianii* (SBZ 19 and 20). The latter two taxa replace *H. r. multifida* and *N. hormoensis* from sample VER 1. All other nummulitids are very rare (especially in sample VER 4) and occur in both older and younger strata, so their stratigraphic significance is limited. Considering the revision of the Bartonian/Priabonian boundary [46,47], the SBZ 19A Subzone corresponds to the early (but not to the earliest as it was earlier suggested in [3]) Priabonian [8].

The rich and diverse orthophragmine assemblage is characteristic of the OZ 14 Zone [5,6]. Considering [7] and the latest, yet unpublished data of the second author, *Discocyclina pratti minor* and *Nemkovella strophiolata tenella* are almost exclusively known only from this zone. This zone is also marked by the lowest occurrence of *D. augustae augustae*, *D. trabayensis elazigensis*, *D. euaensis* and *Asterocyclina alticostata danubica*, and the highest one of *D. dispansa dispansa*, and *Orbitoclypeus varians scalaris*. *Nemkovella daguini*, *A. stellata stellaris* and *O. v. varians* are known from both older and younger strata. The presence of *D. radians* cf. *radians* (represented by only two specimens) is stratigraphically irrelevant (further details in the systematical part). The stratigraphic range of the OZ 14 zone is relatively long, covering the latest Bartonian to early Priabonian interval from the base of the SBZ 18 Zone to the top of the SBZ 19A Subzone [8,45].

## 6. Systematical Part

Order Foraminiferida Eichwald, 1830

LBFs listed in Table 1. belong to three different families, namely Discocyclinidae, Orbitoclypeidae, and Nummulitidae. Due to their morphological similarity and joint occurrence, the first two are often grouped informally under the name of orthophragmines. Their taxa as well as those of nummulitids are described below.

© 2025 by the author(s). Distributed under a Creative Commons CC BY license.

Preprints.org (www.preprints.org) | NOT PEER-REVIEWED | Posted: 24 June 2025 doi:10.20944/preprints202506.1471.v2

Peer-reviewed version available at Geosciences 2025, 15, 334; doi:https://doi.org/10.3390/geosciences15090334

*6.1. Orthophragmines*

Late Paleocene and Eocene orbitoidal larger foraminifera with almost rectangular equatorial chamberlets constitute two systematically independent families, namely Discocylinidae Galloway, 1928 and Orbitoclypeidae Brönnimann, 1945, based on the significantly different microspheric juvenarium of their B-forms [32]. Their morphostructure is otherwise quite similar (for details see [5,7,32,42,48–53]). Therefore, and because these probable symbiont-bearing benthic forms can be found together at least in the peri-Mediterranean region (commonly in the deeper part of the photic zone, i.e., basinward adjacent to the restricted shallow-water environments or transported into deep-marine settings), orthophragmines, an informal collective name, is used to refer to both groups.

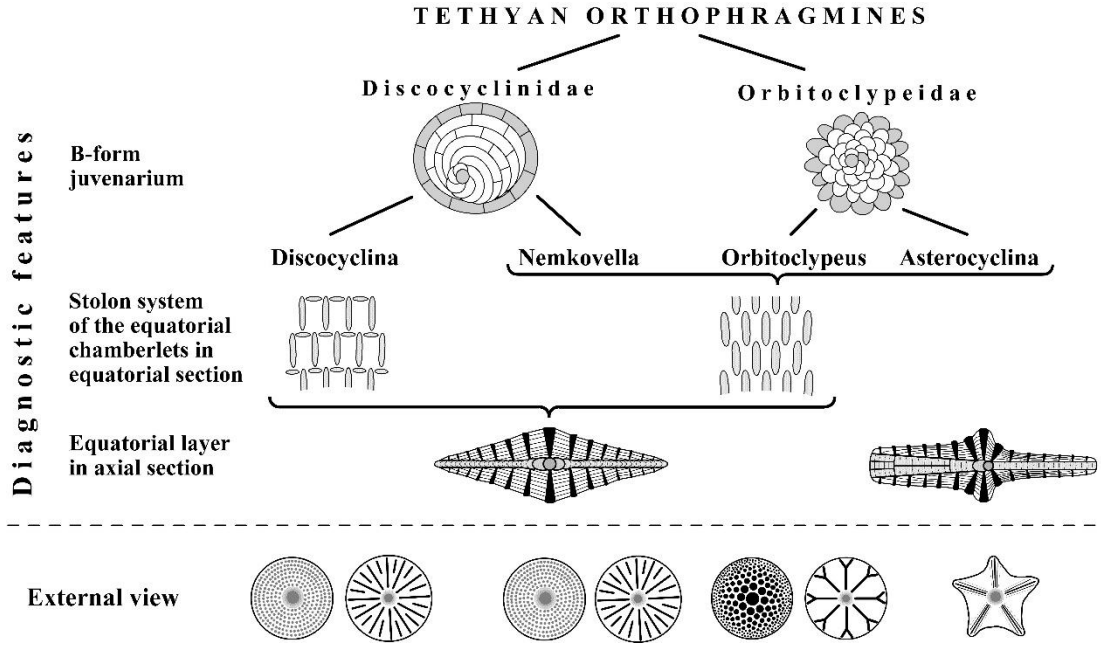


**Figure 3.** Features separating Tethyan orthophragmine families and genera [55].

In the peri-Mediterranean region, Discocyclinidae are represented by two genera: *Discocyclina* Gümbel, 1870 and *Nemkovella* Less, 1987. *Discocyclina* can be distinguished from *Nemkovella* by the presence of annular stolons in the equatorial chamberlets. Orbitoclypeidae have also two genera in this region; *Orbitoclypeus* Silvestri, 1907 and *Asterocyclina* Gümbel, 1870. *Asterocyclina* is differentiated from *Orbitoclypeus* by having an equatorial layer axially subdivided within the ribs. A synoptic summary for distinguishing the four peri-Mediterranean genera is shown in Figure 3. Therefore, ribbing is useful taxonomically only on the specific level (further details in [5,50,54]). [7,53] distinguished also the genus *Hexagonocyclina* within Orbitoclypeidae based on the primitive periembryonal morphology of A-forms.

However, we believe that this feature is not significant enough to distinguish it as a separate genus, and we therefore place these forms in *Orbitoclypeus*. [56] separated the new genus *Virgasterocyclina* from *Asterocyclina* based on the presence of radially thickened lateral walls, i.e., rods, along the ribs. However, this feature appears independently in the peri-Mediterranean Priabonian and also in the American–Caribbean Middle–Upper Eocene, in phylogenetically clearly different *Asterocyclinae*. Therefore, we prefer to keep these forms within *Asterocyclina*.

All four Tethyan genera consist of several, long-living, simultaneously running evolutionary lineages considered to be species in the practice of Tethyan orthophragmines. These species very often coexist in particular samples, in which they are distinguished typologically, by the combination of some clearly qualitative features, such as the external shape (i.e., the presence/absence of ribs and bulges) and other characteristics (Figure 4) that are (excepting the type of rosette) recognizable in the equatorial section of the A-forms. Therefore, the significance of microspheric forms (constituting only

© 2025 by the author(s). Distributed under a Creative Commons CC BY license.

Preprints.org (www.preprints.org) | NOT PEER-REVIEWED | Posted: 24 June 2025 doi:10.20944/preprints202506.1471.v2

Peer-reviewed version available at Geosciences 2025, 15, 334; doi:https://doi.org/10.3390/geosciences15090334

about 1–10% of most of the populations) is subordinate in the specific determination. Some primarily quantitative features (that are in fact evaluated qualitatively and, therefore, recognizable immediately by an experienced expert) are also used in species determination. These are the dimension of the A-form embryo and the shape and width of equatorial chamberlets. Most of the species constitute long-living evolutionary lineages with definite internal development that allows their morphometric subdivision into artificial subspecies (for theoretical background see [42]).

These subspecies are defined by biometric limits of the populational means of the outer cross diameter of the deuteroconch (the second chamber of the A-form embryo) in equatorial section (marked by "d", see Figure 5) [5]. This quantitative feature has been chosen from among several other evolutionary parameters because it is most easily and objectively measurable and because it reveals the fastest and the least variable evolutionary progress [6].

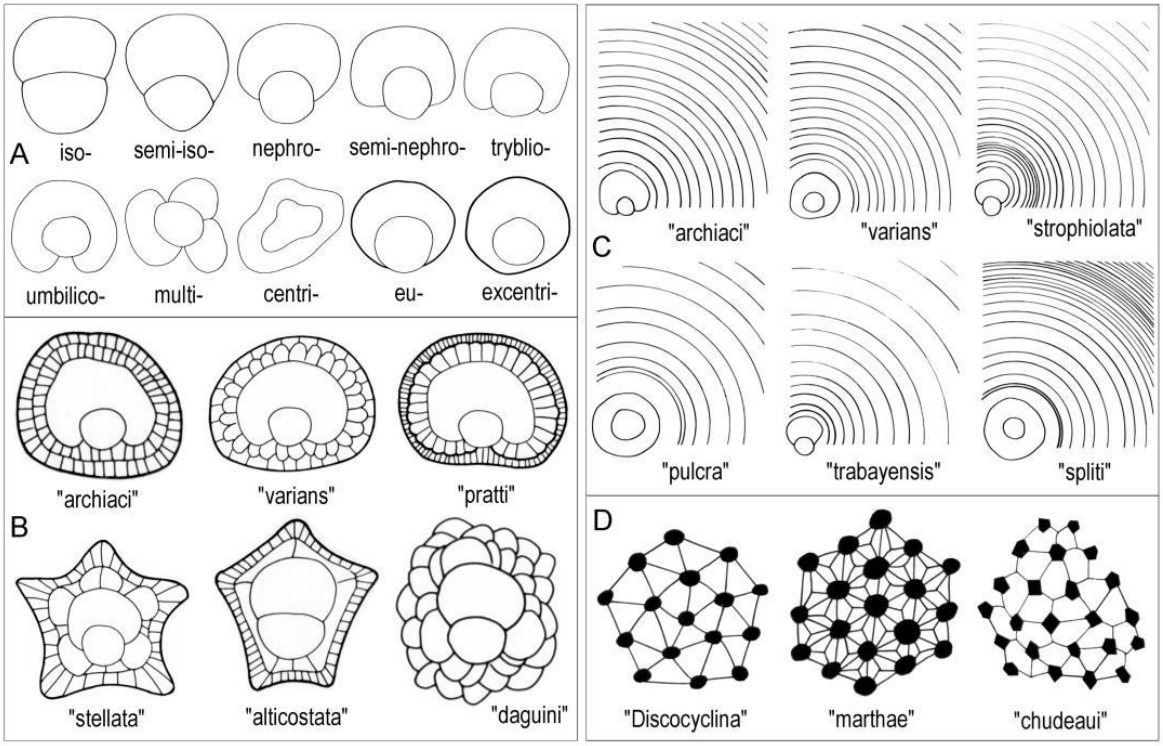


**Figure 4.** Qualitative features of Tethyan orthophragmines. A: Different embryo types (suffix "-lepidine" is to be added to each type); B: Different types of the adauxiliary chamberlets; C: Different growth patterns of the equatorial annuli; D. Different types of the rosette (the network of piles and lateral chamberlets on the test's surface).

Other parameters, shown in Figure 5 are used to describe taxa in detail. They can be very useful to validate determinations in dubious cases. As the orthophragmine assemblage of Castel San Felice is exceptionally diverse and may serve as a key assemblage for the OZ 14 Zone, in this paper we perform a full morphometric analysis to characterize the taxa as completely as possible. It consists of eight measurements and counts in the equatorial section of megalospheric (A) forms as listed below and shown in Figure 5 as well. Morphometric data are summarized in Tables 2–4.

- p and d: outer diameter of the protoconch and deuteroconch perpendicular to their common axis (in μm);
- I and J: outer circumference of the protoconch embraced (I) and not embraced (J) by the deuteroconch;
- N: number of the adauxiliary chamberlets (in Figure 5, N=15);
- H: characteristic height of undeformed adauxiliary chamberlets (in μm);

© 2025 by the author(s). Distributed under a Creative Commons CC BY license.

Preprints.org (www.preprints.org) | NOT PEER-REVIEWED | Posted: 24 June 2025 doi:10.20944/preprints202506.1471.v2

Peer-reviewed version available at Geosciences 2025, 15, 334; doi:https://doi.org/10.3390/geosciences15090334

- n: characteristic number of annuli within 0.5 mm distance measured from the edge of the deuteroconch (in Figure 5, n≈6.7);
- w: characteristic width of the equatorial chamberlets around the peripheral part of the equatorial layer (in μm).

Six of these parameters (p, d, N, H, n and w) are used directly, while five other ones are calculated as follows:

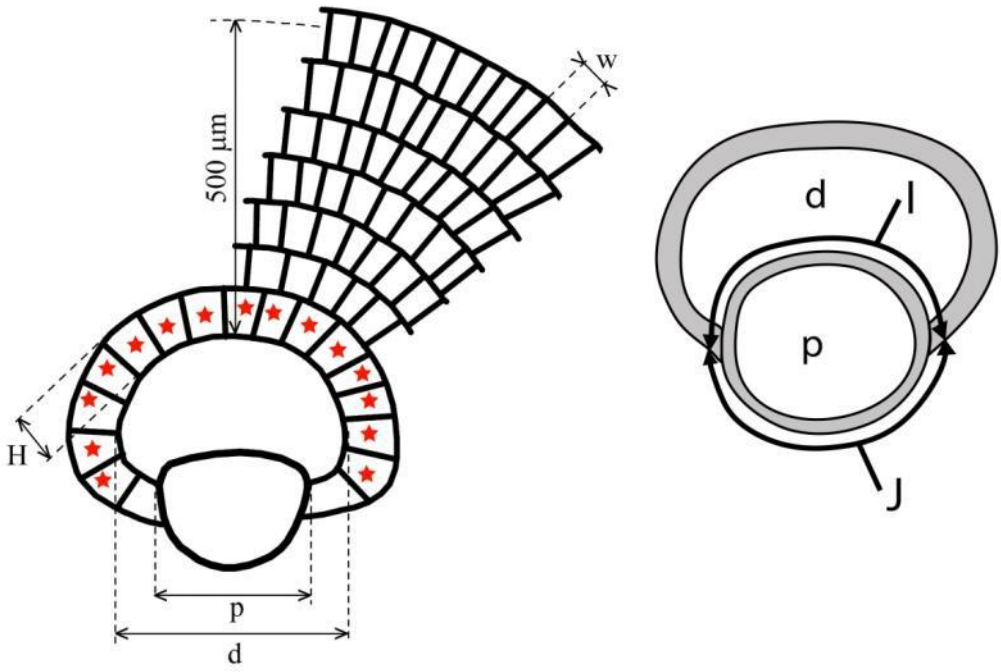


**Figure 5.** Mesurement system for orthophragmines.

- W: estimated width of the adauxiliary chamberlets (in μm) calculated as W=[(d+H)×π–p]/(N+1);
- F: estimated shape of the adauxiliary chamberlets (in %) calculated as F=100×H/(H+W);
- h: estimated height of the equatorial chamberlets close to the embryo (in μm) calculated as h=(500–H)/(n–1);
- G: estimated shape of the equatorial chamberlets close to the embryo (in %) calculated as G=100×h/(h+w).

6.1.1. Family Discocyclinidae Galloway, 1928

Two genera, namely *Discocyclina* and *Nemkovella*, are recorded from Verona. The diagnostic difference between them is the presence (*Discocyclina*) and absence (*Nemkovella*) of proximal annular stolon.

Genus Discocyclina Gümbel, 1870

Representatives of six species of this genus were found in the three samples of Verona, Castel San Felice. For comparison, they are shown together at the same magnification in Figure 6 and Figure 7.

*Discocyclina augustae* van der Weijden, 1940

This very common unribbed species is usually small and flat. It has a very small to small, semi-iso- to nephrolepidine embryo, narrow and low, “archiaci” type adauxiliary chamberlets and also narrow and relatively low equatorial chamberlets mostly with “strophiolata” type growth pattern.

© 2025 by the author(s). Distributed under a Creative Commons CC BY license.

Preprints.org (www.preprints.org) | NOT PEER-REVIEWED | Posted: 24 June 2025 doi:10.20944/preprints202506.1471.v2

Peer-reviewed version available at Geosciences 2025, 15, 334; doi:https://doi.org/10.3390/geosciences15090334

*Discocyclina augustae* forms an evolutionary lineage with four chrono-subspecies such as: *D. a. sourbetensis* ($d_{mean}$ < 145 μm; SBZ 8–13; OZ 4–?9), *D. a. atlantica* ($d_{mean}$=145–180 μm; SBZ 13–17; OZ 9–12), *D. a. olianae* ($d_{mean}$=180–225 μm; SBZ 17–19a; OZ 12–14) and *D. a. augustae* ($d_{mean}$ > 225 μm; SBZ 18c–20; OZ 14–16) [6,7].

This species is the most common one in all three samples (VER 2–4) from Verona Castel San Felice. Their quantitative parameters are very similar (Tables 2–4), therefore they can be jointly evaluated and determined as *Discocyclina augustae augustae*.

*Discocyclina augustae augustae* van der Weijden, 1940

Figure 6: B, Figure 7, Figure 8: A–L, Figure 9.

*Discocyclina (Discocyclina) augustae* n. sp. — [57]: 23–26, Plate 1: 4, 5, 7, 8, Plate 2: 1, 2, 11.

*Discocyclina augustae augustae* van der Weijden. — [5]: 155–156, Plate 10: 5–6, 8–12, Plate 11: 1–4. (with synonymy). — [58]: 689, Plate 4: 5–11. — [59]: Plate 1: 3, 4. — [7]: Figure 52.13.

Remarks. *Discocyclina augustae augustae* and *D. dispansa dispansa* bear very similar qualitative features. *D. a. augustae* differs from *D. d. dispansa* (i) in the smaller embryo (parameters p and d, Table 2), (ii) in the less embraced protoconch by the deuteroconch (parameter A) and the generally lower equatorial chamberlets (parameters n and h). Bivariate plots of Figure 10. also confirm the typological separation of the taxa, although a few specimens appeared quantitatively transitional between the two taxa. The other taxon, which can be confused with *D. a. augustae* is *D. trabayensis elazigensis*. The latter has, however, a significantly smaller embryo, and much less adauxiliary chamberlets (of "varians" type) than for *D. a. augustae* (with "archiaci" type adauxiliary chamberlets) as it is shown on Figure 11. Finally, although the size and type of the embryo is very similar for *D. a. augustae* and *Nemkovella strophiolata tenella*, the equatorial chamberlets of the latter lack proximal annular stolon, therefore they belong to different genera.

*Discocyclina dispansa* (Sowerby, 1840)

This widespread, flat or saddle-shaped, unribbed species has a small to medium-sized, semi-nephro- to trybliolepidine embryo, moderately wide and high, "archiaci" type adauxiliary chamberlets and also moderately wide and high equatorial chamberlets mostly with "strophiolata" or "varians" type growth pattern.

*Discocyclina dispansa* forms an evolutionary lineage with six chrono-subspecies as follows: *D. d. broennimanni* ($d_{mean}$ < 160 μm; SBZ 7–9; OZ 3–4); *D. d. taurica* ($d_{mean}$=160–230 μm; SBZ 10–12; OZ 5–8b); *D. d. hungarica* ($d_{mean}$=230–290 μm; SBZ 12–?17; OZ 8b–?12); *D. d. sella* ($d_{mean}$=290–400 μm; SBZ ?13–18; OZ ?9–14); *D. d. dispansa* ($d_{mean}$=400–520 μm; SBZ 17–19a; OZ 13–14); and *D. d. umbilicata* ($d_{mean}$ > 520 μm; SBZ 19–20; OZ 14–16) [6,7].

This species is a common one in samples VER 3 and 4 from Verona Castel San Felice, however in sample VER 2 it is replaced by *Discocyclina euaensis*. The quantitative parameters in samples VER 3 and 4 are very similar (Tables 2–4), therefore they can be jointly evaluated and determined as *Discocyclina dispansa dispansa*.

*Discocyclina dispansa dispansa* (Sowerby, 1840)

Figure 6: D, Figure 7, Figure 9, Figure 12: A–I.

*Lycophris dispansus* n. sp. — [60]: 327, Plate 24: 16, 16a–b.

*Discocyclina dispansa* (Sowerby). — [61]: 254, 257–259, 262, Plate 3: 1–5, Plate 8: 1, 2, Plate 11: 1–12, Figures 5–7, 11.

*Discocyclina dispansa dispansa* (Sowerby) — [5]: 163–164, Plate 13: 9, 12. Plate 14: 3, 6. (with synonymy). — [55]: Plate 2: 18, Figure 13. — [62]: Figures 28d–f. — [63]: 144, 146, 147, Figures 9B, 10. — [64]: 36, 38, 38, Figures 9, 12, 15, 17. — [65]: Figure 12f. — [7]: Figures 23.3, 4; 30.2,3; 57.5–8, 60.

Remarks. The distinction of *Discocyclina dispansa dispansa* from *D. augustae augustae* is discussed above (see also Figure 10) whereas that from *D. euaensis* can be found below at the latter taxa. *D. d.*

© 2025 by the author(s). Distributed under a Creative Commons CC BY license.

Preprints.org (www.preprints.org) | NOT PEER-REVIEWED | Posted: 24 June 2025 doi:10.20944/preprints202506.1471.v2

Peer-reviewed version available at Geosciences 2025, 15, 334; doi:https://doi.org/10.3390/geosciences15090334

*dispansa* can be safely separated from *D. pratti minor* based on the different type of adauxiliary chamberlets ("archiaci" vs. "pratti" for the latter). Also, the embryo of *D. p. minor* is usually larger, the protoconch is embraced more by the deuteroconch, and the equatorial chamberlets are significantly higher than in the case *D. d. dispansa* (see below).

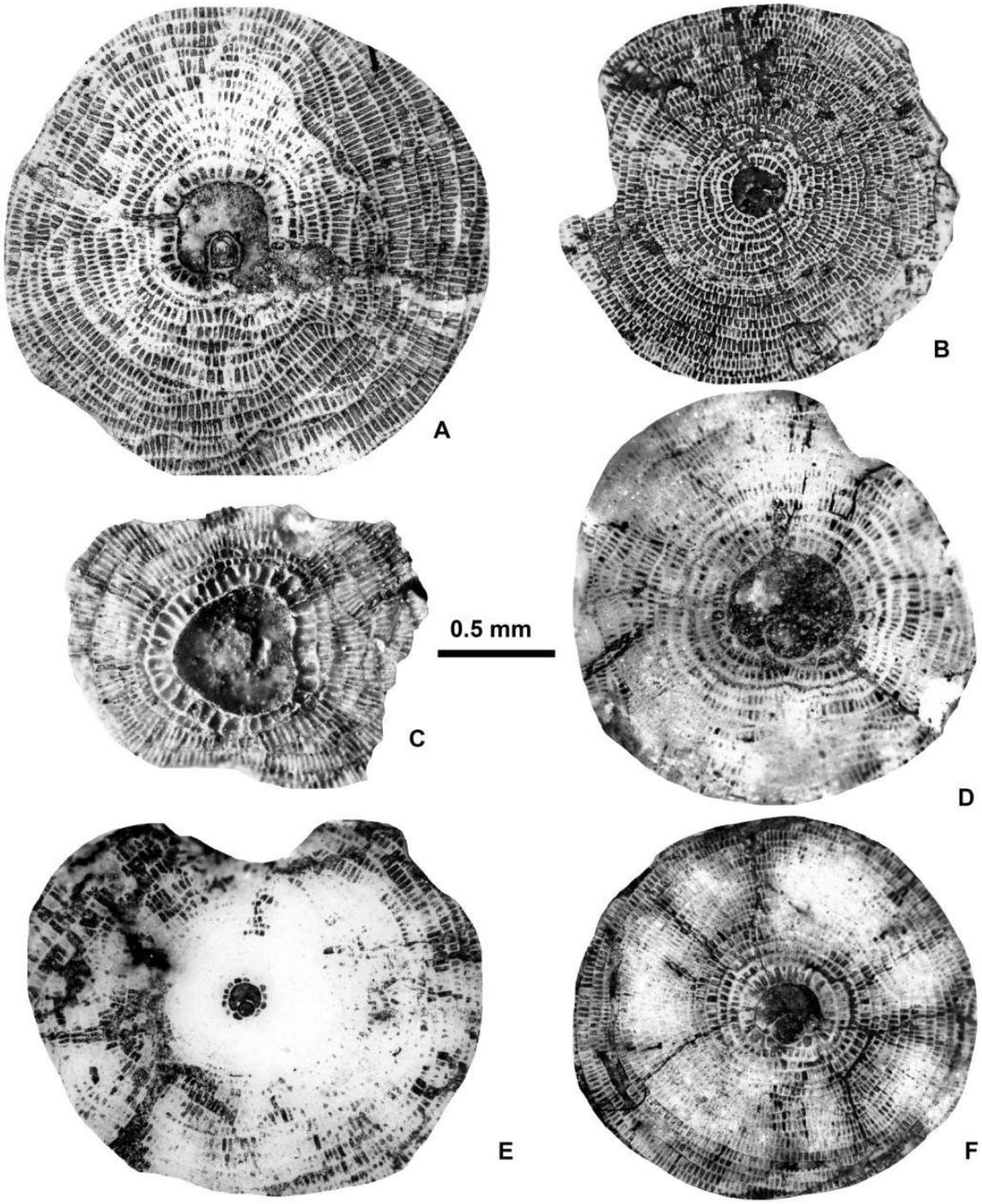


**Figure 6.** Equatorial sections of A-forms of different *Discocyclina* in Castel San Felice, Verona (N Italy). A: *D. euaensis* Whipple, E.2025.44, B: *D. augustae augustae* van der Weijden, E.2025.10, C: *D. pratti minor* Meffert, E.2025.52, D: *D. dispansa dispansa* (Sowerby), E.2025.28, E: *D. trabayensis elazigensis* Özcan & Less, E.2025.57, F: *D. radians* cf. *radians* (d'Archiac), E.2025.56. A, B, E: VER 2; C, F: VER 4; D: VER 3.

© 2025 by the author(s). Distributed under a Creative Commons CC BY license.

Preprints.org (www.preprints.org) | NOT PEER-REVIEWED | Posted: 24 June 2025 doi:10.20944/preprints202506.1471.v2

Peer-reviewed version available at Geosciences 2025, 15, 334; doi:https://doi.org/10.3390/geosciences15090334

**Table 2.** Statistical data of the embryonal part of orthophragmine populations from Verona.

| Parameters | | Outer cross-diameter of the protoconch p (µm) | | | Outer cross-diameter of the deuterococh d (µm) | | | Deuteroconchal embracement A | | | Subspecies |
|---|---|---|---|---|---|---|---|---|---|---|---|
| Species | Sample | № | range | mean ± s.e. | № | range | mean ± s.e. | № | range | mean ± s.e. | |
| *Discocyclina augustae* | **VER 2–4** | **75** | **110 – 195** | **137,4 ± 1,9** | **83** | **170 – 355** | **260,5 ± 4,0** | **75** | **45 – 80** | **60,2 ± 0,8** | *augustae* |
| | VER 2 | 21 | 110 – 155 | 131,2 ± 2,9 | 22 | 180 – 355 | 259,8 ± 7,9 | 22 | 51 – 80 | 62,4 ± 1,6 | |
| | VER 3 | 16 | 120 – 195 | 146,9 ± 5,0 | 18 | 205 – 300 | 270,0 ± 6,0 | 16 | 49 – 68 | 58,8 ± 1,4 | |
| | VER 4 | 38 | 110 – 180 | 136,8 ± 2,5 | 43 | 170 – 335 | 256,9 ± 6,0 | 37 | 45 – 71 | 59,5 ± 1,1 | |
| *D. dispansa* | **VER 3+4** | **30** | **150 – 365** | **245,8 ± 8,2** | **32** | **360 – 655** | **503,8 ± 12,7** | **30** | **60 – 100** | **75,4 ± 1,7** | *dispansa* |
| | VER 3 | 7 | 150 – 260 | 212,9 ± 14,8 | 7 | 360 – 585 | 479,3 ± 34,6 | 7 | 66 – 86 | 76,5 ± 2,7 | |
| | VER 4 | 23 | 195 – 365 | 255,9 ± 8,7 | 25 | 400 – 655 | 510,6 ± 12,7 | 23 | 60 – 100 | 75,1 ± 2,0 | |
| *D. euaensis* | **VER 2** | **24** | **140 – 355** | **199,0 ± 10,2** | **27** | **385 – 715** | **515,6 ± 14,9** | **21** | **66 – 100** | **79,2 ± 1,7** | — |
| *D. pratti* | **VER 4** | **6** | **225 – 340** | **282,5 ± 17,7** | **11** | **500 – 1100** | **778,6 ± 49,4** | **7** | **62 – 100** | **76,7 ± 5,8** | *minor* |
| *D. radians* | **VER 4** | **1** | | **155,0** | **2** | **325 – 375** | **350,0** | **1** | | **56,0** | cf. *radians* |
| *D. trabayensis* | **VER 2–4** | **26** | **60 – 120** | **77,3 ± 2,7** | **25** | **110 – 190** | **137,0 ± 4,0** | **20** | **44 – 73** | **53,2 ± 1,5** | *elazigensis* |
| | VER 2 | 2 | 85 – 120 | 102,5 | 2 | 155 – 160 | 157,5 | 2 | 45 – 54 | 49,2 | |
| | VER 3 | 2 | 65 – 120 | 92,5 | 2 | 130 – 180 | 155,0 | 2 | 56 – 57 | 56,4 | |
| | VER 4 | 22 | 60 – 85 | 73,6 ± 1,3 | 21 | 110 – 190 | 133,4 ± 3,9 | 16 | 44 – 73 | 54,2 ± 1,7 | |
| *Nemkovella strophiolata* | **VER 2–4** | **44** | **100 – 175** | **134,6 ± 2,5** | **48** | **175 – 335** | **235,0 ± 4,3** | **39** | **38 – 67** | **48,8 ± 0,9** | *tenella* |
| | VER 2 | 9 | 100 – 145 | 125,0 ± 5,4 | 13 | 185 – 335 | 238,5 ± 9,6 | 7 | 42 – 67 | 52,5 ± 3,6 | |
| | VER 3 | 7 | 115 – 175 | 144,3 ± 8,0 | 7 | 175 – 285 | 243,6 ± 14,7 | 5 | 38 – 50 | 46,2 ± 1,9 | |
| | VER 4 | 28 | 110 – 160 | 135,3 ± 2,5 | 28 | 195 – 280 | 231,2 ± 4,5 | 27 | 43 – 61 | 48,4 ± 0,8 | |
| *N. daguini* | **VER 4** | **1** | | **60,0** | **1** | | **80,0** | **1** | | **40,0** | — |
| *Orbitoclypeus varians* | **VER 2** | **10** | **180 – 280** | **221,0 ± 8,8** | **10** | **335 – 445** | **375,0 ± 10,2** | **9** | **63 – 100** | **85,8 ± 4,0** | *scalaris* |
| | **VER 3+4** | **27** | **180 – 315** | **235,1 ± 7,8** | **28** | **355 – 580** | **428,0 ± 10,7** | **24** | **60 – 100** | **82,9 ± 2,1** | *varians* |
| | VER 3 | 2 | 225 – 265 | 245,0 | 2 | 355 – 490 | 422,5 | 2 | 62 – 84 | 73,3 | |
| | VER 4 | 25 | 180 – 315 | 234,3 ± 8,3 | 26 | 360 – 580 | 428,5 ± 10,9 | 22 | 60 – 100 | 83,8 ± 2,0 | |
| *Asterocyclina alticostata* | **VER 1** | **1** | | **420,0** | **1** | | **610,0** | **1** | | **40,1** | — |
| | **VER 2–4** | **7** | **260 – 410** | **342,1 ± 22,3** | **7** | **380 – 570** | **472,9 ± 23,0** | **7** | **37 – 55** | **43,0 ± 2,0** | *danubica* |
| | VER 2 | 2 | 280 – 340 | 310,0 | 2 | 415 – 435 | 425,0 | 2 | 40 – 40 | 40,2 | |
| | VER 3 | 2 | 395 – 410 | 402,5 | 2 | 490 – 505 | 497,5 | 2 | 42 – 44 | 43,0 | |
| | VER 4 | 3 | 260 – 410 | 323,3 | 3 | 380 – 570 | 488,3 | 3 | 37 – 55 | 45,0 | |
| *A. stellata* | **VER 1** | **2** | **125 – 145** | **135,0** | **2** | **195 – 205** | **200,0** | **2** | **47 – 47** | **47,2** | cf. *stellaris* |
| | **VER 2–4** | **80** | **100 – 200** | **136,3 ± 2,1** | **83** | **155 – 300** | **211,0 ± 3,0** | **71** | **31 – 64** | **46,7 ± 0,7** | *stellaris* |
| | VER 2 | 26 | 110 – 165 | 136,2 ± 2,8 | 27 | 160 – 270 | 206,3 ± 4,8 | 23 | 31 – 52 | 45,1 ± 1,0 | |
| | VER 3 | 21 | 100 – 165 | 130,7 ± 3,5 | 22 | 175 – 225 | 198,6 ± 3,1 | 18 | 31 – 54 | 44,8 ± 1,3 | |
| | VER 4 | 33 | 100 – 200 | 140,0 ± 3,7 | 34 | 155 – 300 | 222,8 ± 5,4 | 30 | 38 – 64 | 49,1 ± 1,1 | |

© 2025 by the author(s). Distributed under a Creative Commons CC BY license.

Preprints.org (www.preprints.org) | NOT PEER-REVIEWED | Posted: 24 June 2025 doi:10.20944/preprints202506.1471.v2

Peer-reviewed version available at *Geosciences* **2025**, *15*, 334; doi:https://doi.org/10.3390/geosciences15090334

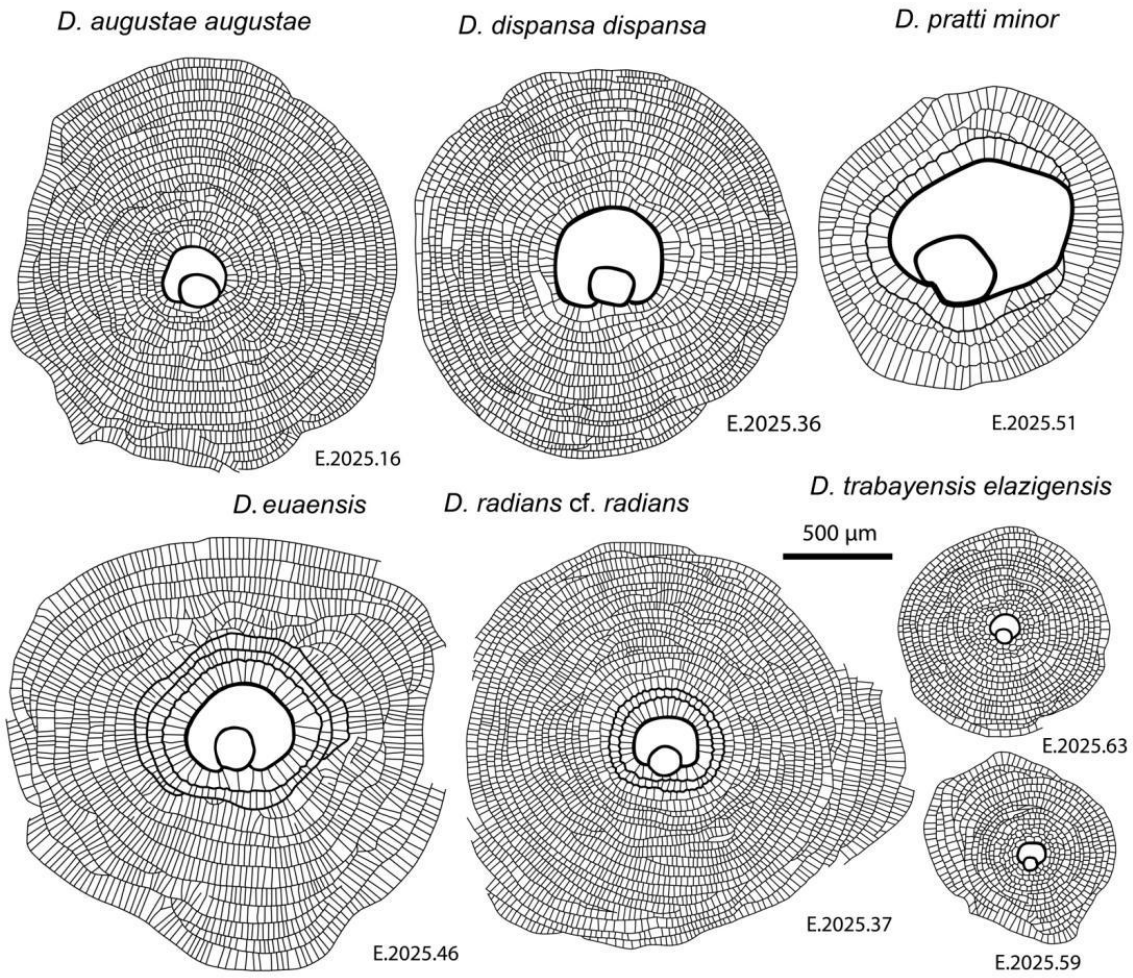


**Figure 7.** Drawings of equatorial sections of different A-forms of *Discocyclina* in Castel San Felice, Verona (N Italy).

© 2025 by the author(s). Distributed under a Creative Commons CC BY license.

Preprints.org (www.preprints.org) | NOT PEER-REVIEWED | Posted: 24 June 2025 doi:10.20944/preprints202506.1471.v2

Peer-reviewed version available at Geosciences 2025, 15, 334; doi:https://doi.org/10.3390/geosciences15090334

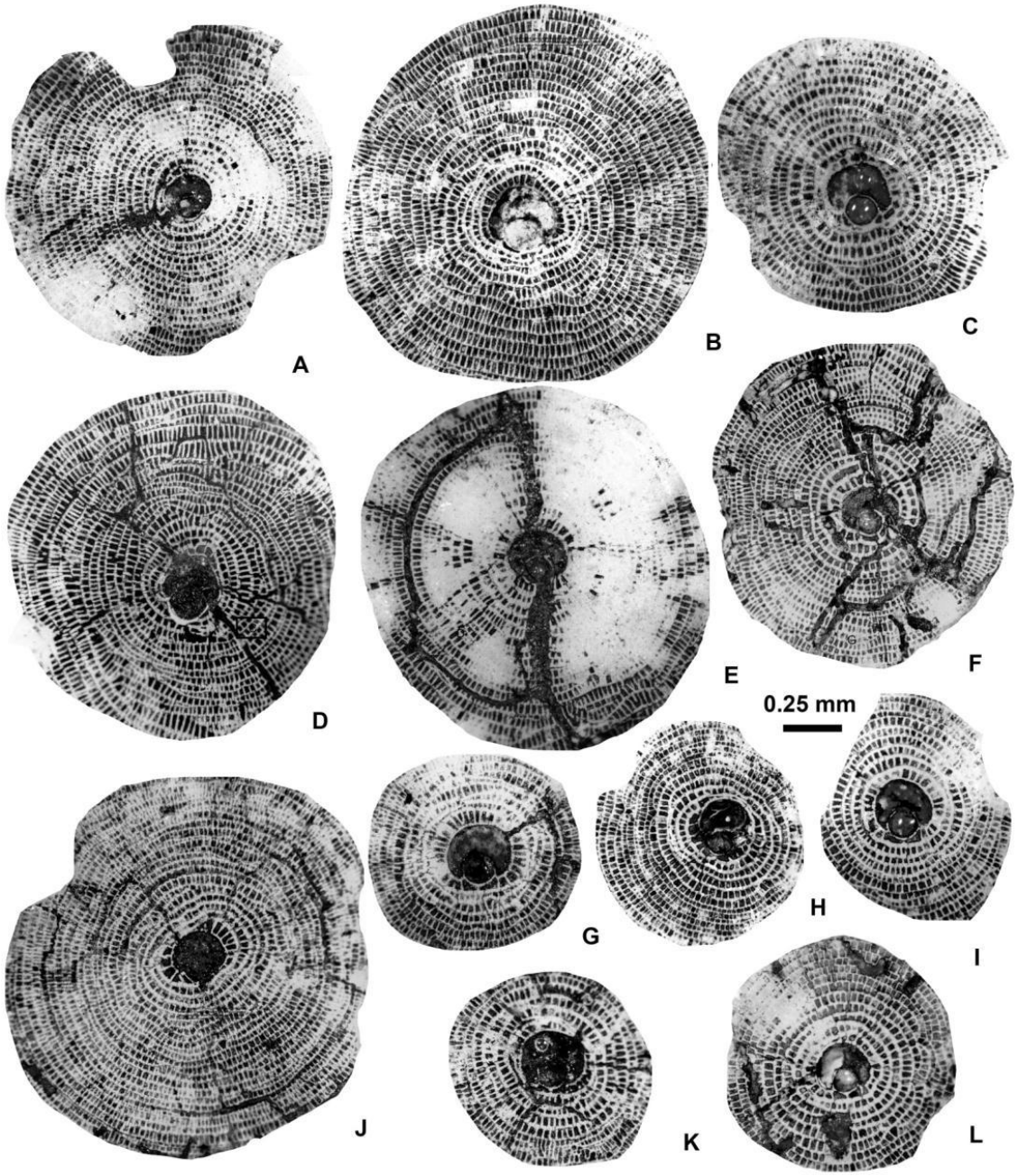


**Figure 8.** Equatorial sections of *Discocyclina augustae augustae* van der Weijden A-forms. A: E.2025.14, B: E.2025.16, C: E.2025.15, D: E.2025.23, F: E.2025.17, G: E.2025.13, H: E.2025.21, I: E.2025.20, J: E.2025.9, K: E.2025.24, L: E.2025.18. A, C: VER 3; D–F, H, I, K, L: VER 4; G, J: VER 2.

© 2025 by the author(s). Distributed under a Creative Commons CC BY license.

Preprints.org (www.preprints.org) | NOT PEER-REVIEWED | Posted: 24 June 2025 doi:10.20944/preprints202506.1471.v2

Peer-reviewed version available at Geosciences 2025, 15, 334; doi:https://doi.org/10.3390/geosciences15090334

**Table 3.** Statistical data of the adauxiliary chamberlets of orthophragmine populations from Verona.

| Parameters | | Number N | | | Height H (μm) | | | Width W (μm) | | | Shape F | | | Subspecies |
|---|---|---|---|---|---|---|---|---|---|---|---|---|---|---|
| Species | Sample | № | range | mean ± s.e. | № | range | mean ± s.e. | № | range | mean ± s.e. | № | range | mean ± s.e. | |
| *Discocyclina augustae* | **VER 2–4** | **58** | **14 – 32** | **22,0 ± 0,47** | **74** | **44 – 81** | **58,9 ± 1,0** | **58** | **30 – 49** | **38,3 ± 0,5** | **58** | **51 – 71** | **60,6 ± 0,6** | *augustae* |
| | VER 2 | 16 | 14 – 32 | 22,3 ± 1,19 | 20 | 44 – 69 | 55,6 ± 1,8 | 16 | 32 – 49 | 37,9 ± 1,2 | 16 | 51 – 68 | 59,9 ± 1,1 | |
| | VER 3 | 10 | 17 – 28 | 22,6 ± 0,95 | 15 | 50 – 81 | 67,8 ± 2,0 | 10 | 33 – 44 | 39,5 ± 1,1 | 10 | 54 – 71 | 63,1 ± 1,5 | |
| | VER 4 | 32 | 16 – 30 | 21,6 ± 0,51 | 39 | 45 – 68 | 57,1 ± 1,1 | 32 | 30 – 47 | 38,1 ± 0,7 | 32 | 54 – 66 | 60,2 ± 0,7 | |
| *D. dispansa* | **VER 3+4** | **25** | **30 – 54** | **40,4 ± 1,29** | **32** | **50 – 102** | **83,1 ± 2,1** | **25** | **28 – 50** | **39,0 ± 1,2** | **25** | **61 – 74** | **68,2 ± 0,7** | *dispansa* |
| | VER 3 | 5 | 35 – 42 | 38,2 ± 1,43 | 7 | 50 – 102 | 86,6 ± 6,9 | 5 | 33 – 50 | 40,4 ± 2,6 | 5 | 67 – 73 | 69,2 ± 1,0 | |
| | VER 4 | 20 | 30 – 54 | 41,0 ± 1,55 | 25 | 61 – 94 | 82,2 ± 1,8 | 20 | 28 – 48 | 38,7 ± 1,3 | 20 | 61 – 74 | 67,9 ± 0,8 | |
| *D. euaensis* | **VER 2** | **21** | **28 – 43** | **35,6 ± 0,86** | **27** | **93 – 137** | **110,7 ± 1,7** | **21** | **36 – 60** | **48,5 ± 1,3** | **21** | **66 – 73** | **69,5 ± 0,4** | — |
| *D. pratti* | **VER 4** | **6** | **34 – 50** | **42,2 ± 2,06** | **11** | **82 – 140** | **104,6 ± 4,8** | **6** | **44 – 75** | **56,3 ± 4,5** | **6** | **52 – 70** | **63,4 ± 2,5** | *minor* |
| *D. radians* | **VER 4** | **2** | **26 – 28** | **27,0** | **2** | **82 – 95** | **88,7** | **2** | **40 – 53** | **46,7** | **2** | **61 – 70** | **65,5** | cf. *radians* |
| *D. trabayensis* | **VER 2–4** | **16** | **8 – 11** | **9,6 ± 0,25** | **20** | **25 – 41** | **33,0 ± 0,8** | **16** | **36 – 51** | **43,0 ± 1,0** | **16** | **36 – 50** | **43,2 ± 0,9** | *elazigensis* |
| | VER 2 | 1 | | 11,0 | 1 | | 41,0 | 1 | | 44,2 | 1 | | 48,1 | |
| | VER 3 | | | | 1 | | 30,0 | | | | | | | |
| | VER 4 | 15 | 8 – 11 | 9,5 ± 0,25 | 18 | 25 – 37 | 32,6 ± 0,7 | 15 | 36 – 51 | 42,9 ± 1,0 | 15 | 36 – 50 | 42,9 ± 0,9 | |
| *Nemkovella strophiolata* | **VER 2–4** | **39** | **11 – 20** | **15,2 ± 0,38** | **48** | **37 – 58** | **43,6 ± 0,5** | **39** | **36 – 54** | **45,9 ± 0,7** | **39** | **42 – 56** | **48,6 ± 0,5** | *tenella* |
| | VER 2 | 9 | 12 – 20 | 14,9 ± 0,79 | 13 | 37 – 58 | 44,0 ± 1,3 | 9 | 36 – 52 | 46,2 ± 1,6 | 9 | 45 – 52 | 48,2 ± 0,9 | |
| | VER 3 | 5 | 12 – 18 | 14,6 ± 1,04 | 7 | 40 – 48 | 44,5 ± 1,1 | 5 | 45 – 51 | 48,2 ± 1,2 | 5 | 44 – 52 | 47,6 ± 1,1 | |
| | VER 4 | 25 | 11 – 19 | 15,4 ± 0,47 | 28 | 37 – 52 | 43,1 ± 0,6 | 25 | 37 – 54 | 45,0 ± 1,0 | 25 | 42 – 56 | 49,1 ± 0,7 | |
| *N. daguini* | **VER 4** | **1** | | **2,0** | **1** | | **25,0** | **1** | | **90,0** | **1** | | **21,7** | — |
| *Orbitoclypeus varians* | **VER 2** | **10** | **23 – 37** | **29,2 ± 1,19** | **10** | **54 – 100** | **78,8 ± 4,6** | **10** | **33 – 53** | **40,5 ± 2,0** | **10** | **59 – 71** | **65,8 ± 1,0** | *scalaris* |
| | **VER 3+4** | **27** | **24 – 38** | **30,3 ± 0,70** | **28** | **55 – 99** | **82,5 ± 2,1** | **27** | **35 – 56** | **44,3 ± 1,2** | **27** | **56 – 71** | **65,1 ± 0,7** | *varians* |
| | VER 3 | 2 | 24 – 37 | 30,5 | 2 | 55 – 93 | 73,9 ± | 2 | 41 – 43 | 41,9 | 2 | 56 – 69 | 62,8 | |
| | VER 4 | 25 | 25 – 38 | 30,3 ± 0,67 | 26 | 67 – 99 | 83,1 ± 1,9 | 25 | 35 – 56 | 44,5 ± 1,3 | 25 | 60 – 71 | 65,2 ± 0,6 | |
| *Asterocyclina alticostata* | **VER 1** | **1** | | **4,0** | **1** | | **68,0** | **1** | | **342,0** | **1** | | **16,6** | — |
| | **VER 2–4** | **7** | **3 – 5** | **4,1 ± 0,24** | **7** | **67 – 99** | **83,4 ± 4,2** | **7** | **229 – 395** | **278,4 ± 20,9** | **7** | **17 – 29** | **23,5 ± 1,5** | *danubica* |
| | VER 2 | 2 | 4 – 4 | 4,0 | 2 | 75 – 87 | 81,2 | 2 | 252 – 260 | 256,1 | 2 | 23 – 25 | 24,0 | |
| | VER 3 | 2 | 5 – 5 | 5,0 | 2 | 97 – 99 | 98,1 | 2 | 241 – 248 | 244,8 | 2 | 29 – 29 | 28,6 | |
| | VER 4 | 3 | 3 – 4 | 3,7 | 3 | 67 – 84 | 75,1 | 3 | 229 – 395 | 315,7 | 3 | 17 – 23 | 19,6 | |
| *A. stellata* | **VER 1** | **2** | **3 – 4** | **3,5** | **2** | **49 – 55** | **52,2** | **2** | **125 – 173** | **148,7** | **2** | **24 – 28** | **26,3** | cf. *stellaris* |
| | **VER 2–4** | **76** | **3 – 6** | **3,5 ± 0,07** | **78** | **40 – 89** | **57,0 ± 1,0** | **76** | **87 – 255** | **156,4 ± 3,0** | **73** | **21 – 38** | **26,7 ± 0,4** | *stellaris* |
| | VER 2 | 24 | 3 – 5 | 3,5 ± 0,12 | 26 | 40 – 69 | 52,2 ± 1,5 | 24 | 109 – 201 | 149,2 ± 4,7 | 23 | 21 – 32 | 25,7 ± 0,5 | |
| | VER 3 | 18 | 3 – 6 | 3,4 ± 0,20 | 19 | 43 – 67 | 56,0 ± 1,5 | 18 | 87 – 188 | 152,0 ± 6,2 | 17 | 21 – 38 | 27,0 ± 1,0 | |
| | VER 4 | 34 | 3 – 5 | 3,6 ± 0,09 | 33 | 40 – 89 | 61,3 ± 1,6 | 34 | 123 – 255 | 163,9 ± 4,3 | 33 | 21 – 32 | 27,1 ± 0,5 | |

This unribbed species has usually a medium-sized flat test. The medium-sized embryonic apparatus is semi-nephro- to trybliolepidine. The adauxiliary chamberlets are wide and moderately high and of the "pratti" type. The equatorial chamberlets are typically narrow and high with a "pulcra" type growth pattern. *Discocyclina euaensis* occurs in the SBZ 17–20 and OZ 13–16 Zones, respectively. It is not yet subdivided into chrono-subspecies, however, it seems that populations with $d_{mean}$ below 400–450 μm are characteristic for the Bartonian while the ones with $d_{mean}$ above this value represent the Priabonian. In Verona, this taxon occurs only in sample VER 2 where it substitutes *D. dispansa dispansa* occurring in the other two samples (VER 3 and 4) from Castel San Felice.

Remarks. Since the *Discocyclina euaensis* population from sample VER 2 is the richest known so far from the peri-Mediterranean region, we had the opportunity to check the possible existence of the species in other localities published in our previous publications. As a result, we found that the populations (i) in [62] determined as *D. pratti* from samples Teke 4 and 6 and (ii) in [69] identified with *D. dispansa* from sample Kırklareli C 19 (see synonymy list) correspond in fact to *D. euaensis*.

© 2025 by the author(s). Distributed under a Creative Commons CC BY license.

Preprints.org (www.preprints.org) | NOT PEER-REVIEWED | Posted: 24 June 2025 doi:10.20944/preprints202506.1471.v2

Peer-reviewed version available at Geosciences 2025, 15, 334; doi:https://doi.org/10.3390/geosciences15090334

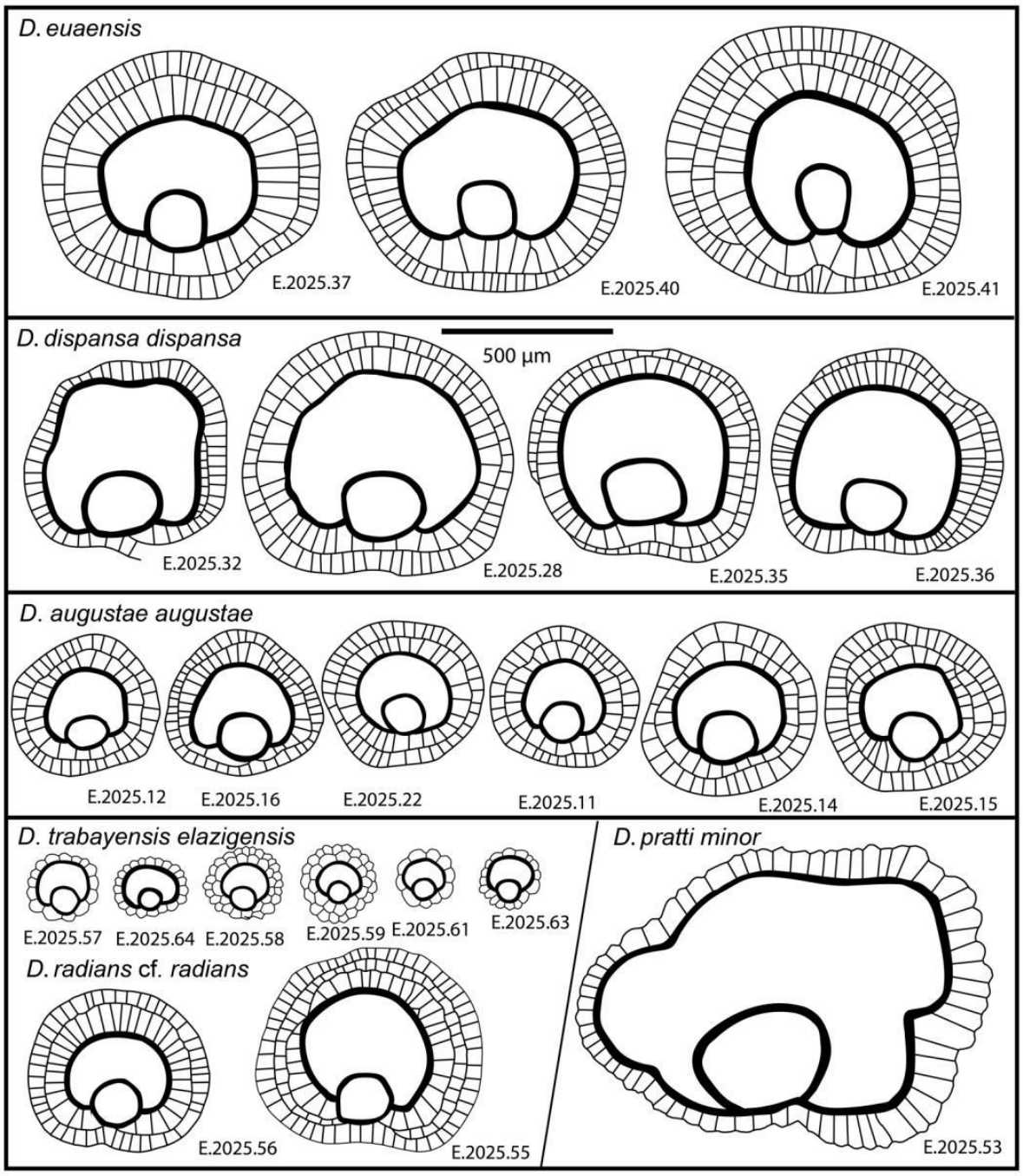


**Figure 9.** Comparative line drawings of the embryonal part of six species of *Discoclina.*

*Discocyclina euaensis* and *D. dispansa dispansa* have a similar size and type embryo, however they are different (i) in the type of adauxiliary chamberlets, which is of the "pratti" type for *D. euaensis* instead of the "archiaci" type for *D. d. dispansa* and (ii) in the height of both the adauxiliary and equatorial chamberlets, which are significantly larger in the case of *D. euaensis* (Figure 14). Although they are similar with *D. pratti minor* in their "pratti" type adauxiliary chamberlets, some size parameters (d, n and h), however, are usually smaller in the case of *D. euaensis* (see below). Finally, it is almost impossible to distinguish it from the advanced members of the *D. radians* lineage (e.g., *D. r. labatlanensis*) based solely on the characteristics of the A-form equatorial sections, however the latter is a ribbed form unlike the unribbed *D. euaensis.*

© 2025 by the author(s). Distributed under a Creative Commons CC BY license.

Preprints.org (www.preprints.org) | NOT PEER-REVIEWED | Posted: 24 June 2025 doi:10.20944/preprints202506.1471.v2

Peer-reviewed version available at Geosciences 2025, 15, 334; doi:https://doi.org/10.3390/geosciences15090334

*Discocyclina pratti* (Michelin, 1846)

This rather widespread, relatively large, flat, rarely saddle-shaped, unribbed species has a medium-sized to large, tryblio- to excentrilepidine embryo, numerous moderately wide and high, "pratti" type adauxiliary chamberlets and narrow but high equatorial chamberlets with "pulcra" type growth pattern.

*Discocyclina pratti* forms an evolutionary lineage with three chrono-subspecies such as *D. p. montfortensis* ($d_{mean}$ < 510 µm; SBZ 13–16; OZ 8b–12); *D. p. pratti* ($d_{mean}$=510–700 µm; SBZ ?15–18; OZ 12–14) and *D. p. minor* ($d_{mean}$ > 700 µm; SBZ 18c–19b; OZ 14–?15) [6,7].

In Verona, *Discocylina pratti* is rather rare, we found it only in sample VER 4, where based on Tables 2–4 it is represented by *D. p. minor*.

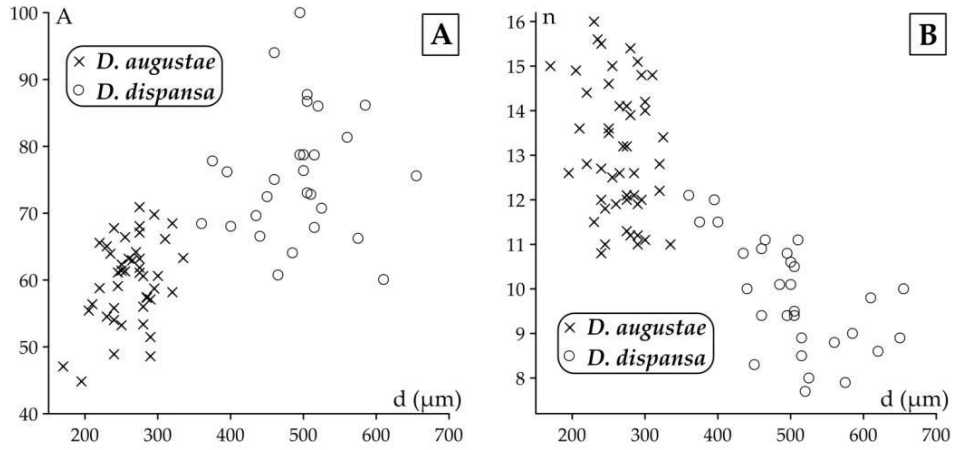


**Figure 10.** Distribution of *Discocyclina augustae augustae* and *D. dispansa dispansa* specimens in samples VER 3 and VER 4 (A) on the d–A (deuteroconch diameter vs. deuteroconchal embracement) and (B) on the d–n (deuteroconch diameter vs. annuli number in the first 0.5 mm from the deuteroconch's rim) bivariate plots.

*Discocyclina pratti minor* Meffert, 1931

Figure 6: C, Figure 7, Figure 9, Figure 15: A–F.

*Discocyclina umbo* var. *minor* n. var. — [70]: 28–31, 54–55, Plate 6: 1–5, Plate 7: 2, Figures 4–6.

*Discocyclina pratti minor* Meffert — [5]: 179–180, Plate 20: 12, Plate 21: 1–3. (with synonymy). — [69]: Figure 33s. — [63]: 151, Figure 15. — [71]: Figures 24c–e, 25a–d. — [7]: Figure 81.

Remarks. The distinction of *Discocyclina pratti minor* from *D. dispansa dispansa* and *D. euaensis* was discussed above, in the remarks to these taxa (see also Figures 16 and 17).

*Discocyclina radians* (d'Archiac, 1850)

Figure 6: F, Figure 7, Figure 9, Figure 17: A, B.

*Orbitolites radians* n. sp. — [1]: 405–406, Plate 8: 15, 15a–b.

*Discocyclina radians* (d'Archiac). — [5]: 166–169, Plate 15: 1–15, Plate 16: 1–7. (with three subspecies and synonymies). — [7]: 52, 54. (with four subspecies).

This ribbed species bears a small to medium-sized semi-nephro- to trybliolepidine type embryo, wide and moderately high, "pratti"-type adauxiliary chamberlets and narrow and high equatorial chamberlets with "pulcra"-type growth pattern.

*Discocyclina radians* forms an evolutionary lineage with four chrono-subspecies as follows: *D. r.* n. ssp. Caupenne (in Less, 1998 with $d_{mean}$ < 240 µm; SBZ 12–13; OZ 8b); *D. r. noussensis* ($d_{mean}$=240–300 µm; SBZ 13; OZ 9); *D. r. radians* ($d_{mean}$=300–375 µm; SBZ 13–19a; OZ ?9–14) and *D. r. labatlanensis* ($d_{mean}$ > 375 µm; SBZ ?16–20; OZ ?12–16) [6,7].

We found only two specimens of this species in sample VER 4 of the Castel San Felice. Based on data of Tables 2–4, it can be determined as *Discocyclina radians* cf. *radians*. This is roughly in agreement

© 2025 by the author(s). Distributed under a Creative Commons CC BY license.

Preprints.org (www.preprints.org) | NOT PEER-REVIEWED | Posted: 24 June 2025 doi:10.20944/preprints202506.1471.v2

Peer-reviewed version available at Geosciences 2025, 15, 334; doi:https://doi.org/10.3390/geosciences15090334

with the data of [31] in the text. See more details in Chapter 3. The specimens Brönnimann studied may have come from a sample (of Castel San Felice) that we have not studied, and where these ribbed forms are more common than in our sites.

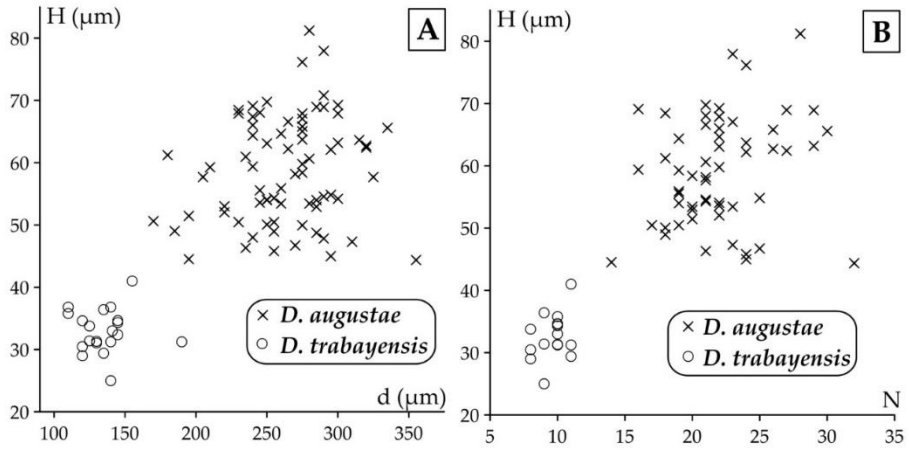


**Figure 11.** Distribution of *Discocyclina augustae augustae* and *D. trabayensis elazigensis* specimens in samples VER 2–4 (A) on the d–H (deuteroconch diameter vs. height of adauxiliary chamberlets) and (B) on the N–H (number of adauxiliary chamberlets vs. height of adauxiliary chamberlets) bivariate plots.

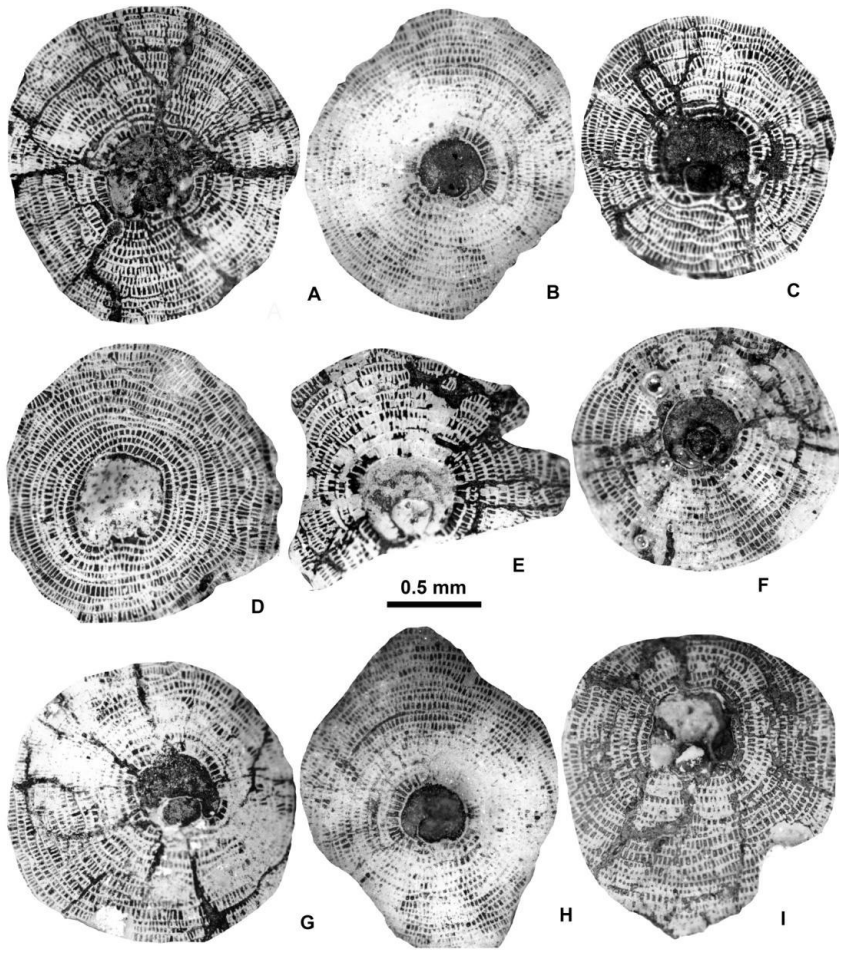


**Figure 12.** Equatorial sections of *Discocyclina dispansa dispansa* (Sowerby) A-forms. A: E.2025.36, B: E.2025.26, C: E.2025.35, D: E.2025.30, E: E.2025.27, F: E.2025.31, G: E.2025.33, H: E.2025.25, I: E.2025.32. A, C, D, F, G, I: VER 4; B, E, H: VER 3.

© 2025 by the author(s). Distributed under a Creative Commons CC BY license.

Preprints.org (www.preprints.org) | NOT PEER-REVIEWED | Posted: 24 June 2025 doi:10.20944/preprints202506.1471.v2

Peer-reviewed version available at Geosciences 2025, 15, 334; doi:https://doi.org/10.3390/geosciences15090334

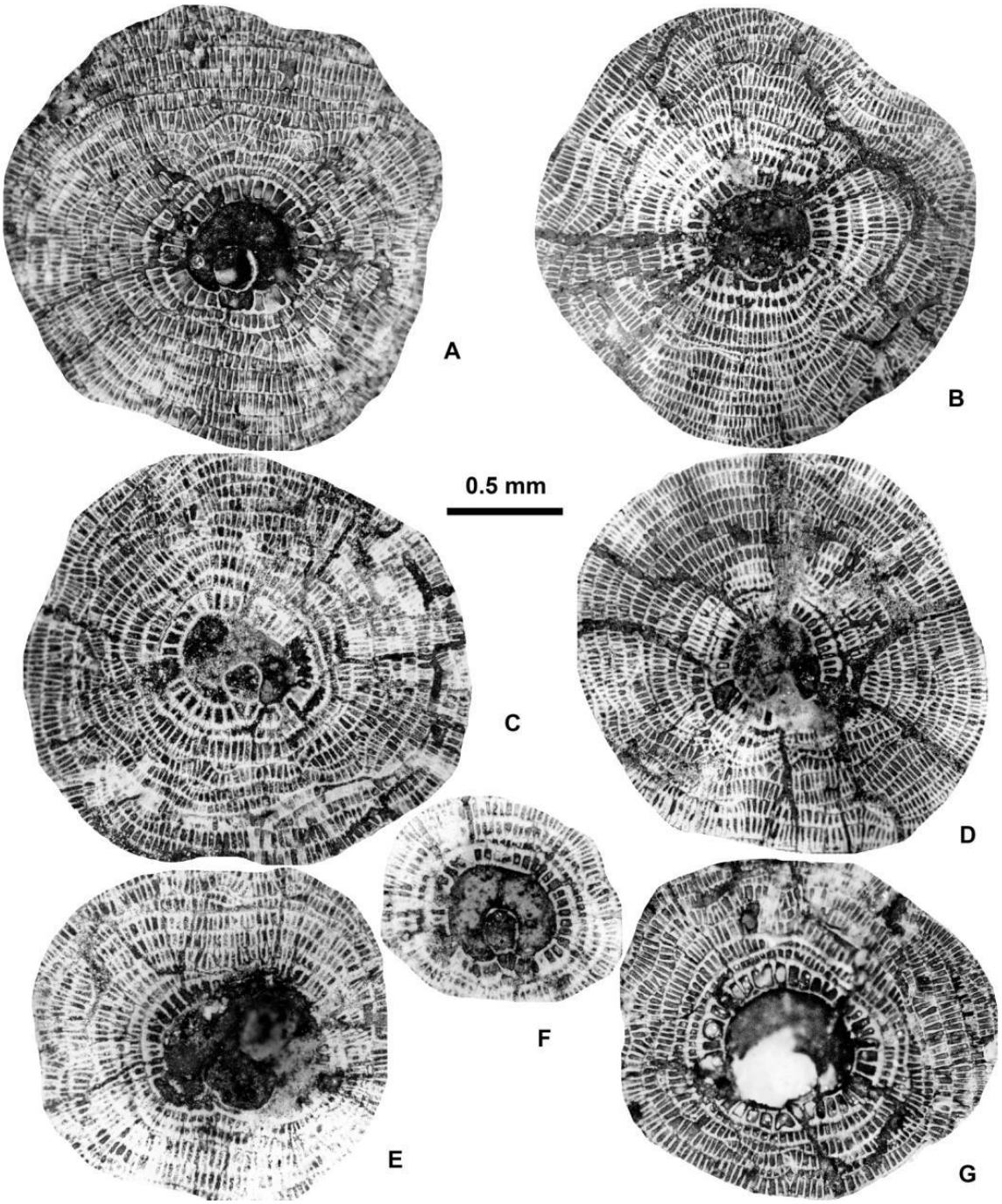


**Figure 13.** Equatorial sections of *Discocyclina euaensis* Whipple A-forms from sample VER 2. A: E.2025.46, B: E.2025.37, C: E.2025.45, D: E.2025.38, E: E.2025.42, F: E.2025.41, G: E.2025.39.

*Discocyclina trabayensis* Neumann, 1955

Figure 6: E, Figure 7, Figure 9, Figure 17: C–I.

This small and flat, unribbed species has a very small, iso- to nephrolepidine embryo, very low, relatively wide, characteristic "varians"-type adauxiliary chamberlets (lobulate in outline) and narrow equatorial chamberlets with "trabayensis" type growth pattern.

*Discocyclina trabayensis* forms an evolutionary lineage with three chrono-subspecies as follows: *D. t. trabayensis* ($d_{mean}$ < 125 μm; SBZ 10–17; OZ 5–13); *D. t. elazigensis* ($d_{mean}$=125–170 μm; SBZ 18–19; OZ 14–15) and *D. t. vicenzensis* ($d_{mean}$ > 170 μm; SBZ 20; OZ 16) [6,7].

© 2025 by the author(s). Distributed under a Creative Commons CC BY license.

Preprints.org (www.preprints.org) | NOT PEER-REVIEWED | Posted: 24 June 2025 doi:10.20944/preprints202506.1471.v2

Peer-reviewed version available at Geosciences 2025, 15, 334; doi:https://doi.org/10.3390/geosciences15090334

In Verona, Castel San Felice, *Discocylina trabayensis* is common in sample VER 4 but rather rare in the other two (VER 2 and 3). Based on their quantitative parameters (Tables 2–4) the three populations can be jointly evaluated and determined as *D. t. elazigensis.*

**Table 4.** Statistical data of the adauxiliary chamberlets of orthophragmine populations from Verona.

| Parameters | | № of annuli in the first 0.5 mm from the deuteroconch | | | Height | | | Width | | | Shape | | | Subspecies |
|---|---|---|---|---|---|---|---|---|---|---|---|---|---|---|
| | | n | | | h (μm) | | | w (μm) | | | G | | | |
| Species | Sample | № | range | mean ± s.e. | № | range | mean ± s.e. | № | range | mean ± s.e. | № | range | mean ± s.e. | |
| *Discocyclina augustae* | **VER 2–4** | **71** | **10,2 – 17,5** | **13,2 ± 0,2** | **70** | **28 – 49** | **36,6 ± 0,6** | **71** | **21 – 32** | **25,7 ± 0,3** | **70** | **49 – 66** | **58,7 ± 0,5** | *augustae* |
| | VER 2 | 20 | 10,2 – 17,5 | 13,6 ± 0,4 | 20 | 28 – 49 | 36,2 ± 1,2 | 20 | 22 – 32 | 25,9 ± 0,6 | 20 | 49 – 65 | 58,1 ± 1,0 | |
| | VER 3 | 15 | 11,0 – 16,0 | 12,5 ± 0,4 | 14 | 30 – 44 | 38,0 ± 1,2 | 15 | 21 – 30 | 25,8 ± 0,7 | 14 | 51 – 66 | 59,6 ± 1,1 | |
| | VER 4 | 36 | 10,8 – 15,6 | 13,3 ± 0,2 | 36 | 30 – 44 | 36,3 ± 0,6 | 36 | 22 – 29 | 25,5 ± 0,3 | 36 | 51 – 64 | 58,6 ± 0,5 | |
| *D. dispansa* | **VER 3+4** | **30** | **7,7 – 12,1** | **9,8 ± 0,2** | **30** | **38 – 61** | **48,0 ± 1,1** | **30** | **23 – 33** | **27,0 ± 0,4** | **30** | **54 – 70** | **63,8 ± 0,6** | *dispansa* |
| | VER 3 | 6 | 7,7 – 12,1 | 10,0 ± 0,8 | 6 | 38 – 61 | 47,9 ± 3,9 | 6 | 24 – 31 | 26,7 ± 1,0 | 6 | 61 – 69 | 63,8 ± 1,4 | |
| | VER 4 | 24 | 8,0 – 11,5 | 9,8 ± 0,2 | 24 | 40 – 60 | 48,1 ± 1,1 | 24 | 23 – 33 | 27,1 ± 0,5 | 24 | 54 – 70 | 63,9 ± 0,7 | |
| *D. euaensis* | **VER 2** | **27** | **5,9 – 8,8** | **7,0 ± 0,1** | **27** | **50 – 79** | **65,8 ± 1,5** | **27** | **22 – 33** | **29,6 ± 0,5** | **27** | **62 – 74** | **68,8 ± 0,6** | — |
| *D. pratti* | **VER 4** | 10 | 4,6 – 6,1 | 5,1 ± 0,1 | 10 | 79 – 110 | 96,8 ± 3,0 | 10 | 28 – 42 | 36,3 ± 1,3 | 10 | 66 – 79 | 72,6 ± 1,2 | *minor* |
| *D. radians* | **VER 4** | **2** | **9,5 – 9,7** | **9,6** | **2** | **47 – 49** | **47,8** | **2** | **25 – 25** | **24,8** | **2** | **65 – 67** | **65,9** | cf. *radians* |
| *D. trabayensis* | **VER 2–4** | **20** | **11,0 – 21,0** | **16,7 ± 0,4** | **19** | **24 – 33** | **29,5 ± 0,6** | **20** | **24 – 32** | **27,9 ± 0,5** | **19** | **48 – 57** | **51,3 ± 0,5** | *elazigensis* |
| | VER 2 | 2 | 11,0 – 15,0 | 13,0 | 1 | | 32,8 | 2 | 27 – 31 | 29,0 | 1 | | 51,4 | |
| | VER 3 | 1 | 17,2 | 17,2 | 1 | | 28,9 | 1 | | 29,9 | 1 | | 49,2 | |
| | VER 4 | 17 | 15,0 – 21,0 | 17,1 ± 0,4 | 17 | 24 – 33 | 29,3 ± 0,6 | 17 | 24 – 32 | 27,6 ± 0,6 | 17 | 48 – 57 | 51,5 ± 0,5 | |
| *Nemkovella strophiolata* | **VER 2–4** | **44** | **12,8 – 19,0** | **15,7 ± 0,2** | **44** | **25 – 39** | **31,4 ± 0,5** | **44** | **23 – 37** | **30,4 ± 0,5** | **44** | **42 – 58** | **50,8 ± 0,5** | *tenella* |
| | VER 2 | 13 | 13,3 – 17,5 | 15,3 ± 0,3 | 13 | 28 – 37 | 32,2 ± 0,8 | 13 | 27 – 35 | 31,2 ± 0,8 | 13 | 44 – 55 | 50,8 ± 0,9 | |
| | VER 3 | 5 | 12,8 – 17,0 | 15,1 ± 0,8 | 5 | 29 – 39 | 33,0 ± 2,0 | 5 | 25 – 33 | 30,0 ± 1,2 | 5 | 49 – 54 | 52,3 ± 1,0 | |
| | VER 4 | 26 | 14,0 – 19,0 | 16,0 ± 0,2 | 26 | 25 – 35 | 30,6 ± 0,5 | 26 | 23 – 37 | 30,1 ± 0,7 | 26 | 42 – 58 | 50,6 ± 0,7 | |
| *N. daguini* | **VER 4** | **1** | | **23,0** | **1** | | **21,6** | **1** | | **26,0** | **1** | | **45,4** | — |
| *Orbitoclypeus varians* | **VER 2** | **10** | **8,8 – 13,0** | **10,4 ± 0,4** | **10** | **37 – 55** | **45,7 ± 1,7** | **10** | **31 – 39** | **34,9 ± 0,6** | **10** | **49 – 64** | **56,5 ± 1,2** | *scalaris* |
| | **VER 3+4** | **28** | **7,2 – 12,1** | **10,2 ± 0,2** | **28** | **39 – 65** | **46,2 ± 1,1** | **28** | **32 – 43** | **36,8 ± 0,6** | **28** | **50 – 61** | **55,5 ± 0,6** | *varians* |
| | VER 3 | 2 | 10,5 – 11,0 | 10,8 | 2 | 41 – 47 | 43,8 | 2 | 34 – 40 | 37,1 | 2 | 50 – 58 | 54,1 | |
| | VER 4 | 26 | 7,2 – 12,1 | 10,1 ± 0,2 | 26 | 39 – 65 | 46,3 ± 1,2 | 26 | 32 – 43 | 36,8 ± 0,6 | 26 | 51 – 61 | 55,6 ± 0,6 | |
| *Asterocyclina alticostata* | **VER 1** | **1** | | **7,2 ±** | **1** | | **69,7** | **1** | | **41,6** | **1** | | **62,6** | — |
| | **VER 2–4** | **7** | **8,5 – 11,8** | **10,2 ± 0,4** | **7** | **39 – 54** | **45,9 ± 1,8** | **7** | **30 – 45** | **37,8 ± 1,7** | **7** | **51 – 61** | **54,8 ± 1,5** | *danubica* |
| | VER 2 | 2 | 9,5 – 11,0 | 10,3 | 2 | 41 – 50 | 45,6 | 2 | 40 – 40 | 40,0 | 2 | 51 – 56 | 53,2 | |
| | VER 3 | 2 | 8,5 – 9,5 | 9,0 | 2 | 47 – 54 | 50,4 | 2 | 30 – 36 | 32,9 | 2 | 60 – 61 | 60,5 | |
| | VER 4 | 3 | 10,0 – 11,8 | 10,9 | 3 | 39 – 48 | 43,0 | 3 | 35 – 45 | 39,6 | 3 | 51 – 54 | 52,1 | |
| *A. stellata* | **VER 1** | **2** | **18,0 – 18,0** | **18,0** | **2** | **26 – 27** | **26,3** | **2** | **25 – 27** | **26,0** | **2** | **49 – 51** | **50,3** | cf. *stellaris* |
| | **VER 2–4** | **57** | **14,5 – 20,7** | **17,3 ± 0,2** | **56** | **23 – 33** | **27,4 ± 0,3** | **58** | **22 – 32** | **27,8 ± 0,4** | **56** | **45 – 56** | **49,8 ± 0,4** | *stellaris* |
| | VER 2 | 20 | 14,5 – 19,5 | 17,4 ± 0,3 | 20 | 25 – 33 | 27,5 ± 0,5 | 21 | 22 – 32 | 28,1 ± 0,7 | 20 | 45 – 56 | 49,8 ± 0,7 | |
| | VER 3 | 13 | 15,0 – 20,0 | 17,2 ± 0,4 | 12 | 23 – 32 | 27,8 ± 0,8 | 13 | 25 – 31 | 28,5 ± 0,4 | 12 | 45 – 56 | 49,3 ± 0,9 | |
| | VER 4 | 24 | 15,8 – 20,7 | 17,3 ± 0,3 | 24 | 23 – 30 | 27,1 ± 0,4 | 24 | 24 – 32 | 27,2 ± 0,5 | 24 | 45 – 55 | 50,0 ± 0,6 | |

*Discocyclina trabayensis elazigensis* Özcan et Less, 2006

*Discocyclina trabayensis elazigensis* n. ssp. — [55]: 495, Plate 2: 7–9, Figure 12. (with synonymy).

*Discocyclina trabayensis elazigensis* Özcan et Less. — [69]: Figure 33l–o. — [7]: Figures 111.4–8, 112.

Remarks. *Discocyclina trabayensis elazigensis* may be confused with *D. augustae augustae*, but due to its very small embryo and characteristic, "varians" type adauxiliary chamberlets, this taxon is easily identified (see also Figure 11).

© 2025 by the author(s). Distributed under a Creative Commons CC BY license.

Preprints.org (www.preprints.org) | NOT PEER-REVIEWED | Posted: 24 June 2025 doi:10.20944/preprints202506.1471.v2

Peer-reviewed version available at Geosciences 2025, 15, 334; doi:https://doi.org/10.3390/geosciences15090334

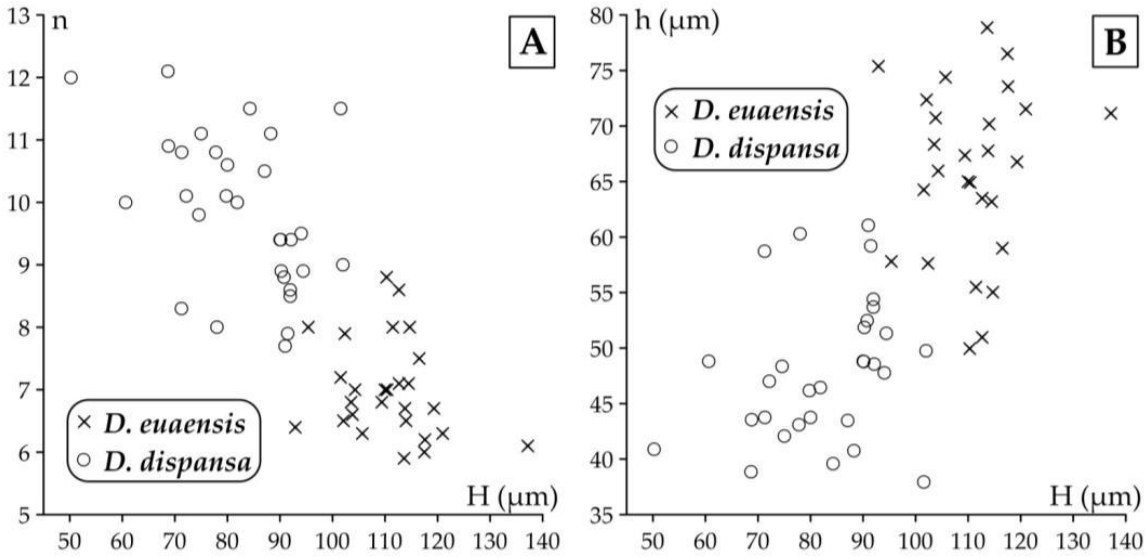


**Figure 14.** Distribution of specimens of *Discocyclina euaensis* (in sample VER 2) and of *D. dispansa dispansa* (in samples VER 3 and VER 4) (A) on the H–n (height of adauxiliary chamberlets vs. annuli number in the first 0.5 mm from the deuteroconch's rim) and (B) on the H–h (height of adauxiliary chamberlets vs. height of equatorial chamberlets) bivariate plots.

Genus *Nemkovella* Less, 1987

Representatives of two species of this genus were found in the three samples of Verona, Castel San Felice.

*Nemkovella strophiolata* (Gümbel, 1870)

This is a small, moderately flat, unribbed species with a small semi-iso to nephrolepidine embryo, low but relatively wide, very diagnostic, arcuate, "varians" type adauxiliary chamberlets and moderately narrow and low, slightly hexagonal equatorial chamberlets with "strophiolata" type growth pattern.

*Nemkovella strophiolata* forms an evolutionary lineage with the following four chrono-subspecies: *N. s. fermonti* ($d_{mean}$ < 150 μm; SBZ 10–13; OZ 6–9); *N. s. strophiolata* ($d_{mean}$=150–185 μm; SBZ 12–16; OZ 8b–12); *N. s.* n. ssp. Padragkút (in Less, 1998 with $d_{mean}$=185–230 μm; SBZ 15–18; OZ 11–14) and *N. s. tenella* ($d_{mean}$ > 230 μm; SBZ 18–19a; OZ 14) [6,7].

This species occurs in all three samples (VER 2–4) from Verona Castel San Felice and is particularly common in sample VER 4. The quantitative parameters of the three populations are very similar (Tables 2–4) and can therefore be evaluated and determined together as *Nemkovella strophiolata tenella*.

Remarks. This easily recognizable taxon can sometimes be confused with *Discocyclina augustae augustae*, which, however, has proximal annular stolons that are absent in *Nemkovella*. Therefore, the equatorial chamberlets of the latter are slightly hexagonal, unlike those of *Discocyclina*, which are rectangular.

© 2025 by the author(s). Distributed under a Creative Commons CC BY license.

Preprints.org (www.preprints.org) | NOT PEER-REVIEWED | Posted: 24 June 2025 doi:10.20944/preprints202506.1471.v2

Peer-reviewed version available at Geosciences 2025, 15, 334; doi:https://doi.org/10.3390/geosciences15090334

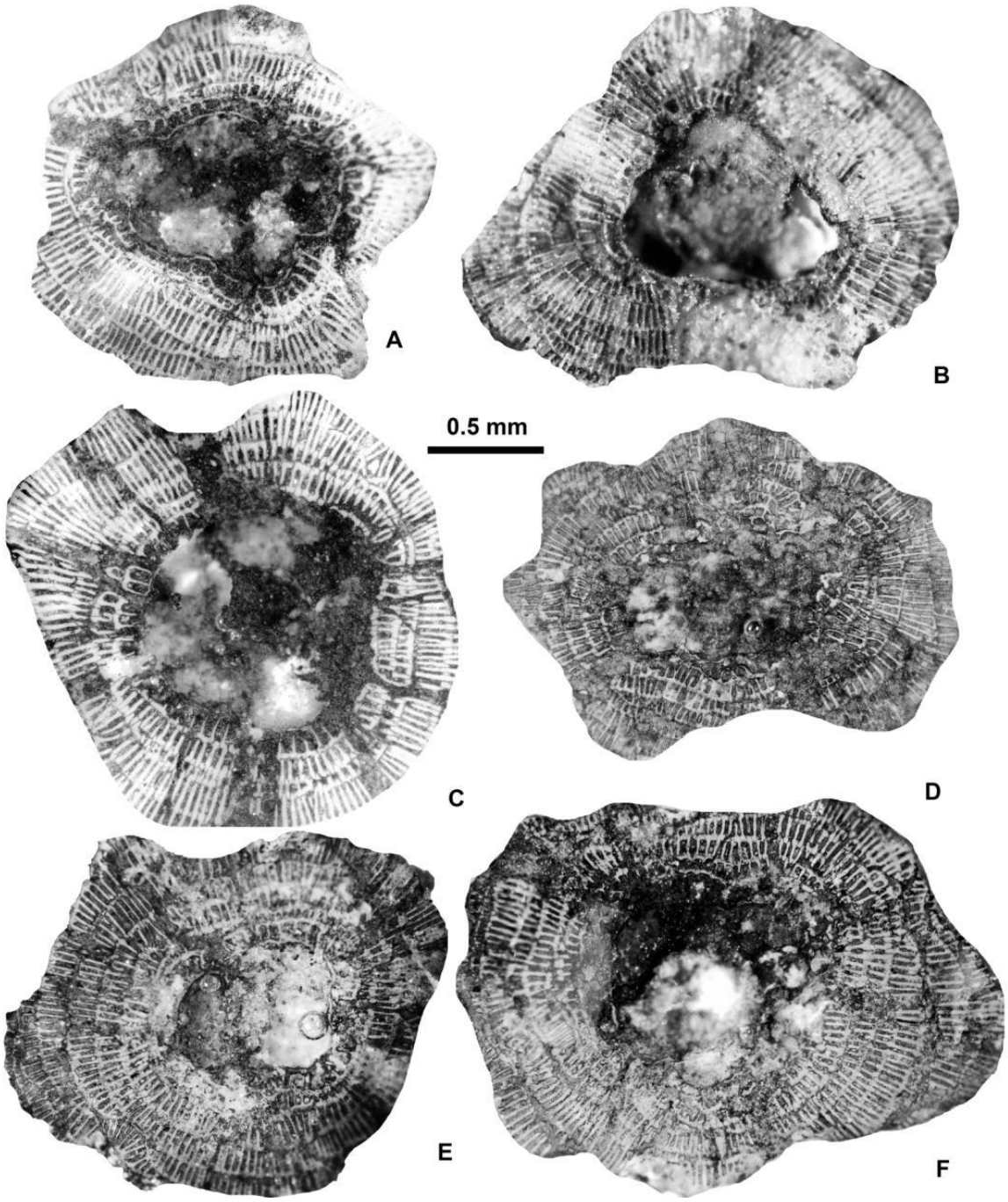


**Figure 15.** *Discocyclina pratti minor* Meffert A-forms from sample VER 4. A: E.2025.53, B: E.2025.48, C: E.2025.54 D: E.2025.47 E: E.2025.50 F: E.2025.49.

Although they belong to different families (which is clear from their microspheric juvenarium, see Figure 3), the megalospheric specimens of *N. strophiolata tenella* and of the advanced *Orbitoclypeus varians* (*O. v. scalaris* and *O. v. varians*) are identical in the absence of proximal annular stolon of equatorial chamberlets and may therefore be confused. Figure 20. shows that their quantitative parameters differ significantly. In addition, the slightly undulated annuli characteristic of *O. varians* are never observed in *N. strophiolata*.

© 2025 by the author(s). Distributed under a Creative Commons CC BY license.

Preprints.org (www.preprints.org) | NOT PEER-REVIEWED | Posted: 24 June 2025 doi:10.20944/preprints202506.1471.v2

Peer-reviewed version available at Geosciences 2025, 15, 334; doi:https://doi.org/10.3390/geosciences15090334

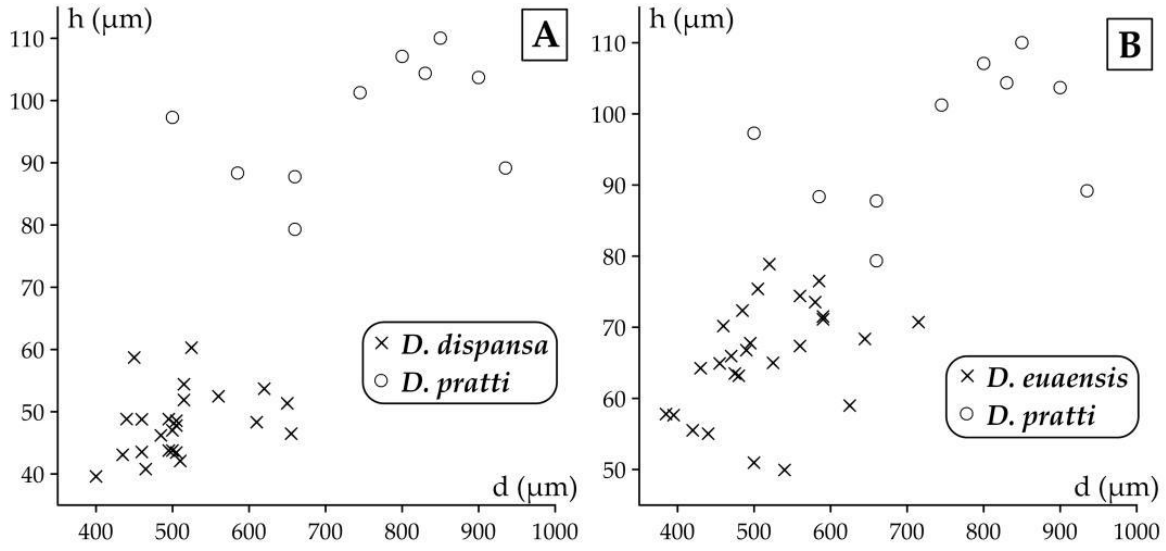


**Figure 16.** Distribution of specimens on the d–h (deuteroconch diameter vs. height of equatorial chamberlets) bivariate plots for (A) *Discocyclina pratti minor* and *D. dispansa dispansa* in sample VER 4 and for (B) *D. pratti minor* in sample VER 4 and *D. euaensis* in sample VER 2.

*Nemkovella daguini* (Neumann, 1958)

Figure 18: L, Figure 19.

*Discocyclina daguini* n. sp. — [73]: 89, Plate 17: 7–10.

*Orbitoclypeus daguini* (Neumann); [5]: 222–224. Plate 36: 1–6, Figures 31a, b (with synonymy).

*Nemkovella daguini* (Neumann) — [55]: 503–504, Plate 2: 1–4, Plate 3: 14, Plate 5: 6, Figure 6. — [74]: 19–23, figs 5A–C, 6A–H, 7A–K, 8, 9A–H, 10A–I, 11A–E. (with synonymy) — [7]: 68, 71, Figures 25.7–8, 36.6–8, 117.1–6, 118. — [67]: 24, Figure 16K.

*Nemkovella daguini* is a very small and strongly inflated taxon without ribs. The very small embryo varies from almost iso- to nephrolepidine type. The pre-annular stage includes auxiliary, adauxiliary and orbitoidal chamberlets. The two principal auxiliary chambers are larger than the nearby orbitoidal chamberlets, tangentially elongated and similar in size and shape to the 1–3 (usually 2) adauxiliary chamberlets. The latter are arcuate in shape, radially low, tangentially wide and are isolated from each other, leading to the formation of 'orbitoidal' chamberlets. The chamberlets following the auxiliary chamberlets on the protoconchal side form very short spirals.

The arrangement of the equatorial chamberlets around the deuteroconch is typically orbitoidal ("daguini"-type of [5]). Annular growth is attained in the successive growth stages following the orbitoidal chamberlets. The annular chamberlets are low, hexagonal, and progressively tend to become rectangular towards the periphery. Most specimens possess wavy annuli, at least in the early part of development, their number varies between 4 and 6. This wavy pattern is attenuated with successive growth, and the latest equatorial chamberlets are in regular annuli with a circular outline. *Nemkovella daguini* ranging from SBZ 11 to SBZ 20 and OZ 8a to OZ 16, respectively, is not yet subdivided into chrono-subspecies.

© 2025 by the author(s). Distributed under a Creative Commons CC BY license.

Preprints.org (www.preprints.org) | NOT PEER-REVIEWED | Posted: 24 June 2025 doi:10.20944/preprints202506.1471.v2

Peer-reviewed version available at Geosciences 2025, 15, 334; doi:https://doi.org/10.3390/geosciences15090334

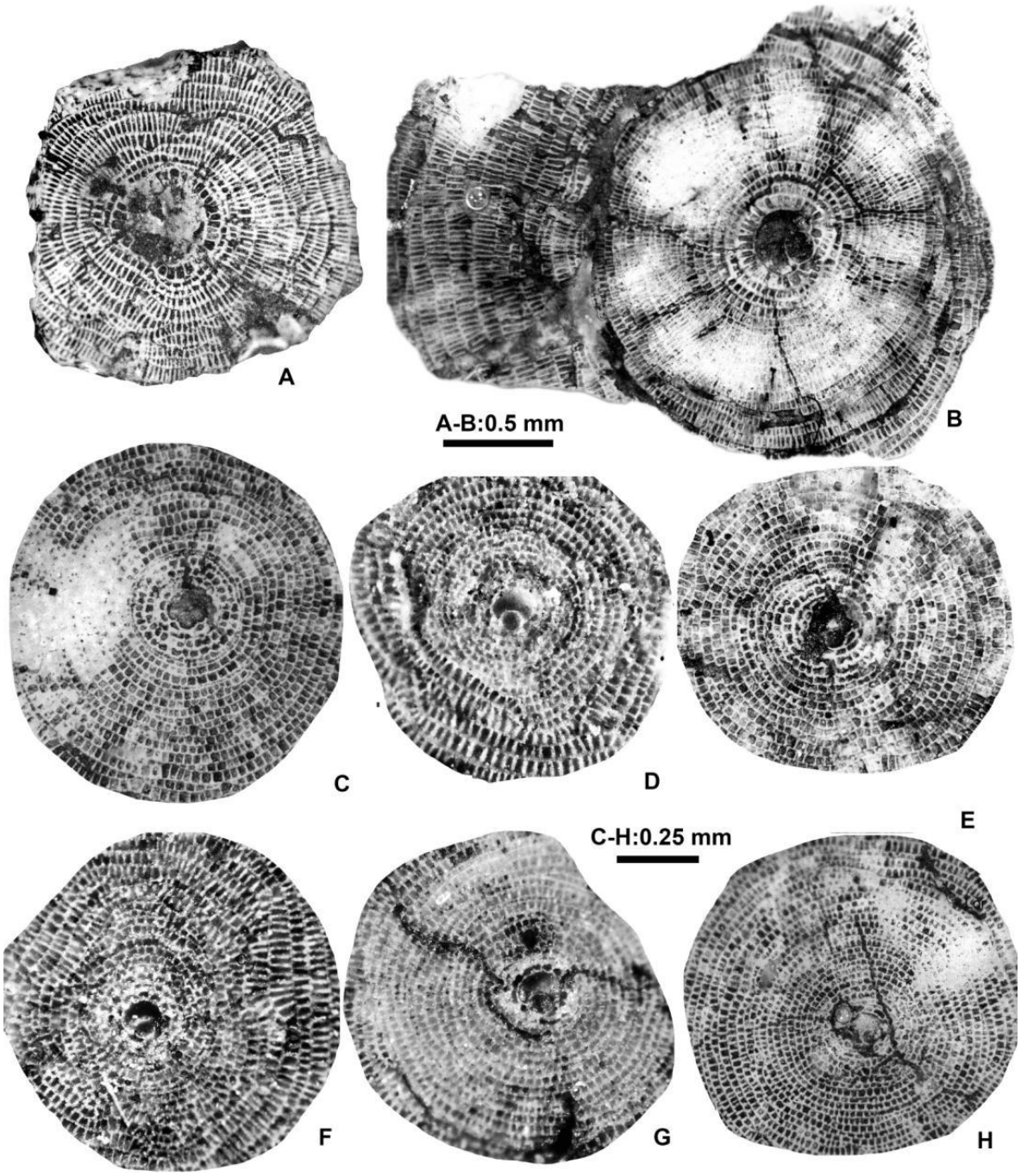


**Figure 17.** Equatorial sections of *Discocyclina radians* cf. *radians* (d'Archiac) (A–B) and *D. trabayensis elazigensis* Özcan & Less (C–H), A: E.2025.55, B: E.2025.56 C: E.2025.60, D: E.2025.63, E: E.2025.62, F: E.2025.61, G: E.2025.59, H: E.2025.64. All A-forms from sample VER 4.

We found only a single specimen of this extremely small, otherwise unconfusable taxon in sample VER 4. Based on its characteristic nepionic arrangement, formerly (see synonymy list) it was assigned to genus *Orbitoclypeus*. However, ([55], Plate 3: 14) found a B-form characteristic of discocyclinids, so it had to be reclassified into the genus *Nemkovella.*

© 2025 by the author(s). Distributed under a Creative Commons CC BY license.

Preprints.org (www.preprints.org) | NOT PEER-REVIEWED | Posted: 24 June 2025 doi:10.20944/preprints202506.1471.v2

Peer-reviewed version available at Geosciences 2025, 15, 334; doi:https://doi.org/10.3390/geosciences15090334

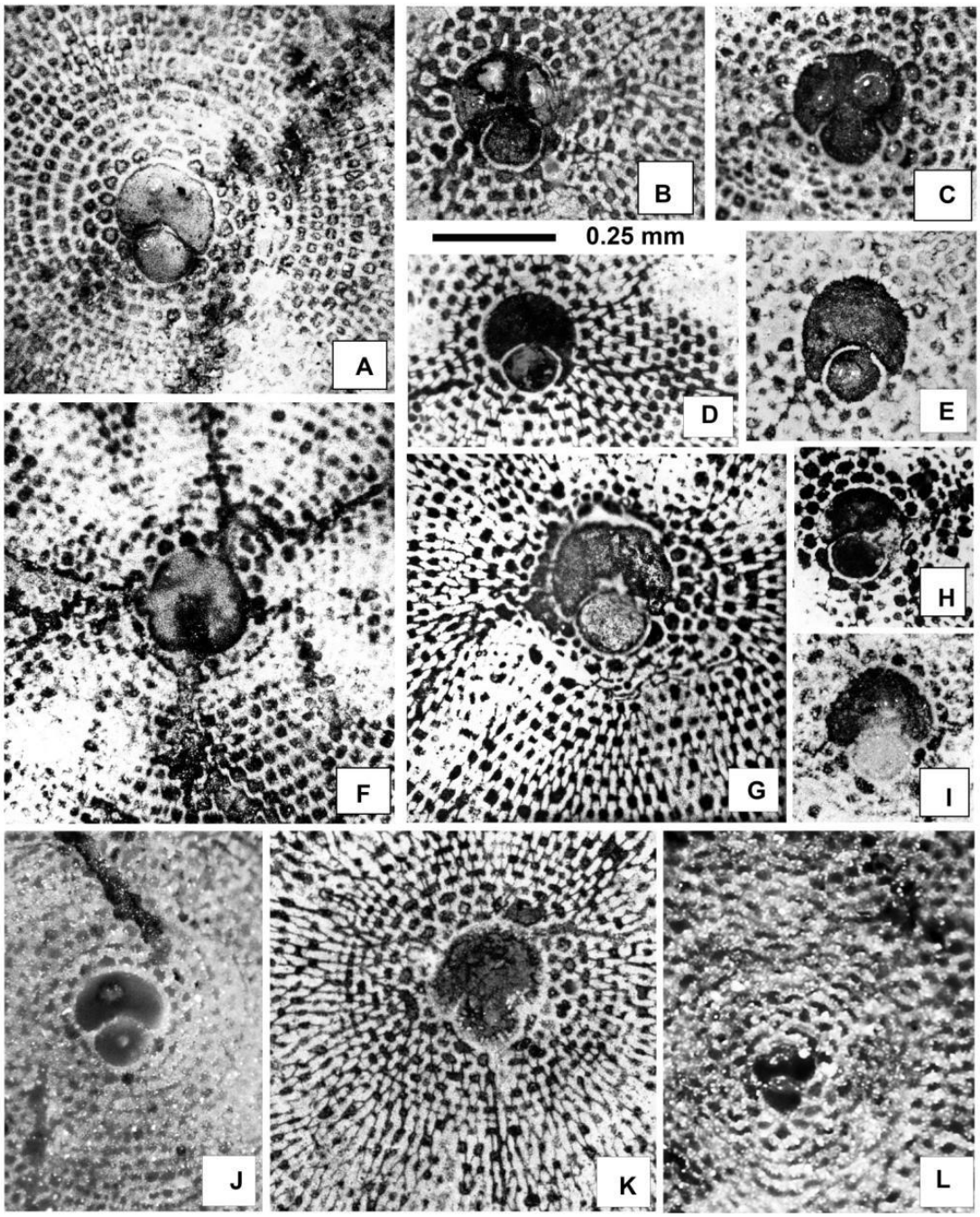


**Figure 18.** Equatorial sections of *Nemkovella strophiolata tenella* (Gümbel) (A–K) and *N. daguini* (Neumann) (L). A: E.2025.163, B: E.2025.84, C: E.2025.74, D: E.2025.77, E: E.2025.71, F: E.2025.162, G: E.2025.81, H: E.2025.82, I: E.2025.164, J: E.2025.76, K: E.2025.80, L: E.2025.85. A, F, I: VER 2; B–E, G–L: VER 4. All A-forms.

6.1.2. Family Orbitoclypeidae Brönnimann, 1945

Two genera, namely *Orbitoclypeus* and *Asterocyclina*, are recorded from Verona. The equatorial layer of the first is unsubdivided into sublayers, whereas it is in the case of the last taxon.

Genus *Orbitoclypeus* Silvestri, 1907

This genus is represented in Verona, Castel San Felice by one single species.

© 2025 by the author(s). Distributed under a Creative Commons CC BY license.

Preprints.org (www.preprints.org) | NOT PEER-REVIEWED | Posted: 24 June 2025 doi:10.20944/preprints202506.1471.v2

Peer-reviewed version available at Geosciences 2025, 15, 334; doi:https://doi.org/10.3390/geosciences15090334

*Orbitoclypeus varians* (Kaufmann, 1867)

This widespread, unribbed species is small- to medium-sized, more or less inflate, with a "marthae"-type rosette. The excentri-to eulepidine embryo is small to medium-sized. Adauxiliary chamberlets are of "varians" type with average size and shape. The equatorial chamberlets are moderately wide and high, arranged into undulated annuli with "varians" type growth pattern.

*Orbitoclypeus varians* forms an evolutionary lineage with six chrono-subspecies as follows: *O. v. portnayae* ($d_{mean}$ < 165 µm; SBZ 10–11; OZ 5–8a); *O. v. ankaraensis* ($d_{mean}$=165–205 µm; SBZ 12–13, OZ 8b); *O. v. angoumensis* ($d_{mean}$=205–255 µm; SBZ 13–14; OZ 9–10); *O. v. roberti* ($d_{mean}$=255–320 µm; SBZ 15–17; SBZ 11–13); *O. v. scalaris* ($d_{mean}$=320–400 µm; SBZ 16–19; OZ 12–15) and *O. v. varians* ($d_{mean}$ > 400 µm; SBZ 17–20; OZ 13–16) [6,7].

*Orbitoclypeus varians* is the only representative of this genus in our samples, and based on its qualitative features cannot be confused with any other taxa. It occurs in all three samples of Castel San Felice but is most common in VER 4 and very rare in VER 3. Based on data in Tables 2–4, the populations of these two samples can be joined and determined as *O. v. varians*. However, the population of the VER 2 sample appears to be slightly less developed based on the values of parameter "d" and can be identified as *O. v. scalaris*.

*Orbitoclypeus varians scalaris* (Schlumberger, 1903)

Figure 19, Figure 21: A, B.

*Orthophragmina scalaris* n. sp. — [75]: 277–278, Plate 8: 4, Plate 9: 12–13.

*Orbitoclypeus varians scalaris* (Schlumberger) — [5]: 211–212, Plate 30: 6–12. (with synonymy) — [55]: Plate 3: 15, Plate 5: 7, 8. — [62]: Figures 28w–x, 29a–e. — [69]: Figures 34l, m, o. —[76]: Figure 14D. — [67]: Figures 18A, B. — [71]: Figure 26a. — [7]: Figures 28.3, 4, 37.10, 153.4–6, 156.

*Orbitoclypeus varians varians* (Kaufmann, 1867)

Figure 19, Figure 21: C–F.

*Orbitoides varians* n. sp. — [77]: 158–160, Plate 10: 1–10.

*Orbitoclypeus varians varians* (Kaufmann). — [5]: 212–214, Plate 31: 1–12, Plate 32: 1–4. (with synonymy). — [78]: 9, Plate 4: 1, Plate 5: 1–2. — [59]: Plate 1: 5, 6. — [55]: Figure 15. — [69]: Figure 34p. — [76]: Figures 14E–G. — [67]: Figure 18C. — [65]: Figure 15e–g. — [71]: Figures 26b– g. — [7]: Figures 153.7–9.

Genus *Asterocyclina* Gümbel, 1870

We found this genus in both Monte Cavro and Castel San Felice. It is represented by two species (*Asterocyclina alticostata* and *A. stellata*), which can be easily distinguished not only by their different types of adauxiliary chamberlets („alticostata" vs. „stellata") but also by their quantitative parameters (Tables 2–4 and Figure 23).

© 2025 by the author(s). Distributed under a Creative Commons CC BY license.

Preprints.org (www.preprints.org) | NOT PEER-REVIEWED | Posted: 24 June 2025 doi:10.20944/preprints202506.1471.v2

Peer-reviewed version available at Geosciences 2025, 15, 334; doi:https://doi.org/10.3390/geosciences15090334

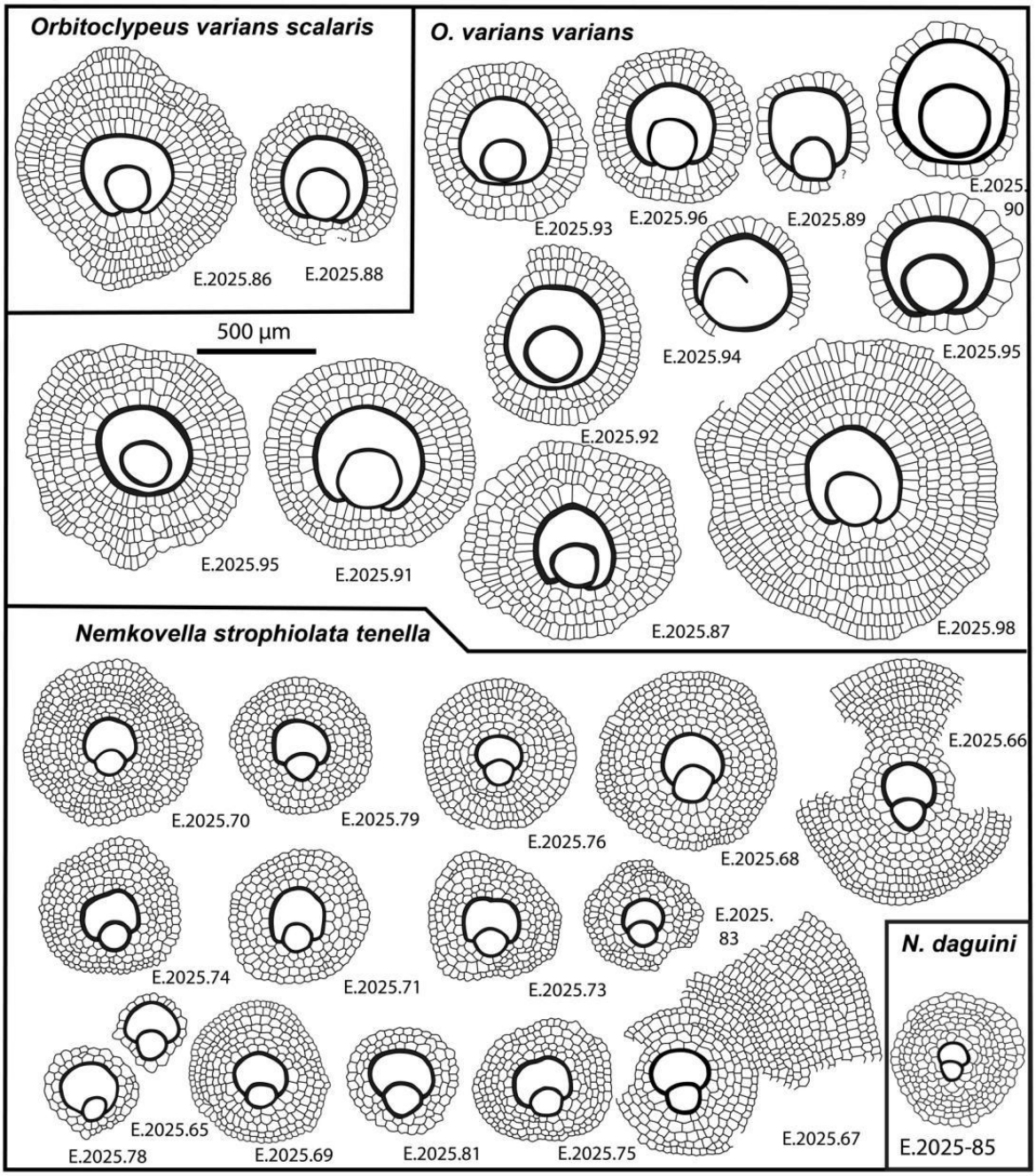


**Figure 19.** Line drawings of Orbitoclypeus varians scalaris (Schlumberger), O. v. varians (Kaufmann), Nemkovella strophiolata tenella (Gümbel) and N. daguini (Neumann).

*Asterocyclina alticostata* (Nuttall, 1926)

This widespread species is star-shaped, usually with five to seven rays and "chudeaui" type rosette. It has a medium-sized to relatively large isolepidine embryo, very few, very wide and moderately low, "alticostata" type adauxiliary chamberlets and also wide and moderately high equatorial chamberlets arranged into asteroidal annuli with "strophiolata" or "varians" type growth pattern.

*Asterocyclina alticostata* includes four subspecies as follows: *A. a. gallica* ($d_{mean}$ < 275 µm; SBZ 10–13; OZ 6–9); *A. a. cuvillieri* ($d_{mean}$=275–350 µm; SBZ 14–15; OZ 10–11); *A. a. alticostata* ($d_{mean}$=350–450 µm; SBZ 16–19a; OZ 12–14) and *A. a. danubica* ($d_{mean}$ > 450 µm; SBZ 18–20; OZ 14–16) [6,7].

© 2025 by the author(s). Distributed under a Creative Commons CC BY license.

Preprints.org (www.preprints.org) | NOT PEER-REVIEWED | Posted: 24 June 2025 doi:10.20944/preprints202506.1471.v2

Peer-reviewed version available at Geosciences 2025, 15, 334; doi:https://doi.org/10.3390/geosciences15090334

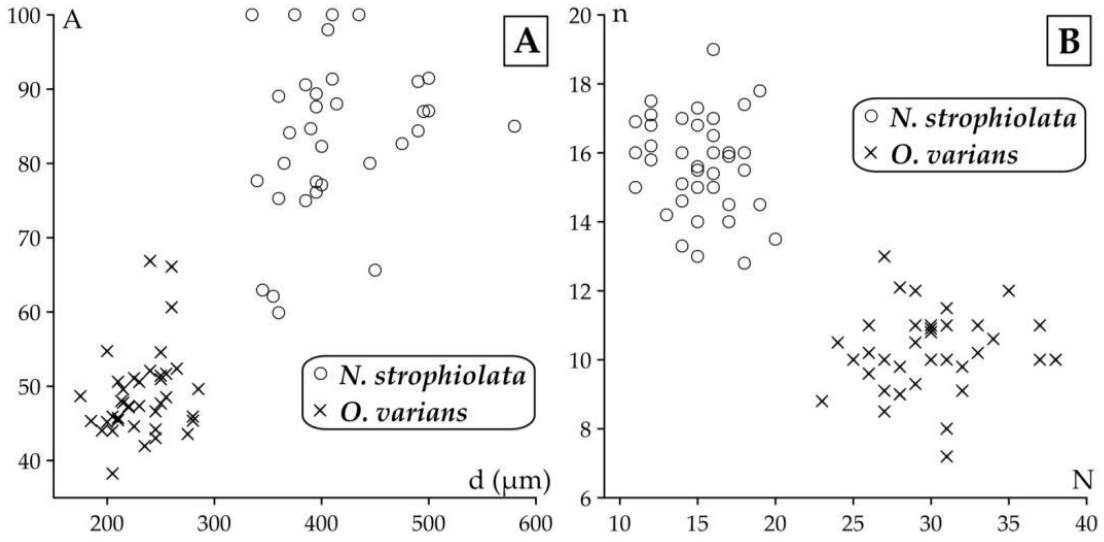


**Figure 20.** Distribution of *Nemkovella strophiolata tenella* and *Orbitoclypeus varians* specimens in samples VER 2–4 (A) on the d–A (deuteroconch diameter vs. deuteroconchal embracement) and (B) on the N–n (number of adauxiliary chamberlets vs. annuli number in the first 0.5 mm from the deuteroconch's rim) bivariate plots.

*Asterocyclina alticostata* occurs in all our samples from Verona, however it is extremely rare in all of them. Therefore, in sample VER 1 from Monte Cavro (where only one single specimen was found) it cannot be determined on the subspecies level, although the numerical parameters (Tables 2–4) are closest to *A. a. danubica*. The quantitative parameters of the three populations from Castel San Felice are similar, thus they can be jointly evaluated and determined as *A. a. danubica*.

*Asterocyclina alticostata danubica* Less, 1987

Figure 23: B–D, Figure 24.

1987 *Asterocyclina alticostata danubica* n. ssp. — [5]: 243–244, Plate 45: 4–11. (with synonymy).

*Asterocyclina alticostata danubica* Less — [55]: Plate 3: 27, 28. — [62]: Figures 31e–g. — [69]: Figure 35t. — [67]: 26, Figures 19A, B. — [71]: Figures 28b–d. — [7]: Figures 27.5, 159.9, 10, 160. — [56]: Figure 2K. — [68]: 467, Figures 4N–P.

*Asterocyclina stellata* (d'Archiac, 1846)

This widespread species is a star-shaped form usually with five rays and "marthae" type rosette. It has a small semi-iso- to nephrolepidine embryo, few, wide and low, "stellata" type adauxiliary chamberlets and also narrow and low equatorial chamberlets arranged into asteroidal annuli with "strophiolata" type growth pattern.

© 2025 by the author(s). Distributed under a Creative Commons CC BY license.

Preprints.org (www.preprints.org) | NOT PEER-REVIEWED | Posted: 24 June 2025 doi:10.20944/preprints202506.1471.v2

Peer-reviewed version available at Geosciences 2025, 15, 334; doi:https://doi.org/10.3390/geosciences15090334

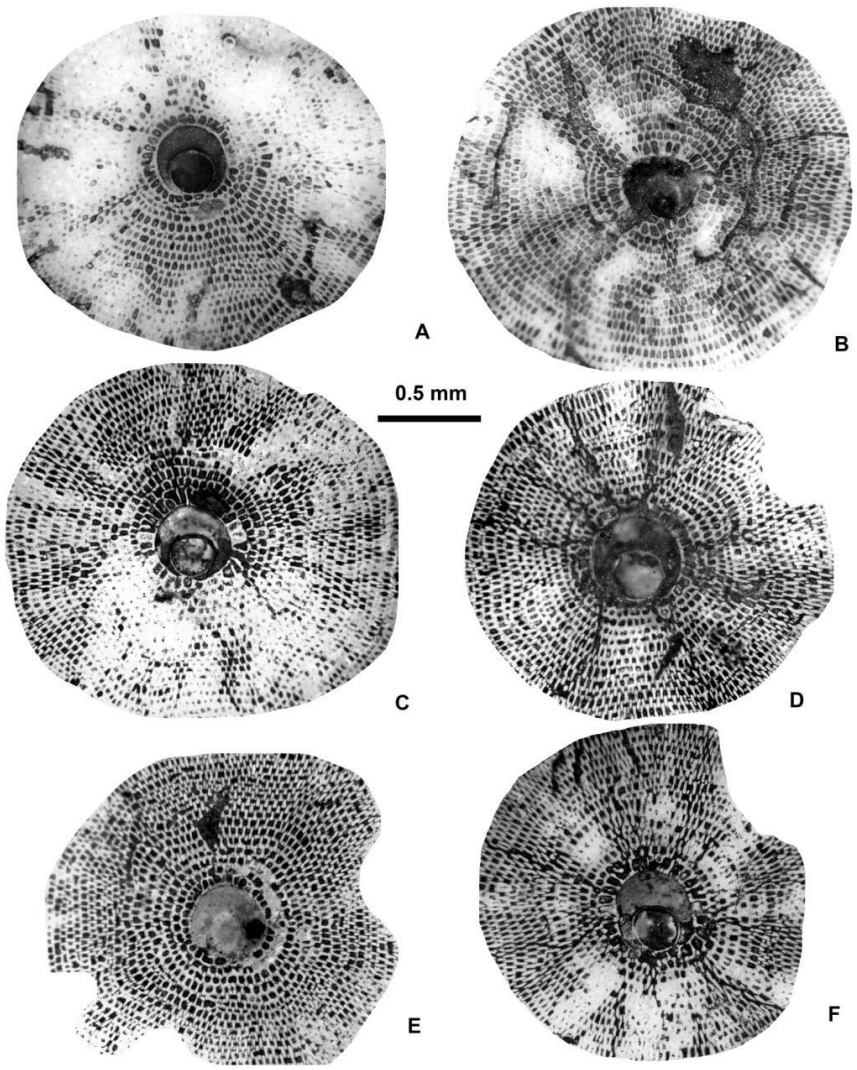


**Figure 21.** Equatorial sections of *Orbitoclypeus varians scalaris* (Schlumberger) (A, B) and *O. v. varians* (Kaufmann) (C–F). A: E.2025.88, B: E.2025.86, C: E.2025.100, D: E.2025.97, E: E.2025.93, F: E.2025.98. A, B: VER 2; C–F: VER 4. All A-forms.

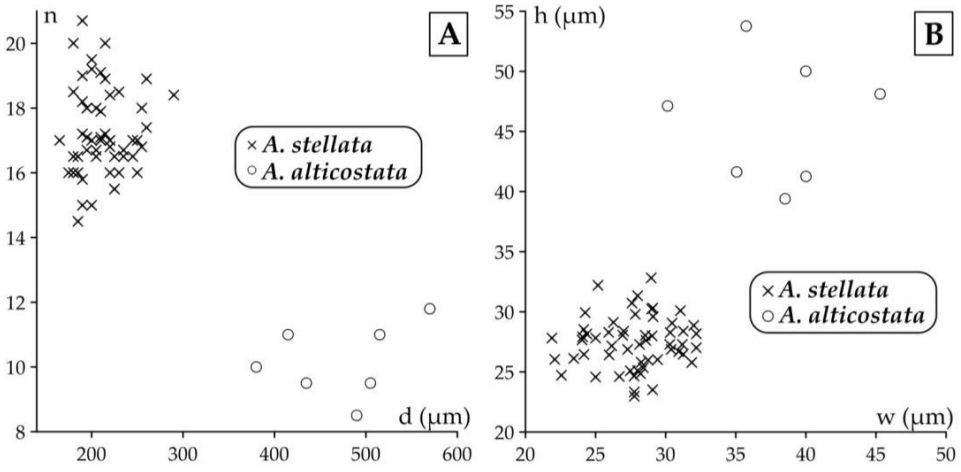


**Figure 22.** Distribution of *Asterocyclina alticostata danubica* and *A. stellata stellaris* specimens in samples VER 2–4 (A) on the d–n (deuteroconch diameter vs. annuli number in the first 0.5 mm from the deuteroconch's rim) and (B) on the w–h (width vs. height of the equatorial chamberlets) bivariate plots.

© 2025 by the author(s). Distributed under a Creative Commons CC BY license.

Preprints.org (www.preprints.org) | NOT PEER-REVIEWED | Posted: 24 June 2025 doi:10.20944/preprints202506.1471.v2

Peer-reviewed version available at Geosciences 2025, 15, 334; doi:https://doi.org/10.3390/geosciences15090334

*Asterocyclina stellata* is arbitrarily subdivided into four chrono-subspecies such as: *A. s. adourensis* ($d_{mean}$ < 150 μm; SBZ 10–16; OZ 6–12); *A. s. stellata* ($d_{mean}$=150–190 μm; SBZ 14–17; OZ 10–13); *A. s. stellaris* ($d_{mean}$=190–240 μm; OZ 13–15) and *A. s. buekkensis* ($d_{mean}$ > 240 μm; SBZ 20; OZ 16) [6,7].

*Asterocyclina stellata* is abundant in all samples from Castel San Felice (VER 2–4) and occurs rarely also in Monte Cavro (VER 1). This latter containing only two specimens can be determined as *A. s.* cf. *stellaris*, whereas the three populations from Castel San Felice (VER 2–4) bear similar quantitative parameters (Tables 2–4). Thus, they can be jointly evaluated and determined as *A. s. stellaris*.

*Asterocyclina stellata stellaris* (Brünner in Rütimeyer, 1850)

Figure 23: F–G, Figure 24, Figure 25: A–H.

*Orbitolites stellaris* Brünner 1848. — [79]: 118, Plate 5: 74.

*Asterocyclina stellata stellaris* (Brünner in Rütimeyer) — [5]: 236–237, Plate 39: 11–12, Plate 40: 1–11, Plate 41: 1–6. (with synonymy). — [80]: Plate 3: 3–5. — [78]: 1–4, Plate 6: 1–7, Figure 4. — [55]: Plate 4: 8–12. — [62]: Figures 29q–s. — [69]: Figures 35a–f. — [65]: Figures 15A–D. — [67]: 26, Figures 18G–K. — [71]: Figures 28e, g. — [7]: Figures 27.6, 172.7–8, 173. — [68]: 467, Plate 4: K. L.

*6.2. Family Nummulitidae de Blainville, 1827*

For the generic classification of the family, we apply the principles and subdivision of [40], with the addition by [81] on the distinction of *Assilina* and *Operculina*. Five genera are recorded in our material: three of them (*Nummulites*, *Assilina* and *Operculina*) with no secondary chamberlets, and the other two (*Heterostegina* and *Spiroclypeus*) with subdivided chambers. Our material from Verona is incorporated into the recent revision of the Eocene representatives of these last two genera [37,38], therefore, here we give only brief information about them. In our material we found only the megalospheric A-forms, so we will not deal with the B-forms in this paper.

© 2025 by the author(s). Distributed under a Creative Commons CC BY license.

Preprints.org (www.preprints.org) | NOT PEER-REVIEWED | Posted: 24 June 2025 doi:10.20944/preprints202506.1471.v2

Peer-reviewed version available at Geosciences 2025, 15, 334; doi:https://doi.org/10.3390/geosciences15090334

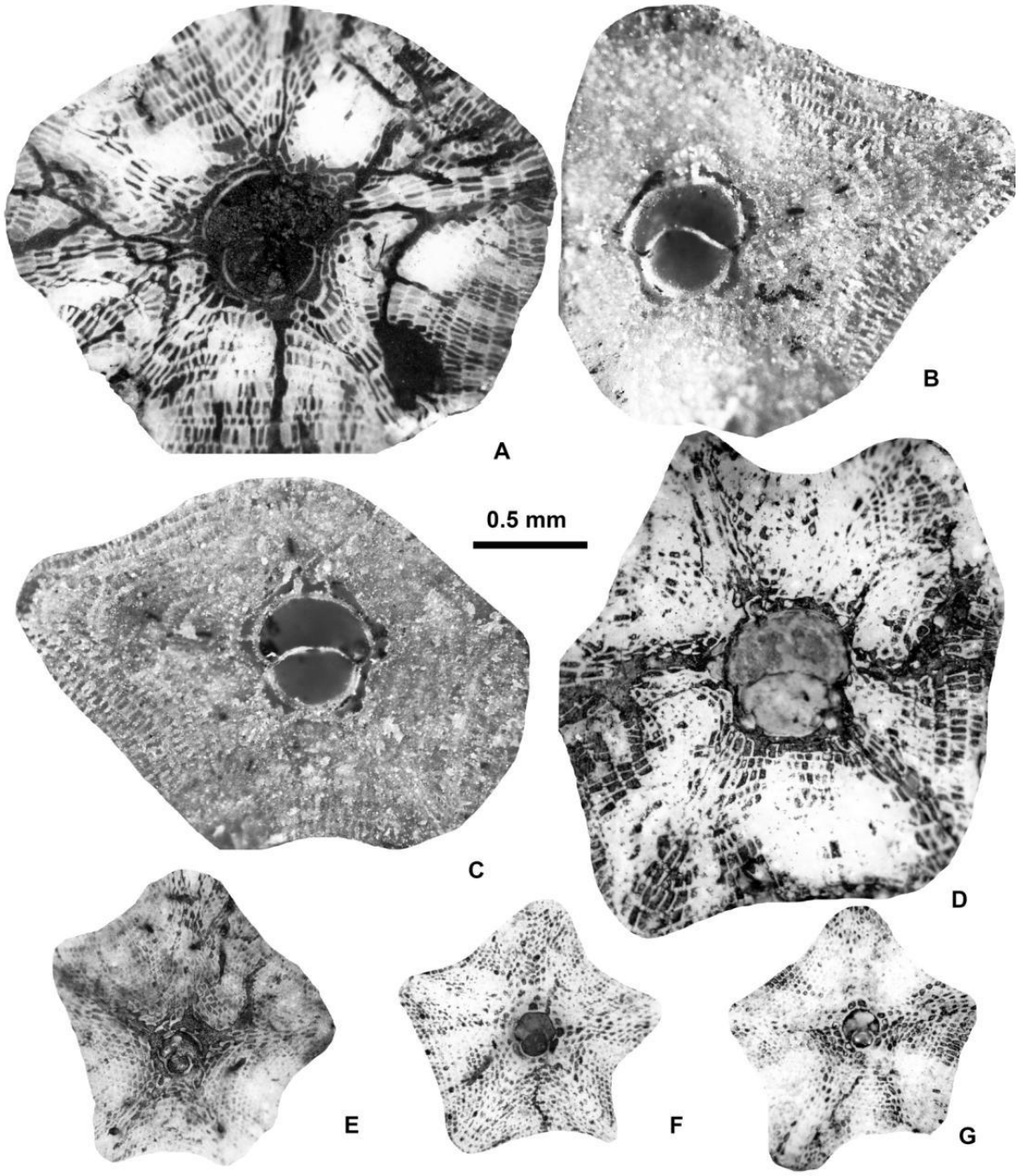


**Figure 23.** Equatorial sections of *Asterocyclina alticostata* indet.ssp. (A), *A. alticostata danubica* Less (B–D), *A. stellata* cf. *stellaris* (Brünner in Rütimeyer) (E) and *A. stellata stellaris* (Brünner in Rütimeyer) (F–G). A: E.2025.101, B: E.2025.104, C: E.2025.103, D: E.2025.106, E: E.2025.107, F: E.2025.118, G: E.2025.117. A, E: VER 1 (Monte Cavro 4); B, C: VER 3; D: VER 4; F, G: VER 2. All A-forms.

© 2025 by the author(s). Distributed under a Creative Commons CC BY license.

Preprints.org (www.preprints.org) | NOT PEER-REVIEWED | Posted: 24 June 2025 doi:10.20944/preprints202506.1471.v2

Peer-reviewed version available at Geosciences 2025, 15, 334; doi:https://doi.org/10.3390/geosciences15090334

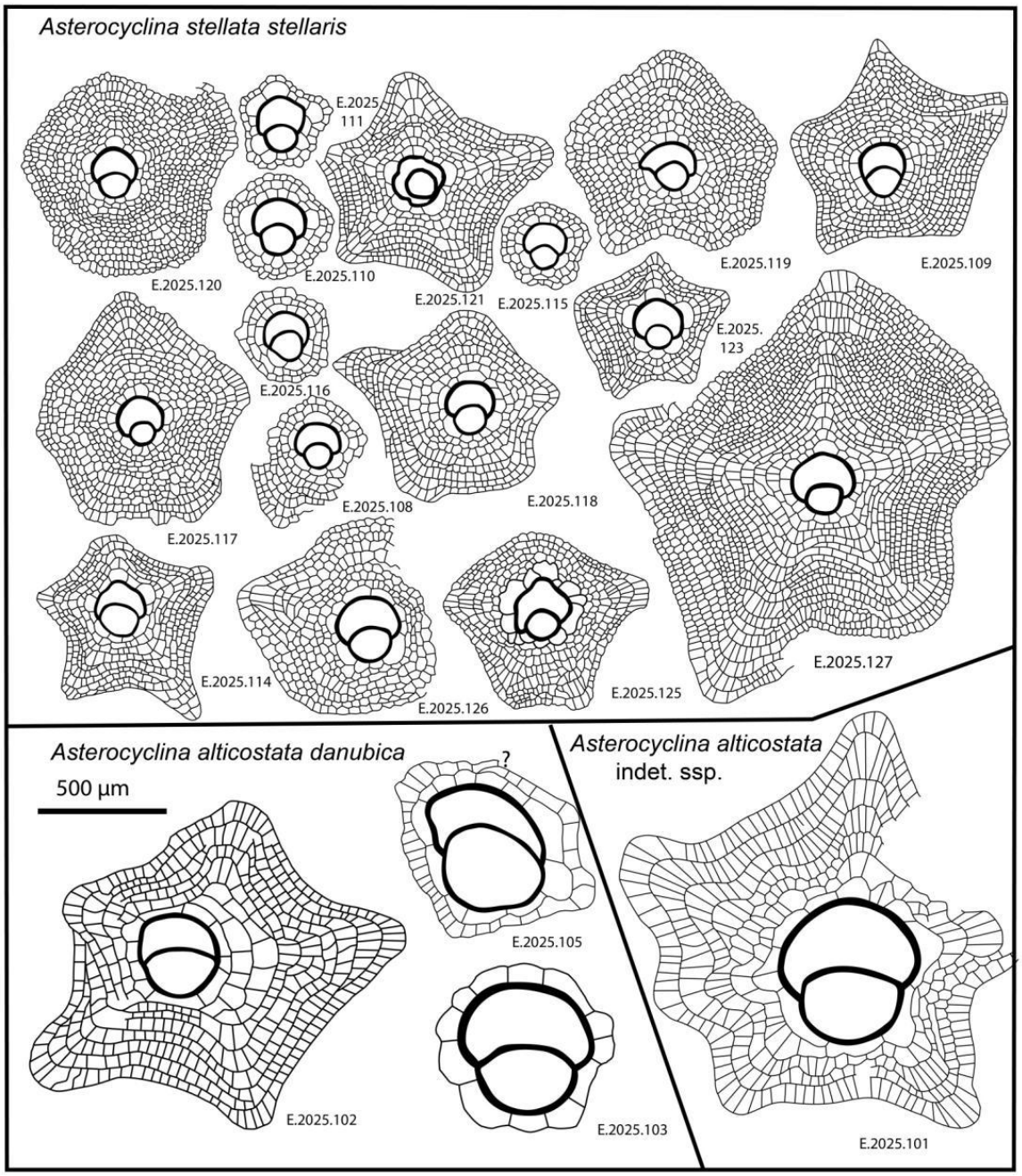


**Figure 24.** Line drawings of *Asterocyclina* from the vicinity of Verona.

6.2.1. Genus Nummulites Lamarck, 1801

The determination of *Nummulites* is based on both the surface characteristics and the features of the equatorial section. Based on their surface characteristics the representatives of genus *Nummulites* in the studied samples can be classified into two categories as follows: *N. hormoensis* and *N. fabianii* (being the successive members of the *N. fabianii* lineage) belong to the reticulate, while *N. incrassatus*, *N. chavannesi*, *N. pulchellus* and *N. budensis* to the radiate forms. Granulate forms are missing from our material.

© 2025 by the author(s). Distributed under a Creative Commons CC BY license.

Preprints.org (www.preprints.org) | NOT PEER-REVIEWED | Posted: 24 June 2025 doi:10.20944/preprints202506.1471.v2

Peer-reviewed version available at Geosciences 2025, 15, 334; doi:https://doi.org/10.3390/geosciences15090334

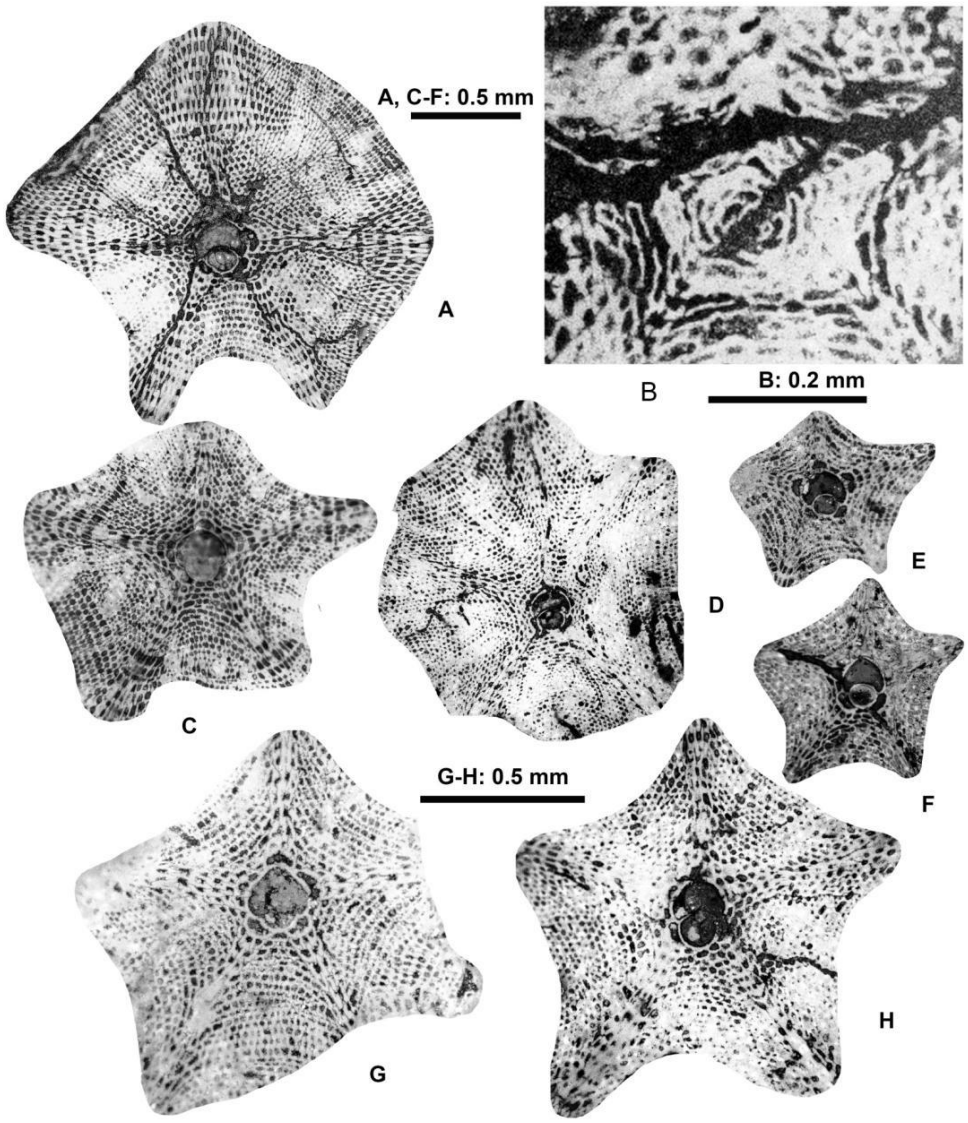


**Figure 25.** Equatorial sections of *Asterocyclina stellata stellaris* (Brünner in Rütimeyer). A: E.2025.113, B: E.2025.107, C: E.2025.128, D: E.2025.126, E: E.2025.123, F: E.2025.124, G: E.2025.121, H: E.2025.122. A: VER 2, B–F; H: VER 4; G: VER 3. B: B form, all the others are A-forms.

Following [59] a measurement and parameter system was introduced [82] to characterize the equatorial section of A-forms that is slightly modified here. It consists of four measurements (in μm) and two counts in the equatorial section of megalospheric (A) forms as listed below and shown in Figure 26. as well.

- P: inner cross-diameter of the proloculus;
- d: outer diameter of the two first whorls along the axis of the embryo;
- E: total number of chambers in the first two whorls (excluding the first two chambers). In Figure 26. these chambers are marked by + (E=19);
- M: inner diameter of the first three whorls along the axis of the embryo;
- D: outer diameter of the first three whorls along the axis of the embryo;
- N: exact number of chambers in the third whorl. In Figure 26. these chambers are marked by * (N=13.6).

Three of these parameters (P, d and E) are used directly; four other parameters are calculated as follows. Morphometric data are summarized in Table 5.

- L: $L=d\times\pi/N$ — estimated average length of chambers in the third whorl (in μm);

© 2025 by the author(s). Distributed under a Creative Commons CC BY license.

Preprints.org (www.preprints.org) | NOT PEER-REVIEWED | Posted: 24 June 2025 doi:10.20944/preprints202506.1471.v2

Peer-reviewed version available at Geosciences 2025, 15, 334; doi:https://doi.org/10.3390/geosciences15090334

- K=100×(D–d)/(D–P) — index of spiral opening (in %) expressed by the ratio of the height of the third whorl vs. the height of the first three whorls (without the proloculus);
- F: F=100×[(D–d)/2]/[(D–d)/2+L] — estimated isometry-index ("shape") of chambers in the third whorl (in %);
- m: m=100×(D–M)/(D–d) — relative width of the spiral cord in the third whorl (in %).

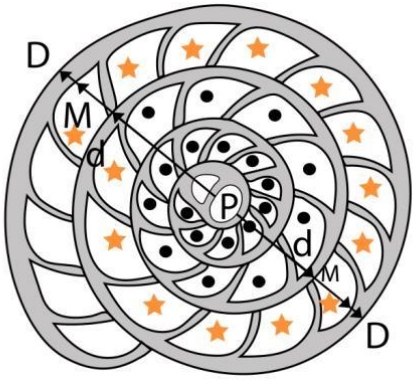


**Figure 26.** Measurement system for nummulitids without secondary chambers.

Although it is generally accepted that (like orthophragmines) *Nummulites* are also arranged in long-lived evolutionary lineages, not only their separation from each other, but also their internal subdivision is typology-based, and their constituent elements are considered separate species [35]. Attempts have been made to subdivide the lineages of *Nummulites* on a morphometric basis only in the case of reticulate forms (*N. fabianii* lineage: [62,69,71,83–87]; *N. ptukhiani* lineage: [88]). The *N. fabianii* lineage (occurring in both Monte Cavro and Castel San Felice) is arbitrarily subdivided into species by using the criteria shown in Table 5. Figure 27. shows the disposition of the two populations observed in our material (Monte Cavro: sample VER 1 and Castel San Felice: sample VER 2) in the P–L bivariate plot of Bartonian and Priabonian populations of the *N. fabianii* lineage.

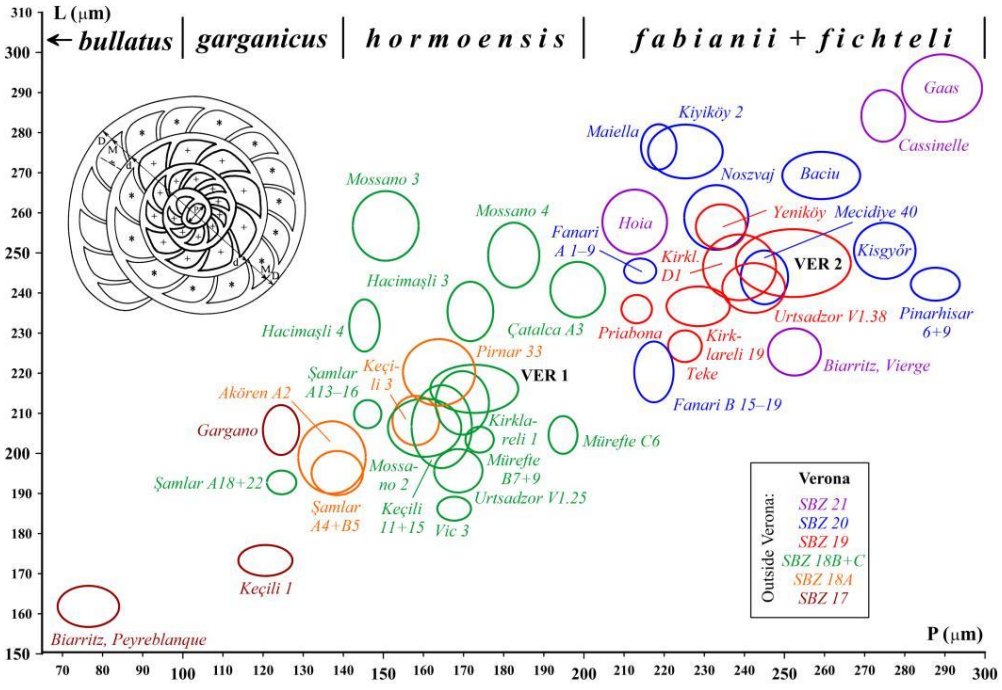


**Figure 27.** Distribution of populations of the *Nummulites fabianii* lineage (with their proposed specific subdivision [62]) from Verona and other localities from the peri-Mediterranean region (mean values at the 68% confidence

© 2025 by the author(s). Distributed under a Creative Commons CC BY license.

Preprints.org (www.preprints.org) | NOT PEER-REVIEWED | Posted: 24 June 2025 doi:10.20944/preprints202506.1471.v2

Peer-reviewed version available at Geosciences 2025, 15, 334; doi:https://doi.org/10.3390/geosciences15090334

level corresponding to 1 s.e.) on the P–L (inner cross diameter of the proloculus vs. average length of chambers in the third whorl) bivariate plot. For localities see [45,68,71].

*Nummulites hormoensis* Nuttall & Brighton, 1931

Figure 28: A–F.

*Nummulites hormoensis* n. sp. — [89]: 53–54, Plate 3: 1–8.

*Nummulites ptukhiani* Z. Kacharava — [35]: 125–126, Plate 49: 33–48.

*Nummulites* cf. *hormoensis* Nuttall & Brighton — [25]: Plate 1: 11, 12.

*Nummulites* '*ptukhiani*' Z. Kacharava — [83]: 161, 164–165, Plate 1: 16–24, Plate 2: 16–21. (with synonymy)

*Nummulites hormoensis* Nuttall & Brighton — [55]: Plate 1: 9, 17. — [62]: 65, Figures 31h–j. — [69]: Figures 37f, l, n–u. — [45]: Figure 5f. — [90]: Figure 13.1. — [65]: 80, figs 17f–h. — [71]: 922, Figures 16d–v.

Remarks. In the VER 1 sample from Monte Cavro, several reticulate *Nummulites* occur. Based on their morphometric data (Table 5), this population can safely be assigned to *N. hormoensis* whose stratigraphic range is limited to the SBZ 18 Zone, which recently [8,65] includes the terminal Bartonian and basal Priabonian. In the last few years, this species is described and discussed in detail from Turkey and Armenia in several papers [62,65,69,71]. Since specimens from the Monte Cavro population fit very well with these, here we do not present a detailed description of this species.

*Nummulites fabianii* (Prever in Fabiani, 1905)

Figure 28: G–K.

*Bruguieria fabianii* n. sp.— Prever in [91]: 1805, 1811.

*Nummulites fabianii* (Prever in Fabiani) — [83]: 165, 168, Plate 1: 1–15, Plate 2: 1–15. (with synonymy) — [62]: 65, Figures 31k, l. — [69]: Figures 37z, A–M. — [45]: Figure 9c. — [90]: Figure 13.2. — [76]: Figures 13A–F. — [92]: Figures 8A, B, D–G. — [71]: 922–924, Figures 16w–z, A–D, 18b, c. — [68]: 456, Plate 1: K–P.

*Nummulites retiatus* Roveda — [59]: 351–352, Plate 1: 13–14.

**Table 5.** Statistical data of *Nummulites* populations from Verona.

| Parameters | | Inner cross-diameter of the proloculus P (μm) | | | Outer diameter of the first two whorls d (μm) | | | Number of post-embryonic chambers in the first two whorls E | | | Index of spiral opening 3. whorl vs. first 3 whorls K=100×(D–d)/(D–P) | | |
|---|---|---|---|---|---|---|---|---|---|---|---|---|---|
| Taxon | Sample | № | range | mean ± s.e. | № | range | mean ± s.e. | № | range | mean ± s.e. | № | range | mean ± s.e. |
| *N. hormoensis* | **VER 1** | **15** | **100 – 235** | **172,7 ± 10,6** | **15** | **960 – 1360** | **1191 ± 30** | **15** | **21 – 26** | **22,87 ± 0,35** | **14** | **29,7 – 39,3** | **33,64 ± 0,70** |
| *N. fabianii* | **VER 2** | **9** | **180 – 340** | **252,2 ± 14,3** | **8** | **1190 – 1745** | **1446 ± 61** | **8** | **18 – 26** | **22,75 ± 0,82** | **7** | **26,8 – 41,0** | **33,09 ± 1,74** |
| *N. chavannesi* | **VER 2–4** | **19** | **150 – 450** | **264,2 ± 16,0** | **19** | **1060 – 2140** | **1507 ± 60** | **19** | **24 – 30** | **26,89 ± 0,45** | **19** | **33,7 – 55,6** | **43,20 ± 1,06** |
| | VER 2 | 15 | 160 – 350 | 259,0 ± 13,0 | 15 | 1060 – 1735 | 1466 ± 51 | 15 | 24 – 30 | 26,93 ± 0,47 | 15 | 37,1 – 55,6 | 44,50 ± 0,98 |
| | VER 3 | 2 | 210 450 | 330,0 | 2 | 1425 2140 | 1783 | 2 | 24 30 | 27,00 | 2 | 33,7 – 34,7 | 34,20 |
| | VER 4 | 2 | 150 – 325 | 237,5 | 2 | 1140 – 1925 | 1533 | 2 | 25 – 28 | 26,50 | 2 | 41,5 – 43,4 | 42,46 |
| *N. budensis* | **VER 1** | **1** | | **70,0** | **1** | | **780** | **1** | | **23,00** | **1** | | **51,70** |
| | **VER 2** | **1** | | **60,0** | **1** | | **650** | **1** | | **24,00** | **1** | | **45,37** |
| *N. pulchellus* | **VER 4** | **2** | **125 – 140** | **132,5** | **2** | **890 – 930** | **910** | **2** | **33 – 34** | **33,50** | **2** | **39,5 – 41,0** | **40,29** |
| *N. incrassatus* | **VER 1** | **5** | **160 – 200** | **185,0 ± 6,6** | **5** | **1090 – 1910** | **1466 ± 122** | **5** | **21 – 25** | **23,60 ± 0,78** | **5** | **30,4 – 38,5** | **34,39 ± 1,21** |
| | **VER 2+3** | **6** | **100 – 225** | **145,0 ± 16,1** | **6** | **990 – 1495** | **1168 ± 84** | **5** | **18 – 25** | **21,00 ± 1,17** | **6** | **32,3 – 42,7** | **38,82 ± 1,47** |
| | VER 2 | 5 | 100 – 225 | 145,0 ± 19,3 | 5 | 990 – 1495 | 1119 ± 84 | 5 | 18 – 25 | 21,00 ± 1,17 | 5 | 35,9 – 42,7 | 40,13 ± 1,02 |
| | VER 3 | 1 | | 145,0 | 1 | | 1415 | | | | 1 | | 32,27 |

| Parameters | | Third whorl: average length of chambers L=d×π/N (μm) | | | average shape of chambers F=100×(D–d)/(D–d+2d×π/N) | | | relative width of the spiral cord m=100×(D–M)/(D–d) | | |
|---|---|---|---|---|---|---|---|---|---|---|
| Taxon | Sample | № | range | mean ± s.e. | № | range | mean ± s.e. | № | range | mean ± s.e. |
| *N. hormoensis* | **VER 1** | **14** | **183 – 259** | **216,1 ± 5,8** | **14** | **48,6 – 60,1** | **54,34 ± 0,87** | **14** | **42,9 – 53,0** | **46,86 ± 0,87** |
| *N. fabianii* | **VER 2** | **7** | **220 – 287** | **247,5 ± 8,5** | **7** | **47,2 – 61,8** | **53,90 ± 1,92** | **7** | **28,5 – 42,2** | **38,00 ± 1,71** |
| *N. chavannesi* | **VER 2–4** | **19** | **170 – 292** | **222,4 ± 7,6** | **19** | **59,5 – 78,6** | **67,73 ± 1,01** | **19** | **8,9 – 23,2** | **12,78 ± 0,85** |
| | VER 2 | 15 | 170 – 278 | 218,3 ± 7,9 | 15 | 60,5 – 78,6 | 68,78 ± 0,98 | 15 | 8,9 – 23,2 | 12,02 ± 0,96 |
| | VER 3 | 2 | 218 292 | 255,3 | 2 | 59,5 59,6 | 59,58 | 2 | 14,0 14,7 | 14,34 |
| | VER 4 | 2 | 188 – 252 | 220,2 | 2 | 66,8 – 69,3 | 68,05 | 2 | 15,8 – 18,1 | 16,93 |
| *N. budensis* | **VER 1** | **1** | | **116,7** | **1** | | **76,51** | **1** | | **27,63** |
| | **VER 2** | **1** | | **113,5** | **1** | | **68,35** | **1** | | **18,37** |
| *N. pulchellus* | **VER 4** | **2** | **106 – 112** | **109,1** | **2** | **70,2 – 71,0** | **70,62** | **2** | **18,2 – 19,0** | **18,59** |
| *N. incrassatus* | **VER 1** | **5** | **200 – 316** | **236,6 ± 18,2** | **5** | **53,3 – 63,2** | **58,35 ± 1,79** | **5** | **25,7 – 54,9** | **33,03 ± 4,98** |
| | **VER 2+3** | **6** | **191 – 232** | **210,3 ± 6,4** | **6** | **52,6 – 65,5** | **60,30 ± 1,60** | **6** | **28,2 – 37,1** | **32,99 ± 1,30** |
| | VER 2 | 5 | 191 – 232 | 211,6 ± 7,6 | 5 | 52,6 – 65,5 | 60,41 ± 1,92 | 5 | 28,2 – 37,1 | 33,63 ± 1,39 |
| | VER 3 | 1 | | 203,9 | 1 | | 59,73 | 1 | | 29,75 |

© 2025 by the author(s). Distributed under a Creative Commons CC BY license.

Preprints.org (www.preprints.org) | NOT PEER-REVIEWED | Posted: 24 June 2025 doi:10.20944/preprints202506.1471.v2

Peer-reviewed version available at Geosciences 2025, 15, 334; doi:https://doi.org/10.3390/geosciences15090334

Remarks. Reticulate *Nummulites* are very rare in the samples from Castel San Felice, in fact only a few of them can be found and only in sample VER 2. Nevertheless, their quantity is just enough to assign them to *N. fabianii* based on their morphometric data (Table 5).

Formerly, *Nummulites fabianii* was believed to be an important leading fossil ("Leitfossil") of the Priabonian (interpreted as consisting of the SBZ 19 and 20 Zones) [83]. However, this needs to be slightly modified due to the revision of the Bartonian/Priabonian boundary [46,47], which induced the displacement of the SBZ 18B and C Subzones (formerly assigned to the terminal Bartonian) to the basal Priabonian [65,77]. Thus, the stratigraphic range of *N. fabianii* remains in the SBZ 19–20 interval (possibly extending to the SBZ 21 Zone), a time-period which, however, does not include the entire Priabonian. In recent years, this species is described and discussed in detail from Italy, Romania, Greece, Turkey and Armenia in several papers (see synonymy list). Since specimens from sample VER 2 fit very well with these, we do not repeat their description here.

*Nummulites budensis* Hantken, 1875

Figure 29: G.

*Nummulites budensis* n. sp. — [93]: 74, Plate 12: 4.

*Nummulites budensis* Hantken — [94]: 229–231, Plate 31: 16–20. — [59]: 354, Plate 2: 5, 6, 9, 10. (with synonymy) — [57]: 687, Plate 3: 19. — [62]: 69, Figure 34k. — [69]: 829, Figures 39K–Q. — [45]: Figure 9d. — [67]: 18. Figures 15A–C. — [68]: 454, Figure 1J.

Remarks. One specimen each of this radiate form was found in sample VER 1 of Monte Cavro and in sample VER 2 of the Castel San Felice. It can easily be identified based on its very small embryo, loose spiral, narrow and high chambers, straight near the base, and then strongly arched. *Nummulites budensis* does not yet fit into any evolutionary lineage. Its stratigraphic range was thought to be SBZ 19–20 [69], however the finding in sample VER 1 allows us to extend the above stratigraphic range a little down to almost the Bartonian/Priabonian boundary (SBZ 18C–19). The distinction from the early Rupelian *N. bouillei* and the Chattian *N. kecskemetii* is discussed in [59].

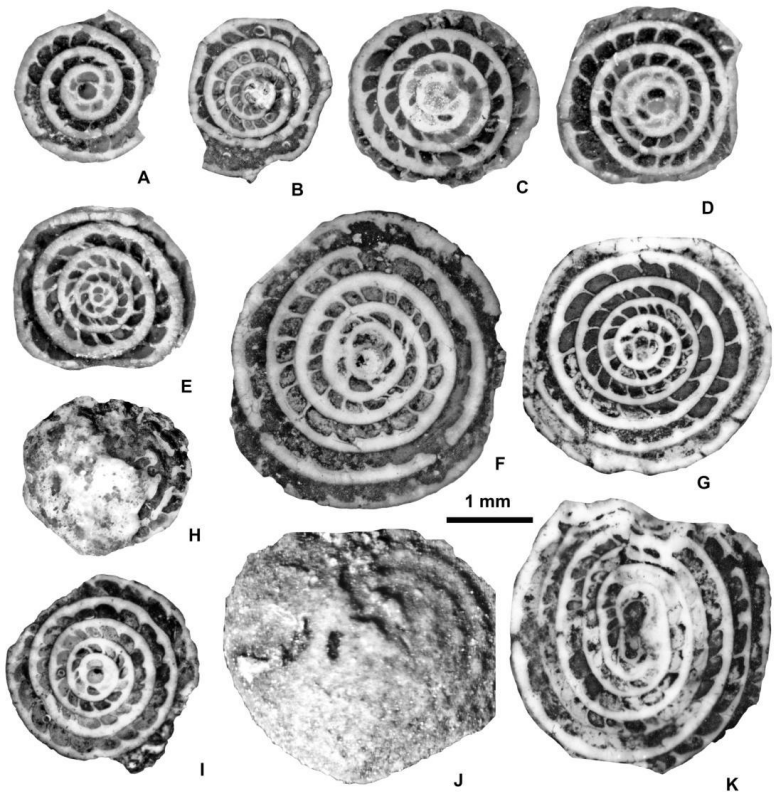


**Figure 28.** Equatorial sections and external views of reticulate *Nummulites*: *N. hormoensis* Nuttall & Brighton (A–F) and *N. fabianii* (Prever in Fabiani) (G–K). A: E.2025.132, B: E.06.36, C: E.2025.131, D: E.2025.130, F: E.06.50, G:

© 2025 by the author(s). Distributed under a Creative Commons CC BY license.

Preprints.org (www.preprints.org) | NOT PEER-REVIEWED | Posted: 24 June 2025 doi:10.20944/preprints202506.1471.v2

Peer-reviewed version available at Geosciences 2025, 15, 334; doi:https://doi.org/10.3390/geosciences15090334

E.06.53, H: E.06.34, I: E.06.33, J: E.06.50, K: E.2025.133. A–E; H, I: VER 1 (Monte Cavro 4); F, G, J, K: VER 2. All A-form.

*Nummulites chavannesi* de la Harpe, 1878

Figure 29: A–F.

*Nummulites chavannesi* n. sp. — [95]: 232 (nomen nudum).

*Nummulites chavannesi* de la Harpe — [96]: Plate 6: 22–41. — [97]: 123–125, Plate 2: 1–3, Figures 14–21. (with synonymy) — [69]: 827, Figures 39v, x–z, A, B. (with synonymy) — [71]: 925, 927, Figures 14g–q. — [68]: 454, 456, Plate 1: G.

Remarks. This radiate taxon with distinct umbo is characterized by a moderately small to medium-sized embryo, moderately opening spiral and moderately arched, relatively high chambers. *Nummulites chavannesi* does not yet fit into any evolutionary lineage. It occurs in all three samples of Castel San Felice: it is quite common in sample VER 2, however rare in the other two ones (VER 3 and 4). Compared to the specimens described under this name from other localities, the Verona individuals have the largest proloculus and differ from them in some other aspects as well. We think that *N. chavannesi* may be a collective term for closely related late Bartonian to Priabonian taxa and will need to be revised in the future. [3] indicate latest Bartonian to Priabonian (SBZ 18–20) for the stratigraphic range of this taxon, which does not need to be modified here.

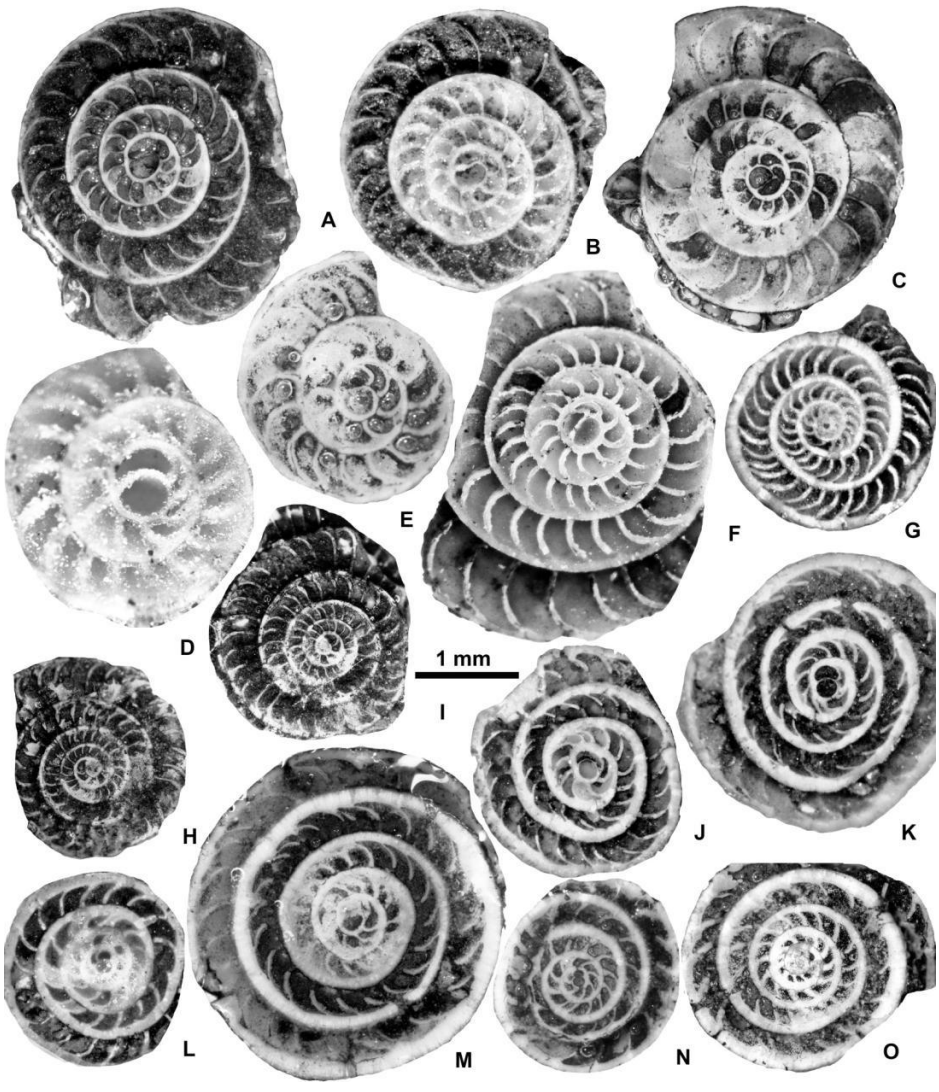


**Figure 29.** Equatorial sections of radiate *Nummulites*: *N. chavannesi* de la Harpe (A–F), *N. budensis* Hantken (G), *N. pulchellus* Hantken in de la Harpe (H, I) and *N. incrassatus* de la Harpe (J–O). A: E.2025.140, B: E.2025.141, C: E.2025.142, D: E.2025.143, E: E.2025.144, F: E.2025.145, G: E.2025.148, H: E.2025.147, I: E.2025.146, J: E.2025.134,

© 2025 by the author(s). Distributed under a Creative Commons CC BY license.

Preprints.org (www.preprints.org) | NOT PEER-REVIEWED | Posted: 24 June 2025 doi:10.20944/preprints202506.1471.v2

Peer-reviewed version available at Geosciences 2025, 15, 334; doi:https://doi.org/10.3390/geosciences15090334

K: E.2025.136, L: E.2025.135, M: E.2025.139, N: E.2025.137, O: E.2025.139. A–E, M–O: VER 2; F, H, I: VER 4, G, J–L): VER 1 (Monte Cavro 4). All A-forms.

*Nummulites incrassatus* de la Harpe, 1883

Figure 29: J–O.

*Nummulites Boucheri* var. *incrassata* n. var.— [96]: Plate 8: 53a.

*Nummulites incrassatus* de la Harpe — [69]: 823, Figures 39a–r. (with synonymy) — [71]: 917, Figures 14r–z. — [68]: 456, Plate 1: A–F.

Remarks. This name is generally used for moderately small radiate *Nummulites* with moderately small embryo, evenly coiled spiral and slightly arched, more or less isometric chambers from the Bartonian and Priabonian. In Verona, such forms occur in the Monte Cavro (sample VER 1) and rarely also in the Castel San Felice (samples VER 2 and VER 3, the latter only with a single specimen). Based on the great variability of such forms especially from N Thrace (NW Turkey) but also from other European sites [69] did not exclude that *N. incrassatus* may be a collective term for some taxa very close to each other, and they need a thorough revision. Until then, we must follow the old practice in joining these forms as *N. incrassatus*, which is believed to be the ancestor of the Rupelian *N. vascus* [35] forming an evolutionary lineage with it. [71] suggests a Bartonian to Priabonian age (SBZ 17–20) for the stratigraphic range of *N. incrassatus*, which is not contradicted in this study.

6.2.2. Genus Assilina d'Orbigny, 1839

Following [40] and [81], we consider *Assilina* as nummulitids with simple short sutural canals and nonfolded septa without apertures. This genus is represented in our material with one single species, belonging to the long-lasting (Ypresian to end-Priabonian), evolute *Assilina parva* – *A. schwageri* – *A. alpina* evolutionary lineage. The early part of this phylum is relatively poorly known. There exist, however, more data from the younger part. Although the morphometric limits between the more primitive, mostly Bartonian *A. schwageri* and the more advanced, mostly Priabonian *A. alpina* are not yet exactly defined, the mean inner cross-diameter of the proloculus for the first species is usually below 120 μm, while for the second it is above this value. Based on our measurements (Table 6) the few specimens from samples VER 3 and 4 can be jointly evaluated and determined as *A. alpina*.

*Assilina alpina* (Douvillé, 1916)

Figure 30: A–F.

*Operculina alpina* n. sp. — [98]: 329, Figure 1.

*Operculina alpina* Douvillé — [40]: 85, Plate 38: 4–6, Figure 34. (with synonymy).

*Assilina alpina* (Douvillé) — [59]: 356, Plate 2: 8. — [57]: 687, 689, Plate 4: 1–3. — [45]: Figure 9e. — [67]: 18, Figure 15I. — [71]: 925, Figures 18g–i, 19a–c. — [68]: 459, 462, Plate 3: A–D.

6.2.3. Genus Operculina d'Orbigny, 1826

Based on [40] and [81] *Operculina* is characterized by evolute or involute flattened test with dense and high chambers and folded septa, which are intersected by stolons [69]. This latter is essential in distinguishing *Operculina* from *Assilina*. This feature can be best observed in painted split equatorial sections (see Figures 29 G–I and also Figure 40. in [69]). This genus (as interpreted above) first appears around the Lutetian/Bartonian boundary and lasts until the end of the Priabonian with a single lineage [45], which starts with *O. bericensis*, followed by *O. roselli* and terminates with *O. gomezi* [40], but did not give their biometric limits.

The inner cross-diameter of the proloculus (P) does not show any clear increasing trend during the Bartonian to Priabonian interval [69] and remains in a range between 65 and 130 μm. Therefore, we rather join these forms under the name of *Operculina* ex gr. *gomezi*. They are very rare in Verona

© 2025 by the author(s). Distributed under a Creative Commons CC BY license.

Preprints.org (www.preprints.org) | NOT PEER-REVIEWED | Posted: 24 June 2025 doi:10.20944/preprints202506.1471.v2

Peer-reviewed version available at Geosciences 2025, 15, 334; doi:https://doi.org/10.3390/geosciences15090334

and recorded only from the Castel San Felice in samples VER 3 and 4 (see Table 6 for morphometric data).

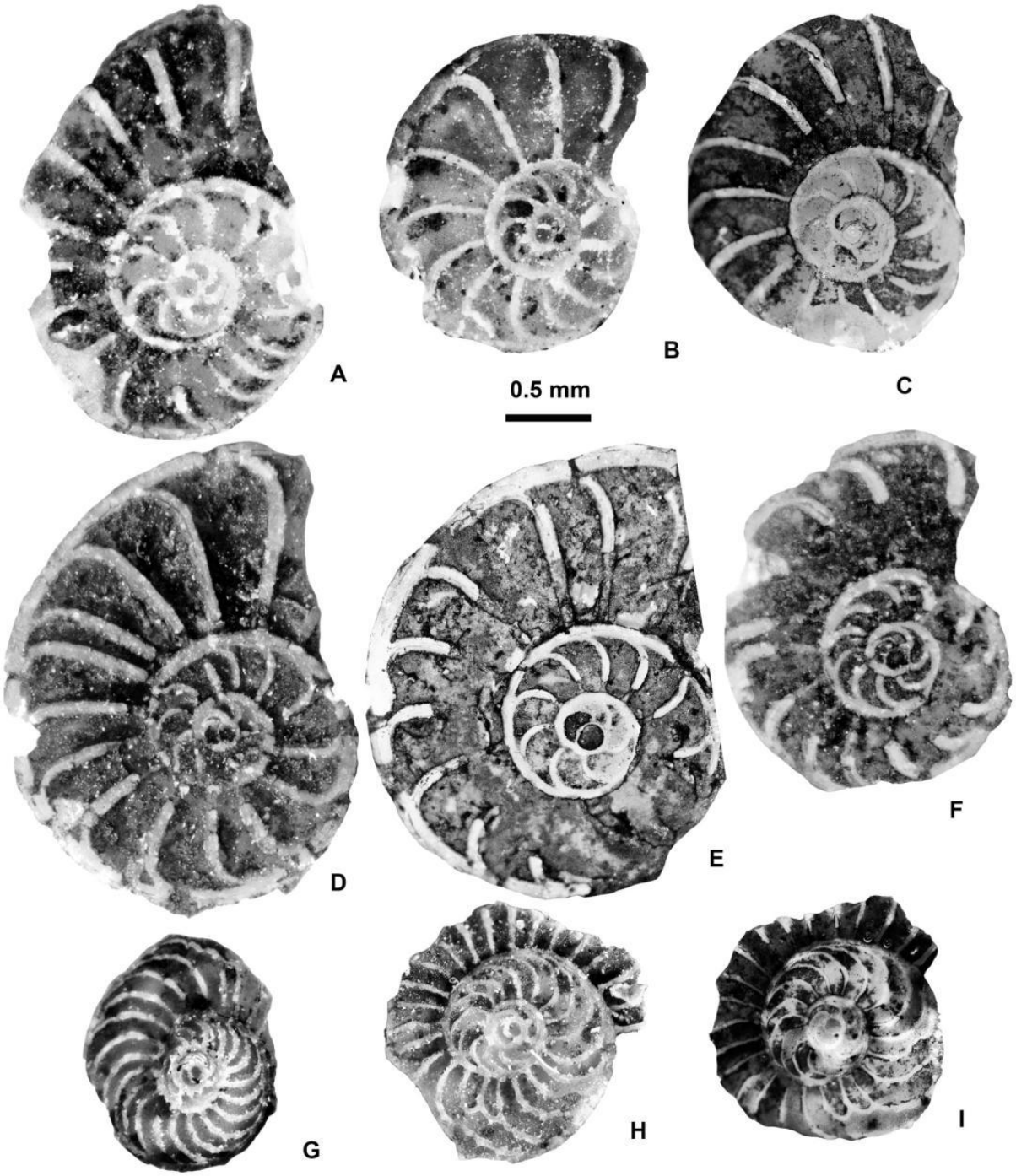


**Figure 30.** All A-forms. Equatorial sections of *Assilina alpina* Douvillé (A–F) and *Operculina* ex gr. *gomezi* Colom & Bauza (G–I). A: E.2025.149, B: E.2025.150, C: E.2025.152, D: E.2025.154, E: E.2025.151, F: E.2025.153, G: E.2025.155, H: E.2025.156, I: E.2025.157. A, B, E, G, H: VER 3; C, D, F, I: VER 4. All A-forms.

*Operculina* ex gr. *gomezi* Colom et Bauzá, 1950

Figure 29: G-I.

*Operculina gomezi* Colom et Bauzá — [40]: 98, 100, Figures 38A–F. (with synonymy). — [67]: 18, Figures 13N–R.

*Assilina gomezi* (Colom et Bauzá) — [59]: 354, Plate 2: 7.

© 2025 by the author(s). Distributed under a Creative Commons CC BY license.

Preprints.org (www.preprints.org) | NOT PEER-REVIEWED | Posted: 24 June 2025 doi:10.20944/preprints202506.1471.v2

Peer-reviewed version available at Geosciences 2025, 15, 334; doi:https://doi.org/10.3390/geosciences15090334

*Operculina* ex gr. *gomezi* Colom et Bauzá — [62]: 71, Figure 32x — [69]: Figures 40j–q — [71]: 925, Figures 19d–l — [68]: 458, 459, Plate 3: E–G.

**Table 6.** Statistical data of the of the inner cross-diameter of the proloculus of *Assilina* and *Operculina* populations from Verona (in μm).

| Taxon | Sample | № | range | mean ± s.e. |
|---|---|---|---|---|
| *Assilina alpina* | **VER 3+4** | **8** | **110 – 160** | **129 ± 6** |
| | VER 3 | 3 | 120 – 160 | 145 |
| | VER 4 | 5 | 110 – 130 | 120 ± 4 |
| *Operculina* ex. gr. *gomezi* | **VER 3+4** | **3** | **80 – 105** | **92** |
| | VER 3 | 2 | 80 – 90 | 85 |
| | VER 4 | 1 | | 105 |

6.2.4. Genus Heterostegina d'Orbigny, 1826

Genus *Heterostegina* bears all characteristics of genus *Operculina* with one exception: following the first, undivided chambers, the next ones are secondarily divided into chamberlets. Based on a widespread Mediterranean material, the Eocene representatives of this genus from the Western Tethys have recently been revised [37] and arranged into three species. These are *H. armenica*, *H. reticulata* and *H. gracilis*; the second of them occurring in our material. The simplified numerical characterization of *Heterostegina* is based on the system introduced for *Cycloclypeus* [100] and consists of two measurements and two counts as follows and shown also in Figure 31. Morphometric data are summarized in Table 7.

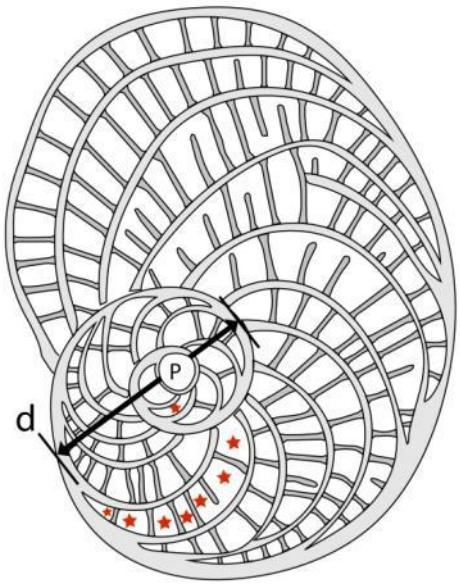


**Figure 31.** Measurement system for nummulitids with secondary chamberlets.

P: the inner cross−diameter of the proloculus in μm. The thickness of the wall is not measured.

X: the number of undivided, "operculinid" chambers before the appearance of the first subdivided, heterosteginid chamber, excluding the embryo (the first two chambers) (degree of „operculinid reduction). Undivided chambers, sometimes reappearing after the first heterosteginid chamber, are not counted. In Figure 31, X = 1.

© 2025 by the author(s). Distributed under a Creative Commons CC BY license.

Preprints.org (www.preprints.org) | NOT PEER-REVIEWED | Posted: 24 June 2025 doi:10.20944/preprints202506.1471.v2

Peer-reviewed version available at Geosciences 2025, 15, 334; doi:https://doi.org/10.3390/geosciences15090334

S: the number of chamberlets in the fourteenth chamber (including the embryo), reflecting the density of secondary chamberlets („heterosteginid escalation"). If this chamber is not subdivided into chamberlets, S = 1. In Figure 31, S = 7.

d: the maximum diameter of the shell in the first whorl as measured along the common symmetry axis of the embryo (the first two chambers) (in μm).

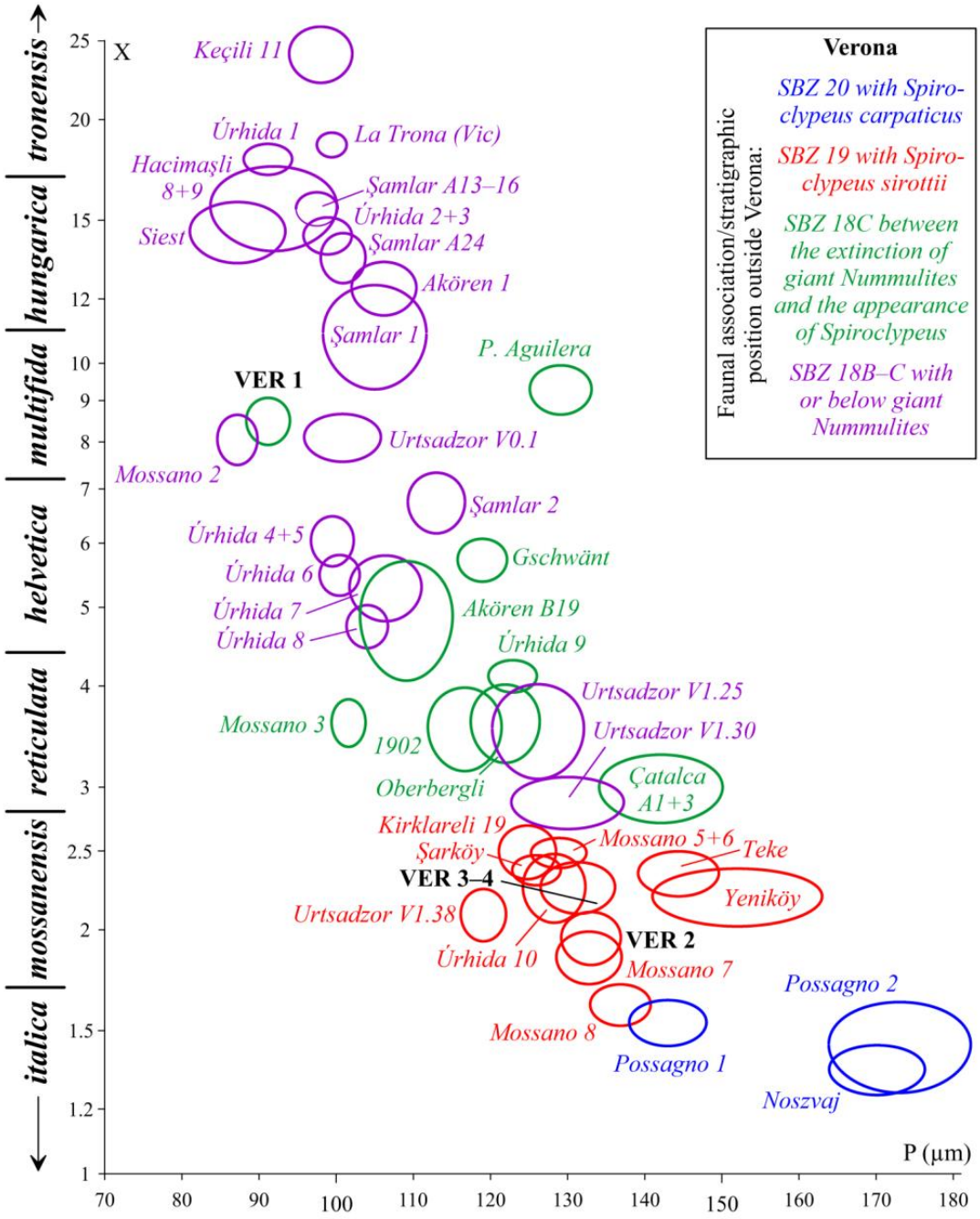


**Figure 32.** Distribution of *Heterostegina* populations from the vicinity of Verona (mean values at the 68% confidence level corresponding to 1 s.e.) on the P–X (proloculus diameter versus the number of undivided postembryonic chambers) bivariate plot (X is on a logarithmic scale) with the subspecific subdivision of *Heterostegina reticulata*. For localities see [45,71].

© 2025 by the author(s). Distributed under a Creative Commons CC BY license.

Preprints.org (www.preprints.org) | NOT PEER-REVIEWED | Posted: 24 June 2025 doi:10.20944/preprints202506.1471.v2

Peer-reviewed version available at Geosciences 2025, 15, 334; doi:https://doi.org/10.3390/geosciences15090334

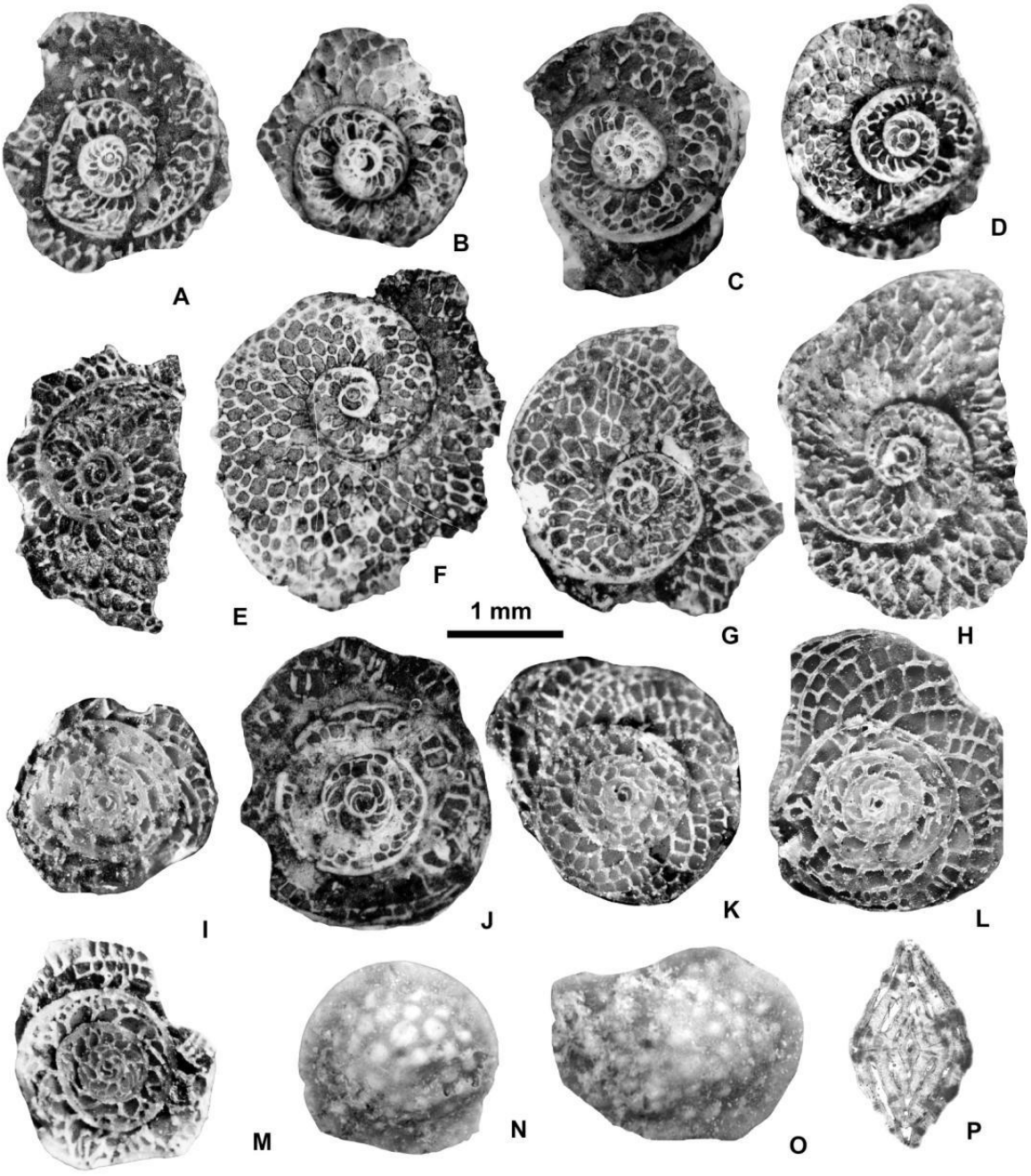


**Figure 33.** Equatorial and axial sections and external views of *Heterostegina reticulata multifida* Bieda (A–D), *H. reticulata mossanensis* Less et al. (E–H) and *Spiroclypeus sirottii* Less & Özcan (I–P). A: E.9527, B: E.9526, C: E.2025.158, D: E.9525, E: E.9562, F: E.9565, G: E.2025.159, H: E. 9563, I: E.2025.160, J: E.9588, K: E.9586, L: E.2025.161, M: E.9587, N: E.07.01, O: E.07.02, P: E.08.02. A–D: VER 1 (Monte Cavro 4); E, G, H, K–P: VER 4; F, J: VER 2; I: VER 3. All A-forms.

*Heterostegina reticulata* Rütimeyer, 1850

This species without granules has an involute, biconvex test with central pile and slightly sigmoid septal sutures passing sooner or later into septal network towards the edges. The size of the proloculus is increasing in stratigraphic order from small to medium-sized chamberlets (with no incomplete secondary septa) are changing simultaneously from rather irregularly arranged and rhomboid to regularly arranged and almost rectangular. Their number in chamber 14 (parameter S) also increases in stratigraphic order but usually does not exceed 7–8. The number of operculinid

© 2025 by the author(s). Distributed under a Creative Commons CC BY license.

Preprints.org (www.preprints.org) | NOT PEER-REVIEWED | Posted: 24 June 2025 doi:10.20944/preprints202506.1471.v2

Peer-reviewed version available at Geosciences 2025, 15, 334; doi:https://doi.org/10.3390/geosciences15090334

(undivided) chambers (parameter X) is strongly reduced during the phylogenesis, which can be very well seen on the P–X bivariate plot of Figure 32. as well.

Based on the operculinid reduction, *Heterostegina reticulata* is subdivided into seven chronosubspecies as follows: *H. r. tronensis* ($X_{mean}$ > 17; SBZ 18B), *H. r. hungarica* ($X_{mean}$ = 11–17; SBZ 18B), *H. r. multifida* ($X_{mean}$ = 7.2–11; SBZ 18C), *H. r. helvetica* ($X_{mean}$ = 4.4–7.2; SBZ 18C), *H. r. reticulata* ($X_{mean}$ = 2.8–4.4; SBZ 18C), *H. r. mossanensis* ($X_{mean}$ = 1.7–2.8; SBZ 19A) and *H. r. italica* ($X_{mean}$ < 1.7; SBZ 19B–20) [37].

*Heterostegina reticulata* occurs in all our samples. The population of sample VER 1 sample from Monte Cavro is determined as *H. r. multifida* whereas those from the Castel San Felice are assigned to *H. r. mossanensis*. The population of sample VER 2 appeared to be slightly more advanced than those of samples VER 3 and 4 very similar to each other and, therefore, could be evaluated jointly as well.

*Heterostegina reticulata multifida* (Bieda, 1949)

Figure 33: A–D, Figure 34.

*Grzybowskia multifida* sp. nov. — [101] (partim): 153–158, 168–173, Plate 3: 1, 3, 7; Plate 4: 1. (non 2).

*Heterostegina reticulata multifida* (Bieda) — [37]: 335–336, Figures 12J–M, O–Q. (with synonymy) — [71]: Figures 20a–f.

*Heterostegina reticulata mossanensis* Less, Özcan, Papazzoni & Stockar, 2008

Figure 33: E–H, Figure 34.

*Heterostegina reticulata mossanensis* n. ssp. — [37]: 336, 338, Figures 14G–R, 15A–C (with synonymy)

*Heterostegina reticulata mossanensis* Less, Özcan, Papazzoni & Stockar — [62]: Figures 32b–f. — [69]: Figures 42r–s. — [45]: Figure 9b. — [71]: Figure 21b.

**Table 7.** Statistical data of *Heterostegina* and *Spiroclypeus* populations from Verona.

| Parameters | | Inner cross-diameter of the proloculus P (μm) | | | Number of post-embryonic pre-heterosteginid chambers X | | | Number of chamberlets in the fourteenth chamber S | | | Outer diameter of the first whorl d (μm) | | | Subspecific determination |
|---|---|---|---|---|---|---|---|---|---|---|---|---|---|---|
| Taxon | Sample | № | range | mean ± s.e. | № | range | mean ± s.e. | № | range | mean ± s.e. | № | range | mean ± s.e. | |
| *Heterostegina reticulata* | **VER 1** | **28** | **60 – 135** | **91,2 ± 2,8** | **28** | **4 – 17** | **8,50 ± 0,57** | **28** | **1 – 3** | **2,00 ± 0,12** | **28** | **442 – 760** | **569 ± 15** | *multifida* |
| | **VER 2** | **23** | **100 – 160** | **133,0 ± 3,9** | **23** | **1 – 4** | **1,96 ± 0,15** | **22** | **3 – 6** | **4,41 ± 0,18** | **22** | **427 – 1120** | **832 ± 35** | *mossanensis* |
| | **VER 3+4** | **27** | **90 – 185** | **131,3 ± 4,8** | **27** | **1 – 5** | **2,26 ± 0,17** | **25** | **3 – 6** | **4,68 ± 0,19** | **26** | **510 – 1200** | **862 ± 31** | |
| | VER 3 | 11 | 90 – 185 | 137,4 ± 9,2 | 11 | 1 – 3 | 2,27 ± 0,24 | 9 | 3 – 6 | 5,00 ± 0,41 | 10 | 510 – 1200 | 885 ± 70 | *mossanensis* |
| | VER 4 | 16 | 105 – 185 | 127,2 ± 5,2 | 16 | 1 – 5 | 2,25 ± 0,23 | 16 | 3 – 5 | 4,50 ± 0,18 | 16 | 710 – 1080 | 848 ± 28 | |
| *Spiroclypeus sirottii* | **VER 2–4** | **52** | **55 – 115** | **86,6 ± 2,0** | **52** | **2 – 10** | **4,52 ± 0,26** | **52** | **2 – 5** | **2,87 ± 0,11** | **52** | **340 – 710** | **532 ± 11** | — |
| | VER 2 | 12 | 72 – 105 | 91,9 ± 3,1 | 12 | 2 – 6 | 3,92 ± 0,34 | 12 | 2 – 5 | 3,25 ± 0,27 | 12 | 461 – 710 | 572 ± 24 | |
| | VER 3 | 19 | 55 – 110 | 86,8 ± 3,3 | 19 | 2 – 10 | 5,11 ± 0,49 | 19 | 2 – 4 | 2,79 ± 0,12 | 19 | 340 – 660 | 524 ± 20 | |
| | VER 4 | 21 | 57 – 115 | 83,5 ± 3,2 | 21 | 2 – 8 | 4,33 ± 0,41 | 21 | 2 – 4 | 2,71 ± 0,17 | 21 | 410 – 650 | 518 ± 14 | |

Genus *Spiroclypeus* Douvillé, 1905

*Spiroclypeus* is a planispiral, lamellar, finely perforated, involute foraminifer [40]. Externally (Figure 33: N, O), the test is biconvex with a very slightly eccentric outline. Most of the surface is covered by granules. Its chambers in the equatorial plane become secondarily subdivided into regularly arranged secondary chamberlets by well–developed, complete secondary septa at different moments of their ontogeny. The spiral chambers never develop into annular ones. The diagnostic feature of *Spiroclypeus* that distinguishes it from *Heterostegina* is the presence of lateral chamberlets (Figure 33: P), symmetrically on both sides of the spiral. The network of chamberlets can be frequently seen on its very edge.

Based on widespread Mediterranean material, the Eocene representatives of this genus from the Western Tethys have recently been revised, and one single evolutionary lineage was recognized [38].

© 2025 by the author(s). Distributed under a Creative Commons CC BY license.

Preprints.org (www.preprints.org) | NOT PEER-REVIEWED | Posted: 24 June 2025 doi:10.20944/preprints202506.1471.v2

Peer-reviewed version available at Geosciences 2025, 15, 334; doi:https://doi.org/10.3390/geosciences15090334

Due to the similar architecture of their equatorial plane, the same measurement system is applied to *Spiroclypeus* as to *Heterostegina* (see above). Morphometric data are summarized in Table 7.

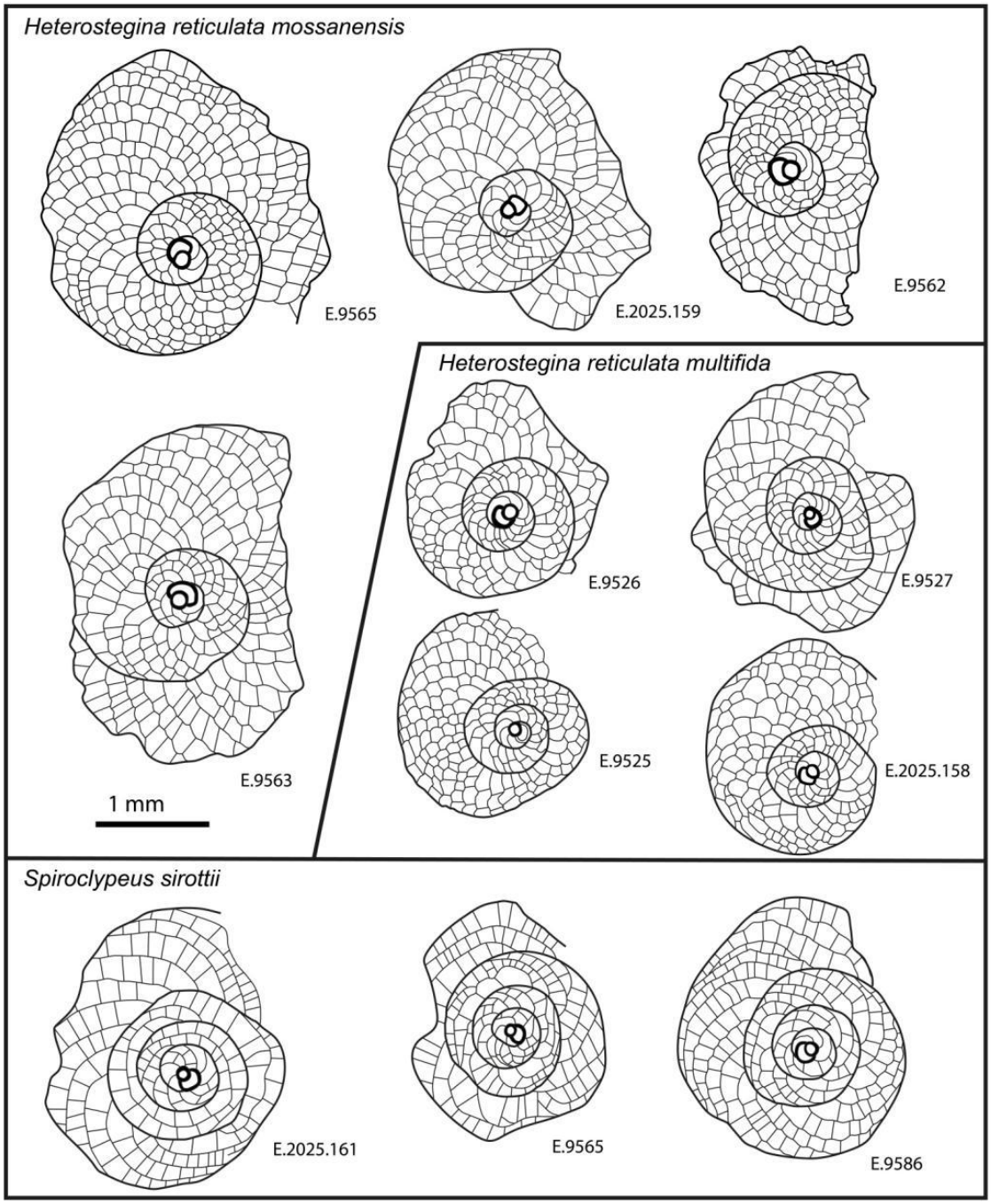


**Figure 34.** Line drawings of the *Heterostegina* and *Spiroclypeus* from the vicinity of Verona.

The developmental trends within the evolutionary lineage of Tethyan *Spiroclypeus* are the same as discussed in detail at *Heterostegina reticulata*. Based on these two separate taxa could be distinguished that are interpreted as species since no gradual transition could be observed between them (unlike in the case of *Heterostegina reticulata* with subspecies). Based on the operculinid reduction (see also the P–X bivariate plot of Figure 35), the evolutionary lineage of Eocene *Spiroclypeus* in the Western Tethys is subdivided into two species [38] as follows: *S. sirottii* ($X_{mean}$ > 2.7; SBZ 19) and *S. carpaticus* ($X_{mean}$ < 2.7; SBZ 20).

© 2025 by the author(s). Distributed under a Creative Commons CC BY license.

Preprints.org (www.preprints.org) | NOT PEER-REVIEWED | Posted: 24 June 2025 doi:10.20944/preprints202506.1471.v2

Peer-reviewed version available at Geosciences 2025, 15, 334; doi:https://doi.org/10.3390/geosciences15090334

*Spiroclyeus* is absent in sample VER 1 from Monte Cavro, however common in all three samples (VER 2–4) of the Castel San Felice. Due to their similar morphometric parameters, they can be jointly evaluated and determined as *S. sirottii.*

6.2.5. *Spiroclypeus sirottii* Less & Özcan, 2008

Figure 33: I–P, Figure 34.

*Spiroclypeus sirottii* n. sp.— [38]: 310–311, Figures 7A–N, P, Q, T. (with synonymy)

*Spiroclypeus sirottii* Less & Özcan — [62]: 72, Figures 32g–m. — [69]: 838, Figures 40D, E. — [45]: Figure 9a. — [90]: Figures 13.5, 6. — [71]: 928, Figure 21c.

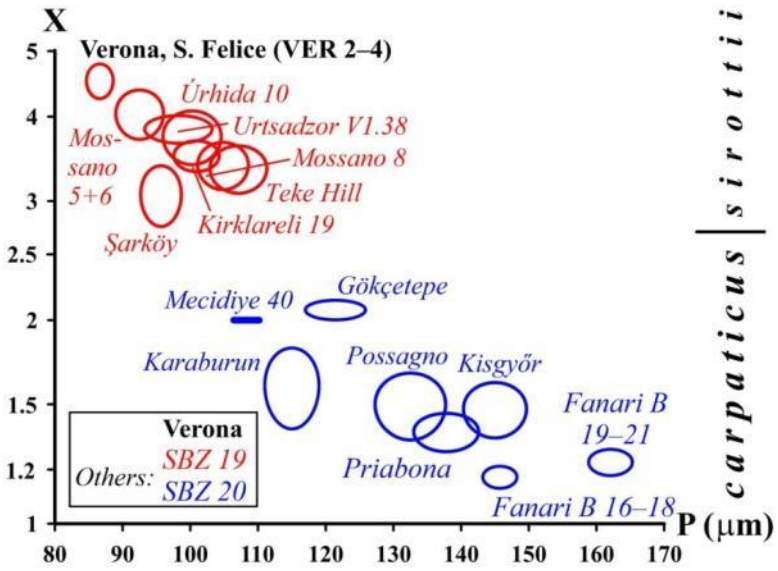


**Figure 35.** Distribution of the *Spiroclypeus* population from Verona (mean values at the 68% confidence level corresponding to 1 s.e.) on the P–X (proloculus diameter v. the number of undivided postembryonic chambers) bivariate plot (X is on a logarithmic scale) with the specific subdivision of Eocene *Spiroclypeus*. Information on localities in Turkey, Armenia and Europe was given by [38,62,67–69,71].

## 7. Discussion

*7.1. Comparison with Other LBF Key Assemblages*

The LBF fauna found in sample VER 1 on Monte Cavro is rather poor. Nevertheless, it contains a sufficient number of *Heterostegina reticulata multifida*, which clearly defines the SBZ 18C subzone. This is supported by the fact that *Nummulites hormoensis*, characteristic of SBZ 18, is also present in significant numbers whereas genus *Spiroclypeus,* first appearing in SBZ 19, is missing. However, since radiate *Nummulites* and especially orthophragmines occur only sporadically, this assemblage cannot be considered as a key LBF fauna, just as the upper part of Monte Cavro is not really a key locality for the SBZ 18C Subzone. The most diverse LBF assemblages of this age are found in Şamlar (NW Turkey, samples 1 and 2) [69], Úrhida (Hungary, samples 4–9, mostly yet unpublished) [37] and in Urtsadzor (Armenia, samples V.01, V1 25 and 30) [71].

On the other hand, the LBF fauna around Castel San Felice is both very diverse and very well preserved. From the point of view of dating the most important is the presence of *Heterostegina reticulata mossanensis*, which is limited to SBZ 19A Subzone. This age is also supported by the mass occurrence of *Spiroclypeus sirottii*, which is characteristic of the SBZ 19 Zone, and the sporadic presence of *Nummulites fabianii* (SBZ 19–20 Zones). The orthophragmines, characteristic of the OZ 14 Zone, are abundant, and significantly predominate over the radiate *Nummulites*.

© 2025 by the author(s). Distributed under a Creative Commons CC BY license.

Preprints.org (www.preprints.org) | NOT PEER-REVIEWED | Posted: 24 June 2025 doi:10.20944/preprints202506.1471.v2

Peer-reviewed version available at Geosciences 2025, 15, 334; doi:https://doi.org/10.3390/geosciences15090334

**Table 8.** Distribution of LBF in some key-localities for the SBZ 19A Zone. Thick lines indicate transitional (ex. interc.) populations. [1][6,25], [2][37] and GL's unpublished data, [3][55], [4][62], [5][69], [6][71].

| Taxa/localities | | Verona, Castel San Felice (this work) | Mossano, Priabona Marl, basal layers[1] | Úrhida 10[2] | Şarköy 2+4[3] | Teke 1–8[4] | Kırklareli C 19[5] | Urtsadzor V1. 38[6] |
|---|---|---|---|---|---|---|---|---|
| *Discocyclina augustae olianae* | | | | | × | | | |
| *D. augustae augustae* | | × | × | × | | | × | cf. |
| *D. dispansa dispansa* | | × | × | × | | | | cf. |
| *D. dispansa umbilicata* | | | | | × | | | |
| *D. euaensis* | | × | | × | | × | × | |
| *D. nandori* | | | × | × | × | | | |
| *D. pratti minor* | | × | | × | | | | cf. |
| *D. radians radians* | | cf. | | × | | | cf. | cf. |
| *D. samantai* | | | | | | | × | |
| *D. trabayensis elazigensis* | | × | × | | × | | | |
| *Nemkovella strophiolata tenella* | | × | × | × | | | | |
| *N. daguini* | | × | | | × | | | |
| *Orbitoclypeus varians scalaris* | | × | | | | × | | |
| *O. varians varians* | | × | × | × | | | × | × |
| *O. zitteli* | | | × | | | × | | × |
| *Asterocyclina alticostata alticostata* | | | × | | | | × | cf. |
| *A. alticostata danubica* | | × | | | | cf. | | |
| *A. kecskemetii* | | | | × | | × | | |
| *A. stella stella* | | | × | × | × | | | × |
| *A. stellata stellaris* | | × | × | × | × | × | × | |
| *A. ferrandezi ferrandezi* | | | | | × | × | × | |
| *Nummulites fabianii* | | × | rare | | | × | × | × |
| radiate *Nummulite* | *N. incrassatus* | × | × | to be studied | not studied | not studied | × | × |
| | *N. chavannesi* | × | × | | | | × | × |
| | *N. pulchellus* | × | × | | | | | |
| | *N. budensis* | × | | | | | | × |
| | *N. cunialensis* | | | | | | × | × |
| | *N. stellatus* | | × | | | | × | × |
| *Assilina alpina* | | × | × | × | × | × | × | × |
| *Operculina* ex gr. *gomezi* | | × | × | × | × | | | × |
| *Heterostegina reticulata mossanensis* | | × | × | × | × | × | × | × |
| *Spiroclypeus sirottii* | | × | × | × | × | × | × | × |
| *Pellatispira madaraszi* | | | | | | | | × |

In Table 8 the LBF fauna of Castel San Felice (samples VER 2–4) is compared with other rich assemblages of similar age (SBZ 19A). The table shows that they are very similar to each other, with minimal differences. All of these sites are considered key-localities for both the SBZ 19A and OZ 14 zones. However, the preservation of the fauna is considerably better in Verona, Mossano, Úrhida and Kırklareli than in Şarköy, Teke and Urtsadzor. Finally, both Verona Castel San Felice and Mossano are easily accessible, making them ideal key-localities for the discussed time-spans.

© 2025 by the author(s). Distributed under a Creative Commons CC BY license.

Preprints.org (www.preprints.org) | NOT PEER-REVIEWED | Posted: 24 June 2025 doi:10.20944/preprints202506.1471.v2

Peer-reviewed version available at Geosciences 2025, 15, 334; doi:https://doi.org/10.3390/geosciences15090334

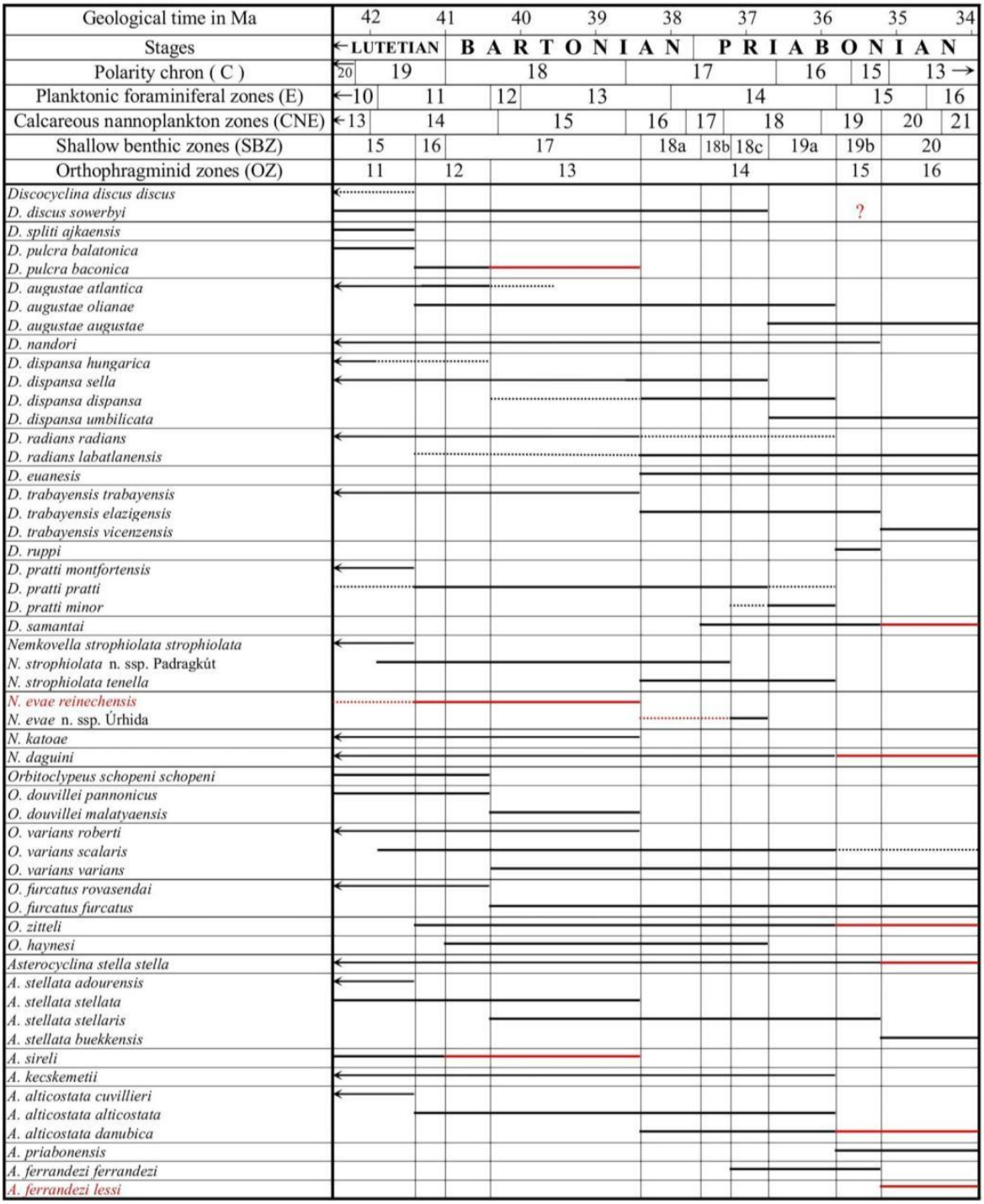


**Figure 36.** Updated orthophragmine range-chart for the late Lutetian to terminal Priabonian interval in the Western and Central Tethys. Updates compared to the range-chart in [69] are marked in red. Dashed lines indicate uncertain occurrences. Red question mark corresponds to the erratic occurrence of one single specimen of *Discocyclina discus sowerbyi* from Switzerland [56]. The time scale, position of stages, polarity chrons and zonal subdivision by planktonic foraminifera, calcareous nannoplankton and larger benthic foraminifera are based on [102].

### *7.2. Updating late Lutetian–Priabonian LBF Range Charts*

In recent years, several important new data have been published on LBF assemblages from the second half of the Eocene [7,56,63–65,67,68,71,103]. These significantly enriched our knowledge on the stratigraphic ranges of LBF taxa living in this period, which made it necessary to update previously published summaries [45,69] on this topic.

© 2025 by the author(s). Distributed under a Creative Commons CC BY license.

Preprints.org (www.preprints.org) | NOT PEER-REVIEWED | Posted: 24 June 2025 doi:10.20944/preprints202506.1471.v2

Peer-reviewed version available at Geosciences 2025, 15, 334; doi:https://doi.org/10.3390/geosciences15090334

The updated stratigraphic ranges of particular orthophragmine taxa (subspecies and unsubdivided species) are shown in Figure 36. Note that the arbitrary subdivision of the (supposedly gradual) evolutionary lineages causes overlaps between the stratigraphical ranges of neighboring subspecies (Figure 37) since there are always spatial, ecological and random deviations from the 'medium' evolutionary track, and thus the latter has a range of variation.

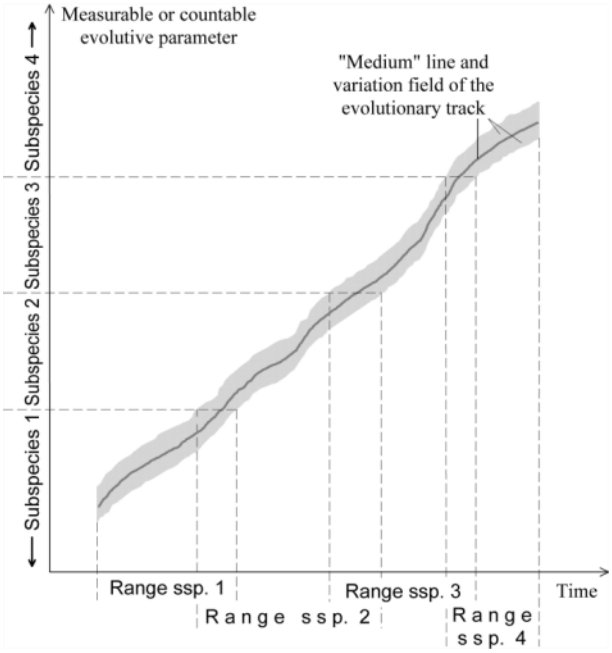


**Figure 37.** Relationship between the arbitrary subdivision of evolutionary lineages and the stratigraphic ranges of the obtained subspecies.

The updated ranges of most important Bartonian–Priabonian LBF taxa are summarized in Figure 38. Figures 36 and 38 are spatially valid for the peri-Mediterranean region, including the territory from Spain to Armenia, and from the Alps to Tunisia, but not including the Indian subcontinent. One of the reasons is that the taxonomical composition of the orthophragmine fauna in this region is significantly different from that of the more western territories, although several common taxa enable the correlation between them [7,63,64,104]. The other reason is that in our opinion the nummulitids from the Indian subcontinent need a comprehensive revision because the nomenclature used for them is significantly different for (mainly) the Western Tethys [35] and for India [105,106].

© 2025 by the author(s). Distributed under a Creative Commons CC BY license.

Preprints.org (www.preprints.org) | NOT PEER-REVIEWED | Posted: 24 June 2025 doi:10.20944/preprints202506.1471.v2

Peer-reviewed version available at *Geosciences* **2025**, *15*, 334; doi:https://doi.org/10.3390/geosciences15090334

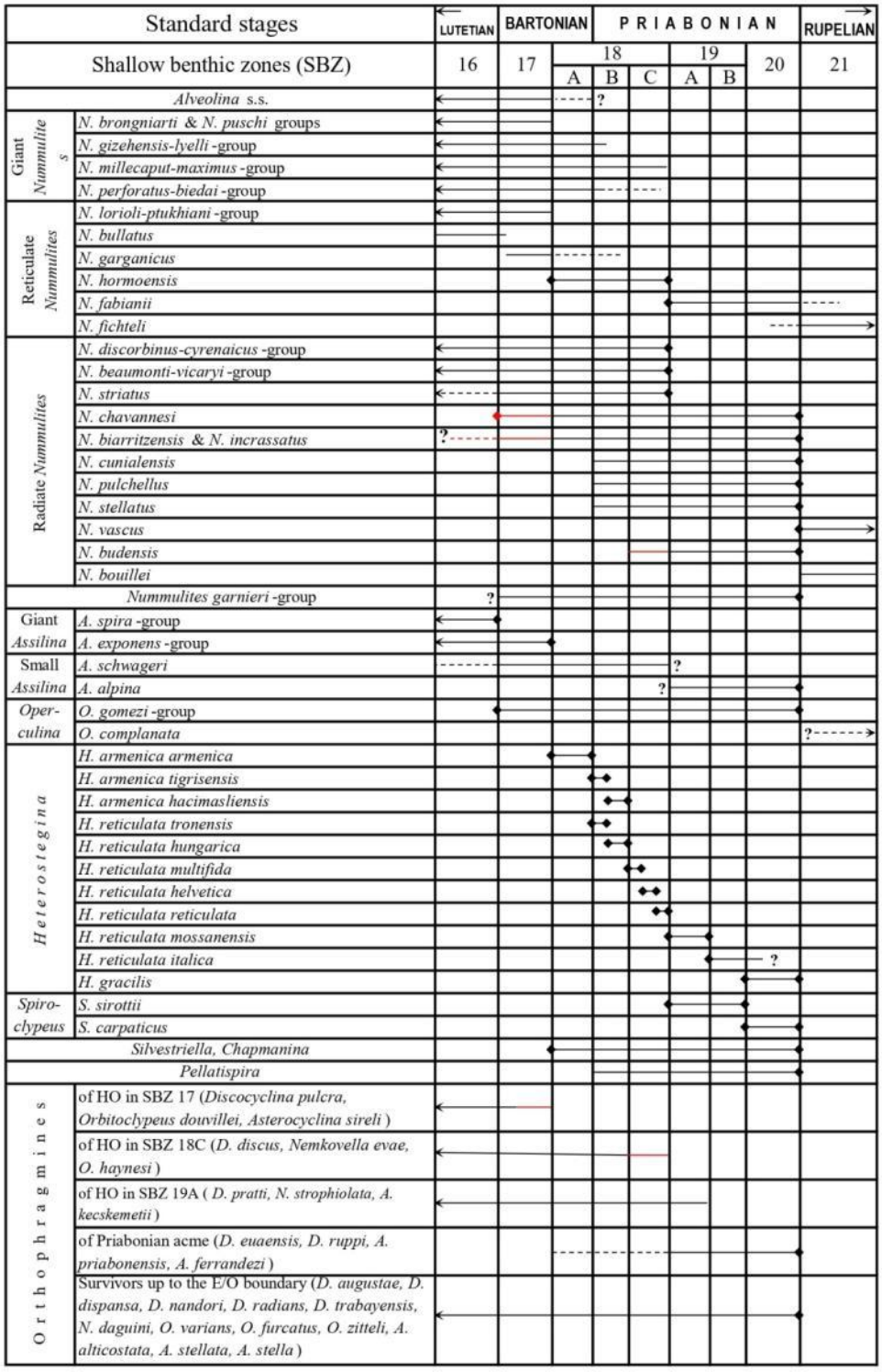


**Figure 38.** Updated range chart for some late Lutetian to early Rupelian larger benthic foraminiferal taxa of the peri-Mediterranean region [45] with modifications (updates are marked in red). The stratigraphic subdivision is not time-proportional.

**Author Contributions:** Conceptualization, L.S.E. and G.L.; methodology, G.L and C.A.P.; validation, L.S.E., G.L. and C.A.P.; investigation, L.S.E. and G.L.; data curation, G.L.; writing—original draft preparation, L.S.E., G.L. and C.A.P.; writing—review and editing, L.S.E.; visualization, L.S.E.; supervision, G.L. All authors have read and agreed to the published version of the manuscript.

**Funding:** This research received no external funding.

© 2025 by the author(s). Distributed under a Creative Commons CC BY license.

Preprints.org (www.preprints.org) | NOT PEER-REVIEWED | Posted: 24 June 2025 doi:10.20944/preprints202506.1471.v2

Peer-reviewed version available at Geosciences 2025, 15, 334; doi:https://doi.org/10.3390/geosciences15090334

**Data Availability Statement:** The raw data will be made available by the authors on request.

**Acknowledgments:** The authors are grateful to the late Prof. Achille Sirotti (University of Modena) for introducing the geology of the area and presenting the localities. L.S.E received support through the Stipendium Hungaricum program for his related researches. He also would like to express profound gratitude to his late MSc advisor, Prof. Ercan Özcan, for his invaluable guidance, support, and the lasting impact he had on his academic journey. We would like to thank the whole staff of the Institute of Exploration Geosciences of the University of Miskolc for introducing the use of the equipment. The useful comments of the two reviewers greatly improved the quality of the paper.

**Conflicts of Interest:** The authors declare no conflict of interest.

## Abbreviations

SBZShallow Benthic Zone
LBFLarger benthic foraminifera
OZ Orthophragmine Zone
№ number of specimens
s.e. standard error
HO highest occurrence

## References

1. Archiac, E. J. A. d'. Description des fossiles du groupe nummulitique recueillis par M. S. P. Pratt et M. J. Delbos aux environs de Bayonne et de Dax. *Mém. Soc. Géol. Fr*., 2nd series, 1850, *3*, 397–456. (in French).
2. Archiac, E. J. A. d', Haime, J. *Description des animaux fossils du groupe nummulitique de l'Inde, précédé d'un résumé géologique et d'une monographie des Nummulites*. Paris, France: Gide et J. Baudry Libraires-Éditeurs, 1853. (in French).
3. Serra-Kiel, J.; Hottinger, L.; Caus, E.; Drobne, K.; Ferrández, C.; Jauhri, A. K.; Less, G.; Pavlovec, R.; Pignatti, J.; Samsó, J. M. Larger Foraminiferal Biostratigraphy of the Tethyan Paleocene and Eocene. *Bull. Soc. Géol. Fr*. 1998, *169*, 281–299.
4. Cahuzac, B.; Poignant, A. Essai de Biozonation de l'Oligo-Miocène Dans Les Bassins Européens à l'aide Des Grands Foraminifères Néritiques. *Bull. Soc. Géol. Fr*. 1997, *168*, 155–169.
5. Less, Gy. Paleontology and stratigraphy of the European *Orthophragminae*. *Geol. Hung., Series Palaeontologica* 1987, *51*, 1–373.
6. Less, Gy. The zonation of the Mediterranean Upper Paleocene and Eocene by *Orthophragminae*. *Opera Dela Slovenska Akademija Znanosti in Umetnosti* 1998, *34*, 21–43.
7. Özcan, E.; Yücel, A. O.; Erkızan, L. S.; Gültekin, M. N.; Kayğılı, S.; Yurtsever, S. *Atlas of the Tethyan Orthophragmines*. *Mediterr. Geosci. Rev*. 2022, *4*, 3–213.
8. Papazzoni, C. A.; Ćosović, V.; Briguglio, A.; Drobne, K. Towards a calibrated larger foraminifera biostratigraphic zonation: Celebrating 18 years of the application of shallow benthic zones. *Palaios* 2017, *32*, 1–5.
9. Pignatti, J.; Papazzoni, C. A. Oppelzones and their heritage in current larger foraminiferal biostratigraphy. *Lethaia* 2017, *50*, 369–380.
10. Doglioni, C.; Bosellini, A. Eoalpine and Mesoalpine tectonics in the Southern Alps. *Geol. Rundsch*. 1987, *76*, 735–754.
11. Carminati, E.; Doglioni, C. Alps vs. Apennines: The paradigm of a tectonically asymmetric Earth. *Earth-Sci. Rev*. 2012, *112*, 67–96.
12. Curzi, M.; Viola, G.; Zuccari, C.; Aldega, L.; Billi, A.; van der Lelij, R.; Kylander-Clark, A.; Vignaroli, G. Tectonic evolution of the Eastern Southern Alps (Italy): A reappraisal from new structural data and geochronological constraints. *Tectonics* 2024, *43*, e2023TC008013.
13. Bosellini, A. Dynamics of Tethyan carbonate platforms. In Crevello, P. D.; Wilson, J. L.; Sarg, J. F.; Read, J. F., Eds. *Controls on carbonate platform and basin development*; SEPM Special Publication 44; Society of Economic Paleontologists and Mineralogists: 1989, 3–13.

© 2025 by the author(s). Distributed under a Creative Commons CC BY license.

Preprints.org (www.preprints.org) | NOT PEER-REVIEWED | Posted: 24 June 2025 doi:10.20944/preprints202506.1471.v2

Peer-reviewed version available at Geosciences 2025, 15, 334; doi:https://doi.org/10.3390/geosciences15090334


14. Zampieri, D. Tertiary extension in the Southern Trento Platform, Southern Alps, Italy. *Tectonics* 1995, *14*, 645–657.
15. Winterer, E. L.; Bosellini, A. Subsidence and sedimentation on Jurassic passive continental margin, Southern Alps, Italy. *AAPG Bull*. 1981, *65*, 394–421.
16. Luciani, V. Stratigrafia sequenziale del Terziario nella catena del Monte Baldo (provincie di Verona e Trento). *Mem. Sci. Geol*. 1989, *41*, 263–351.
17. Rasser, M. W.; Harzhauser, M.; Anistratenko, O. Y.; Anistratenko, V. V.; Bassi, D.; Belak, M.; Berger, J.-P.; Bianchini, G.; Čičić, S.; Ćosović, V. Palaeogene and Neogene. In *The Geology of Central and Eastern Europe*; McCann, T., Ed.; Geological Society of London: London, UK, 2008; 1031–1137.
18. Martire, L.; Clari, P.; Lozar, F.; Pavia, G. The *Rosso Ammonitico Veronese* (Middle-Upper Jurassic of the Trento Plateau): A Proposal of Lithostratigraphic Ordering and Formalization. *Rivista Italiana di Paleontologia e Stratigrafia* 2006, *112*, 227.
19. Roghi, G.; Romano, R. Le Formazioni Geologiche del Veronese nella Nuova Cartografia Geologica Nazionale. La Lessinia—Ieri Oggi Domani. *Quaderno Culturale* 2009, 32.
20. Bosellini, A.; Carraro, F.; Corsi, M.; De Vecchi, G.; Gatto, G.; Malaroda, R.; Sturani, C.; Ungaro, S.; Zanettin, B. *Note illustrative della Carta geologica d'Italia. F. 49, Verona*; Servizio Geologico d'Italia: Roma, Italy, 1967.
21. Zorzin, R. Geologia e paleontologia dell'area collinale di Verona. In *Storia naturale della città di Verona*; Latella, L., Ed.; Cierre Edizioni: Caselle di Sommacampagna (VR), 2018; pp. 71–74.
22. De Zanche, V.; Sorbini, L.; Spagna, V. Geologia del territorio del Comune di Verona. *Mem. Mus. Civ. St. Nat. Verona, II Ser., Sez. Sci. Terra* 1977, *1*, 1–52.
23. Barbieri, G. *I macroforaminiferi dell'Eocene superiore nei Lessini a Nord di Verona*. Unpublished BSc thesis, Università degli Studi di Modena – Istituto di Paleontologia 1985, 198 pp., 2 tabs., 13 pls., 1 geological map.
24. Giusberti, L.; Bannikov, A.; Galazzo, F. B.; Fornaciari, E.; Frieling, J.; Luciani, V.; Papazzoni, C. A.; Roghi, G.; Schouten, S.; Sluijs, A. A New Fossil-Lagerstätte from the Lower Eocene of Lessini Mountains (Northern Italy): A Multidisciplinary Approach. *Palaeogeogr., Palaeoclimatol., Palaeoecol.* 2014, *403*, 1–15.
25. Papazzoni, C. A.; Sirotti, A. *Nummulite* biostratigraphy at the Middle/Upper Eocene boundary in the Northern Mediterranean Area. *Riv. Ital. Paleontol. Stratigr.* 1995, *101*, 63–80.
26. Fabiani, R. Guida geologica delle Colline di Verona. *Atti Accad. Agricolt. Scienze Lett. Verona* 1920, *21*, 241–252.
27. Catullo, A. Memoria geognostico-paleozoica sulle Alpi Venete, con Appendice e Seconda Appendice al Catalogo degli Ammoniti delle Alpi Venete. *Mem. Soc. Ital. Sci. Res. Modena* 1848, *24*, 187–339.
28. Bittner, A. Das Alpengebiet zwischen Vicenza und Verona. *Verh. Geol. Bundesanstalt* 1877, *8*, 226–231.Oppenheim, P. Die Eocaenfauna des Monte Postale bei Bolca in Veronesischen. *Palaeontographica* 1896, *43*, 125–222.
29. Oppenheim, P. Die Eocaenfauna des Monte Postale bei Bolca in Veronesischen. *Palaeontographica* 1896, *43*, 125–222.
30. Fabiani, R. Il Paleogene del Veneto. *Mem. Istit. Geol. Univ. Padova* 1915, *3*, 1–336.
31. Brönnimann, P. Zur Morphologie von *Aktinocyclina* Gümbel 1868. *Eclogae Geol. Helv.* 1945a, *38*, 560–579.
32. Brönnimann, P. Zur Frage der verwandtschaftlichen Beziehungen zwischen *Discocyclina* s.s. und *Asterocyclina*. *Eclogae Geol. Helv.* 1945b, *38*, 579–617.
33. Hottinger, L. Recherches sur les *Alvéolines* paléocènes et éocènes. *Schweiz. Paläontol. Abh.* 1960, *75–76*, 1–236 + Atlas.
34. Schaub, H. Contribution à la stratigraphie du *Nummulitique* du Véronais et du Vicentin. *Mem. Soc. Geol. Ital.* 1962, *3*, 59–66.
35. Schaub, H. *Nummulites* et *Assilinae* de la Tethys Paléogène. Taxonomies, phylogenèse et biostratigraphie. *Schweiz. Paläontol. Abh.* 1981, *104–106*, 1–236 + Atlas I–II.
36. Arni, P.; Lanterno, E. Considérations paléoécologiques et interprétation des calcaires de l'Éocène du Véronais. *Arch. Sci.* 1972, *25*, 251–283..
37. Less, Gy.; Özcan, E.; Papazzoni, C. A.; Stockar, R. The Middle to Late Eocene Evolution of Nummulitid Foraminifer *Heterostegina* in the Western Tethys. *Acta Palaeontol. Pol.* 2008, *53*, 317–350.


© 2025 by the author(s). Distributed under a Creative Commons CC BY license.

Preprints.org (www.preprints.org) | NOT PEER-REVIEWED | Posted: 24 June 2025 doi:10.20944/preprints202506.1471.v2

Peer-reviewed version available at Geosciences 2025, 15, 334; doi:https://doi.org/10.3390/geosciences15090334


38. Less, Gy.; Özcan, E. The Late Eocene Evolution of Nummulitid Foraminifer *Spiroclypeus* in the Western Tethys. *Acta Palaeontol. Pol.* 2008, *53*, 303–316.
39. Less, Gy. New method for the examination of equatorial sections of orbitoidal larger foraminifera. *Magy. Áll. Földt. Int. Évi Jelentése 1979* 1981, 445–457.
40. Hottinger, L. Foraminifères operculiniformes. *Mém. Mus. Natl. Hist. Nat.* 1977, *57*, 1–159.
41. Drobne, K. Alvéolines paléogènes de la Slovénie et de l'Istrie. *Schweiz. Paläontol. Abh.* 1977, *99*, 1–132.
42. Drooger, C. W. Radial Foraminifera: Morphometrics and Evolution. *Verh. Kon. Ned. Akad. Wetensch., Afd. Natuurk.* 1993, *41*, 1–242.
43. Khan, M. A.; Drooger, C. W. On variation in *Nummulites* assemblages. I and II. *Proc. Kon. Ned. Akad. Wetensch., B* 1971, *72*, 97–121.
44. Less, Gy.; Kovács, L. Ó. Typological versus morphometric separation of orthophragminid species in single samples–a case study from Horsarrieu (upper Ypresian, SW Aquitaine, France). *Rev. Micropaléontol.* 2009, *52*, 267–288.
45. Less, Gy.; Özcan, E. Bartonian–Priabonian larger benthic foraminiferal events in the Western Tethys. *Austrian J. Earth Sci.* 2012, *105*, 129–140.
46. Agnini, C.; Fornaciari, E.; Giusberti, L.; Grandesso, P.; Lanci, L.; Luciani, V.; et al. Integrated biomagnetostratigraphy of the Alano section (NE Italy): A proposal for defining the middle–late Eocene boundary. *Bull. Geol. Soc. Am.* 2011, *123*, 841–872.
47. Agnini, C.; Backman, J.; Boscolo-Galazzo, F.; Condon, D. J.; Fornaciari, E.; Galeotti, S.; … Wade, B. S. Proposal for the global boundary stratotype section and point (GSSP) for the Priabonian stage (Eocene) at the Alano section (Italy). *Episodes* 2021, *44*, 151–173.
48. Caudri, C. B. Systematics of the American *Discocyclinas*. *Eclogae Geol. Helv.* 1972, *65*, 211–219.
49. Ferràndez-Cañadell, C.; Serra-Kiel, J. Morphostructure and paleobiology of *Discocyclina* Gümbel, 1870. *J. Foraminifer. Res.* 1992, *22*, 147–165.
50. Ferràndez-Cañadell, C. A new, ribbed species of *Nemkovella* Less 1987 (Discocyclinidae), and discussion of the genus *Actinocyclina* Gümbel, 1870. *J. Foraminifer. Res.* 1997, *27*, 175–185.
51. Ferràndez-Cañadell, C. An asterigerinacean origin for *Orbitoclypeus* and *Asterocyclina* (Orbitoclypeidae, Foraminifera). *J. Foraminifer. Res.* 1998, *28*, 135–140.
52. Özcan, E.; Less, Gy.; Kertész, B. Late Ypresian to Middle Lutetian orthophragminid record from central and northern Turkey: Taxonomy and remarks on zonal scheme. *Turk. J. Earth Sci.* 2007, *16*, 281–318.
53. Özcan, E.; Mitchell, S. F.; Less, Gy.; Robinson, E.; Bryan, J. R.; Pignatti, J.; Yücel, A. O. A revised suprageneric classification of American orthophragminids with emphasis on late Paleocene representatives from Jamaica and Alabama. *J. Syst. Palaeontol.* 2019, *17*, 1551–1579.
54. Less, Gy. Numeric characterization of 'Orthophragmina' populations. *Acta Geol. Hung.* 1993, *35*, 193–215.
55. Özcan, E.; Less, Gy.; Báldi-Beke, M.; Kollányi, K.; Kertész, B. Biometric analysis of middle and upper Eocene Discocyclinidae and Orbitoclypeidae (Foraminifera) from Turkey and updated orthophragmine zonation in the western Tethys. *Micropaleontology* 2006, *52*, 485–520.
56. Ferràndez-Cañadell, C.; Baumgartner-Mora, C.; Baumgartner, P. O.; Epard, J.-L. Priabonian (upper Eocene) larger foraminifera from the Helvetic Nappes of the Alps (Western Switzerland): New markers for Shallow Benthic Zones 19–20. *Micropaleontology* 2023, *69*, 401–450.
57. van der Weijden, W. J. M. *Het genus Discocyclina in Europa. Een monografie naar aanleiding van een heronderzoek van het Tertiair-profiel van Biarritz*; Utrecht, 1940.
58. Rasser, M. W.; Less, Gy.; Báldi-Beke, M. Biostratigraphy and facies of late Eocene sediments of the western Austrian Molasse zone with special reference to the larger foraminifera. *Abh. Geol. Bundesanst.* 1999, *56*, 679–698.
59. Less, Gy. The late Paleogene larger foraminiferal assemblages of the Bükk Mts. (NE Hungary). *Rev. Esp. Micropaleontol.* 1999, *31*, 51–60.
60. Sowerby, J. De C. Systematic list of organic remains, the plants determined by Mr. John Morris, and the remainder by Mr. James de Carl Sowerby. *Trans. Geol. Soc. Lond.*, Ser. 2, 1840, *5*, 327–329, pls. 21–26.


© 2025 by the author(s). Distributed under a Creative Commons CC BY license.

Preprints.org (www.preprints.org) | NOT PEER-REVIEWED | Posted: 24 June 2025 doi:10.20944/preprints202506.1471.v2

Peer-reviewed version available at Geosciences 2025, 15, 334; doi:https://doi.org/10.3390/geosciences15090334


61. Samanta, B. K.; Lahiri, A. The occurrence of *Discocyclina* Gümbel in the middle Eocene Fulra Limestone of Cutch, Gujarat, Western India, with notes on species reported from the Indian region. *Bull. Geol. Min. Metall. Soc. India* 1985, *52*, 211–295.
62. Özcan, E.; Less, Gy.; Okay, A. I.; Báldi-Beke, M.; Kollányi, K.; Yılmaz, İ. Ö. Stratigraphy and larger foraminifera of the Eocene shallow-marine and olistostromal units of the southern part of the Thrace Basin, NW Turkey. *Turk. J. Earth Sci.* 2010, *19*, 27–77.
63. Özcan, E.; Saraswati, P. K.; Yücel, A. O.; Ali, N.; Hanif, M. Bartonian orthophragminids from the Fulra Limestone (Kutch, W India) and coeval units in Sulaiman Range, Pakistan: A synthesis of shallow benthic zone (SBZ) 17 for the Indian Subcontinent. *Geodinamica Acta* 2018, *30*, 137–162.
64. Ali, N.; Özcan, E.; Yücel, A. O.; Hanif, M.; Hashmi, S. I.; Ullah, F.; Pignatti, J. Bartonian orthophragminids with new endemic species from the Pirkoh and Drazinda formations in the Sulaiman Range, Indus Basin, Pakistan. *Geodinamica Acta* 2018, *30*, 31–62.
65. Özcan, E.; Less, Gy.; Jovane, L.; Catanzariti, R.; Frontalini, F.; Coccioni, R.; Giorgioni, M.; Rodelli, D.; Rego, E.S.; Kayğılı, S.; Asgharian Rostami, M. Integrated biostratigraphy of the middle to upper Eocene Kırkgeçit Formation (Baskil section, Elazığ, eastern Turkey): Larger benthic foraminiferal perspective. *Mediterr. Geosci. Rev.* 2019, *1*, 55–90.
66. Whipple, G.L. Eocene Foraminifera. In *Geology of Eua, Tonga*; Hoffmeister, I.E., Ed.; Bulletin of the Bernice P. Bishop Museum: Honolulu, HI, USA, 1932; Volume 96, pp. 79–90.
67. Yücel, A.O.; Özcan, E.; Erbil, Ü. Latest Priabonian larger benthic foraminiferal assemblages at the demise of the Soğucak Carbonate Platform (Thrace Basin and Black Sea shelf, NW Turkey): Implications for the shallow marine biostratigraphy. *Turk. J. Earth Sci.* 2019, *29*, 85–114.
68. Dimou, V.G.; Koukousioura, O.; Less, G.; Triantaphyllou, M.V.; Dimiza, M.D.; Syrides, G. Systematic paleontology and biostratigraphy of upper Eocene larger benthic foraminifera from Fanari (Thrace Basin, Greece). *Micropaleontology* 2023, *69*, 457–486.
69. Less, Gy.; Özcan, E.; Okay, A.I. Larger foraminiferal stratigraphy and paleoenvironments of the Middle Eocene to Lower Oligocene shallow-marine units in the northern and eastern parts of the Thrace Basin, NW Turkey. *Turk. J. Earth Sci.* 2011, *20*, 793–845.
70. Meffert, B.F. Eocenovaja fauna iz Daralageza v Armenii. *Tr. Glav. Geol.-Razved. Upravl.* 1931, *99*, 1–64. Leningrad–Moscow. (in Russian).
71. Zakrevskaya, E.; Less, G.; Bugrova, E.; Shcherbinina, E.; Grigoryan, T.; Sahakyan, L. Integrated biostratigraphy and benthic foraminifera of the middle-upper Eocene deposits of Urtsadzor section (Southern Armenia). *Turk. J. Earth Sci.* 2020, *29*, 896–945.
72. Gümbel, C.W. Beiträge zur Foraminiferenfauna der nordalpinen älteren Eocängebilde oder der Kressenberger Nummulitenschichten. *Abh. K. Bayer. Akad. Wiss., Math.-Phys. Kl.*, 1870, *10*, 581–730.
73. Neumann, M. Révision des *Orbitoididés* du Crétacé et de l'Éocène en Aquitaine Occidentale. *Mém. Soc. Géol. Fr.* 1958, *37*(83), 1–174.
74. Özcan, E.; Erbay, S.; Abbasi, A.I.; Pereira, C.D.; Erkızan, L.S.; Kayğılı, S. The first record of *Nemkovella daguini* (Neumann, 1958) from the middle-late Eocene of Oman (Arabian Peninsula) and Meghalaya (Indian Subcontinent) and its significance in Tethys: Correlations and paleobiogeography. *Riv. Ital. Paleontol. Stratigr.* 2019, *125*, 13–28.
75. Özcan, E.; Okay, A.İ.; Bürkan, K.A.; Yücel, A.O.; Özcan, Z. Middle–Late Eocene marine record of the Biga Peninsula, NW Anatolia, Turkey. *Geologica Acta* 2018, *16*, 133–162.
76. Schlumberger, C. Troisième note sur les *Orbitoïdes*. *Bull. Soc. Géol. Fr.* 1903, *4*, 273–289.
77. Kaufmann, F.J. *Geologische Beschreibung des Pilatus*. Beitr. Geol. Karte Schweiz 1867, *5*, 1–169.
78. Stöckar, R. I macroforaminiferi eocenici negli inclusi dei depositi Quaternari della collina di Prella (Ticino meridionale, Svizzera). *Geologia Insubrica* 1999, *4*, 1–20.
79. Rütimeyer, L. *Ueber das schweizerische Nummulitenterrain, mit besonderer Berücksichtigung des Gebirges zwischen dem Thunersee und der Emme*. Neue Denkschr. Schweiz. Naturforsch. Ges. 1850, *11*, 1–120.
80. Less, Gy. Amendments to the monograph *Paleontology and Stratigraphy of the European Orthophragminae* [Kiegészítések az európai Orthophragminák őslénytana és rétegtana c. monográfiához]. *Magy. Áll. Földt. Int. Évi Jel.* 1987, *1987*, 313–321.


© 2025 by the author(s). Distributed under a Creative Commons CC BY license.

Preprints.org (www.preprints.org) | NOT PEER-REVIEWED | Posted: 24 June 2025 doi:10.20944/preprints202506.1471.v2

Peer-reviewed version available at Geosciences 2025, 15, 334; doi:https://doi.org/10.3390/geosciences15090334

81. Romero, J.; Hottinger, L.; Caus, E. Early appearance of larger foraminifera supposedly characteristic for the late Eocene in the Igualada Basin, NE Spain. *Rev. Esp. Paleontol.* 1999, *14*, 79–92.
82. Drooger, C.W.; Marks, P.; Papp, A. Smaller radiate *Nummulites* of northwestern Europe. *Utrecht Micropalaeontol. Bull.* 1971, *5*, *1–137*.
83. Papazzoni, C.A. Biometric analyses of *Nummulites "ptukhiani"* Z.D. Kacharava, 1969 and *Nummulites fabianii* (Prever in Fabiani, 1905). *J. Foraminifer. Res.* 1998, *28*, 161–176.
84. Less, Gy.; Kertész, B.; Özcan, E. Bartonian to end-Rupelian reticulate *Nummulites* of the Western Tethys. *Anu. Inst. Geociênc.* 2006, *29*, 344–345.
85. Less, Gy.; Frijia, G.; Özcan, E.; Saraswati, P.K.; Parente, M.; Kumar, P. *Nummulitids*, lepidocyclinids and Sr-isotope data from the Oligocene of Kutch (western India) with chronostratigraphic and paleobiogeographic evaluations. *Geodinamica Acta* 2018, *30*, 183–211.
86. Özcan, E.; Less, Gy.; Báldi-Beke, M.; Kollányi, K.; Acar, F. Oligo-Miocene Foraminiferal Record (Miogypsinidae; Lepidocyclinidae and Nummulitidae) from the Western Taurides (SW Turkey): Biometry and Implications for the Regional Geology. *J. Asian Earth Sci.* 2009, *34*, 740–760.
87. Özcan, E.; Less, Gy.; Báldi-Beke, M.; Kollányi, K. Oligocene hyaline larger foraminifera from Kelereşdere Section (Muş, Eastern Turkey). *Micropaleontology* 2010, *56*, 465–493.
88. Cotton, L.J.; Pearson, P.N.; Renema, W. A place for *Nummulites ptukhiani*? A new lineage of reticulate *Nummulites* from Kilwa District, Tanzania. *Journal of Systematic Palaeontology* 2015, *13*, 465–486.
89. Nuttall, W.L.F.; Brighton, A.G. Larger Foraminifera from the Tertiary of Somaliland. *Geol. Mag.* 1931, *68*, 49–65.
90. Cotton, L.J.; Zakrevskaya, E.Y.; van der Boon, A.; Asatryan, G.; Hayrapetyan, F.; et al. Integrated stratigraphy of the Priabonian (upper Eocene) Urtsadzor section, Armenia. *Newsl. Stratigr.* 2017, *50*, 269–295.
91. Fabiani, R. Studii geo-paleontologichi dei Colli Berici. *Atti R. Istituto Veneto di Scienze, Lettere ed Arti* 1905, *64*, 1805–1825.
92. Okay, A. İ.; Çolak, D.; Özcan, E. Eocene–Oligocene succession at Kıyıköy (Midye) on the Black Sea coast of Turkey: Stratigraphy, larger benthic foraminifera, and paleoenvironments. *Turk. J. Earth Sci.* 2020, *29*, 1–22.
93. Hantken, M. von. Die Fauna der Clavulina-Szaboi–Schichten. I. Foraminiferen. *Mitt. Jahrb. Königl. Ungar. Geol. Anstalt* 1875, *4*, 1–93. (in German).
94. Nemkov, G.I. Nummulitides of the Soviet Union and their biostratigraphic significance. *Mater. K poznan. geol. stroen. SSSR* 1967, *16*, 1–319. (in Russian).
95. Harpe, P. de la. Note sur les *Nummulites* des Alpes occidentales. *Acta Soc. Helv. Sci. Nat.* 1878, *60*, 227–232.
96. Harpe, P. de la. Étude des *Nummulites* de Suisse et révision des espèces éocènes des genres *Nummulites* et *Assilina*. Troisième et dernière partie (Posthume). *Mém. Soc. Paléontol. Suisse / Abh. Schweiz. Paläontol. Ges.* 1883, *10*, 141–180.
97. Herb, R.; Hekel, H. *Nummuliten* aus dem Obereozän von Possagno. *Schweiz. Paläontol. Abh.* 1975, *97*, 113–135.
98. Douvillé, H. Le Crétacé et le Tertiaire aux environs de Thônes (Haute-Savoie). *C. R. Acad. Sci. Paris* 1916, *163*, 324–331.
99. Colom, G.; Bauzá, J. *Operculina canalifera gomezi* n. subsp. de Bartoniense de Cataluña. *Bol. Real Soc. Esp. Hist. Nat.* 1950, *47*, 219–221.
100. Drooger, C.W.; Roelofsen, J.W. *Cycloclypeus* from Ghar Hassan, Malta. *Proc. Kon. Ned. Akad. Wetensch.* 1982, *85*, 203–218.
101. Bieda, F. Sur quelques foraminifères nouveaux ou peu connus du flysch des Carpates polonaises. *Ann. Soc. Géol. Pologne* 1949, *18*, 151–179.
102. Speijer, R.P.; Pälike, H.; Hollis, C.J.; Hooker, J.J.; Ogg, J.G. The Paleogene Period. In: *Geologic Time Scale 2020*; Gradstein, F.M., Ogg, J.G., Schmitz, M.D., Ogg, G.M., Eds.; Elsevier: Amsterdam, 2020; pp. 1087–1140.
103. Ben Ismail-Lattrache, K.; Özcan, E.; Boukhalfa, K.; Saraswati, P.K.; Soussi, M.; Jovane, L. Early Bartonian orthophragminids (Foraminiferida) from Reineche Limestone, North African platform, Tunisia: Taxonomy and paleobiogeographic implications. *Geodinamica Acta* 2014, *26* (spec. issue 1–2), 94–121.

© 2025 by the author(s). Distributed under a Creative Commons CC BY license.

Preprints.org (www.preprints.org) | NOT PEER-REVIEWED | Posted: 24 June 2025 doi:10.20944/preprints202506.1471.v2

Peer-reviewed version available at Geosciences 2025, 15, 334; doi:https://doi.org/10.3390/geosciences15090334

104. Özcan, E.; Saraswati, P.K.; Hanif, M.; Ali, N. Orthophragminids with new axial thickening structures from the Bartonian of the Indian subcontinent. *Geologica Acta* 2016, *14*, 261–282.
105. Samanta, B.K.; Bandopadhyay, K.P.; Lahiri, A. The occurrence of *Nummulites* Lamarck (Foraminiferida) in the Middle Eocene Harudi Formation and Fulra Limestone of Cutch, Gujarat, western India. *Bull. Geol. Min. Metall. Soc. India* 1990, *55*, 1–66.
106. Saraswati, P.K.; Patra, P.K.; Banerji, R.K. Biometric study of some Eocene *Nummulites* and *Assilina* from Kutch and Jaisalmer, India. *J. Palaeontol. Soc. India* 2000, *45*, 91–122.

**Disclaimer/Publisher's Note:** The statements, opinions and data contained in all publications are solely those of the individual author(s) and contributor(s) and not of MDPI and/or the editor(s). MDPI and/or the editor(s) disclaim responsibility for any injury to people or property resulting from any ideas, methods, instructions or products referred to in the content.

© 2025 by the author(s). Distributed under a Creative Commons CC BY license.